Application of Intense Pulsed Light for Surface Sterilization and Food Quality Improvement

by

Sanjiv H. Avashia

Thesis submitted to the Faculty of the
Virginia Polytechnic Institute and State University
in partial fulfillment of the requirements for the degree of

Master of Science
in
Food Science and Technology

APPROVED:

Dr. George J. Flick

Dr. James K. Palmer

Dr. Joseph Dunn

January, 1988
Blacksburg, Virginia

Application of Intense Pulsed Light for Surface Sterilization and Food Quality Improvement

by

Sanjiv H. Avashia

ABSTRACT

Flashblast™ (a registered trademark) is an intense broad spectrum pulsed light source developed by Maxwell Laboratories, San Diego, California which utilizes a Xenon flashlamp for emitting a mixed spectrum of ultraviolet, visible and infrared light. The project's objective was to determine the feasibility of ultra-high intensity light for improving food quality by reducing surface microbial contamination and selected mold metabolites (aflatoxins).

Flashblast™ light was found to be highly effective in inactivating vegetative cells of E. coli, S. aureus, B. cereus and B. subtilis. Bacilli and A. niger spores were also susceptible to Flashblast light at somewhat higher fluences.

Ultrastructural study with the scanning and transmission electron microscopes indicated that Flashblast™ treated gram-negative E. coli population is more susceptible to membrane damage when compared to other

microorganisms. This suggests that photoinactivation involves effects on sensitive sites (genetic material) within the treated organisms which do not lead to significant changes in the microorganism morphology.

Food acceptability studies on cheese, bread, strawberries and turkey breasts did not show a significant alteration in color, flavor and texture ($p \leq 0.05$). The results obtained with bread and strawberries showed commercial feasibility with an approximate 50% shelf-life extension. Flashblast^{TM} treatment caused photodegradation of most aflatoxin types when multiple flash sequences were employed.

It was concluded that full spectrum Flashblast^{TM} light is highly effective for the inactivation of microorganisms and destruction of aflatoxins without causing undesirable sensory changes in foods.

ACKNOWLEDGEMENTS

I wish to express sincere appreciation and gratitude to my research advisor, Dr. G. J. Flick, for his suggestions, guidance and assistance during the entire course of this study and in the preparation of this manuscript.

Further appreciation is extended to my committee members, Drs. J. K. Palmer and Joseph Dunn for their interest and advice throughout the research work. I would like to thank Dr. N. R. Krieg, Dr. O. K. Miller, Dr. G. W. Claus and Dr. A. A. Yousten of the Biology Department at Virginia Tech for their assistance in the micrographs interpretation.

Deepest appreciation is given to Dr. R. L. Grayson for his help and guidance in developing my electron microscopy skills. I am also grateful to Sandy Perkins for her continued technical assistance in developing the micrographs and providing encouragement in the electron microscopy studies. I appreciate the guidance provided by Dr. Diane Van Hekken for the development and arrangement of selected micrographs compiled in this manuscript.

Thanks are extended to Mr. Richard E. Keith, Laboratory Support Services, for his assistance in solving electrical problems that occured in the Flashblast apparatus during the initial studies.

Maxwell Laboratories, San Diego, California supplied the Flashblast apparatus and other accessories required for this investigation. Their interest and cooperation is appreciated. I am grateful to my brother and sister-in-law for their constant encouragement and financial support during my graduate studies.

TABLE OF CONTENTS

CHAPTER 1

INTRODUCTION

Food irradiation has been recognized as a new physical technique in food preservation. During the process of irradiation, food is exposed to electromagnetic radiation of various kinds, e.g. ionizing or non-ionizing, which produce bactericidal effects or may induce alterations in the physical and chemical properties of matter by transferring the photon energy into susceptible molecules. The wave length and the intensity of radiation per unit area determine the extent of damage and types of alterations in irradiated matter.

Among ionizing radiation, gamma radiation is the most common. These are emitted by the decay of a radioactive isotope such as Cobalt-60 and possess considerable penetrating power. Applications of ionizing radiation in the food and agriculture processing industry include: extending shelf-life of fresh produce or processed/packaged food products; prolonging the quality of certain crops by delaying ripening; inhibiting sprouting; and hence reducing requirements for chemical preservation and pest control.

In spite of the enormous advantages of ionizing radiations and approval by U.S. Food & Drug Administration for specific applications, modern food technology has not yet fully exploited gamma radiation use. One of the reasons

for this setback is the question of safety and the wholesomeness of gamma-irradiated foods which are still under public controversy. Ionizing radiation may cause a potential induction of radioactivity into some of the food constituents due to the formation of free radicals. The indirect effects caused by the chain reactions may in turn result in the formation of toxic compounds or Unique Radiolytic Products (URP) which have not been studied in conjuction with human metabolism.

Ultraviolet light (UV) does not induce ionization in the atoms and molecules of matter on exposure. Hence, UV light does not pose a problem of food product radioactivity. However, its use is limited to surfaces and thin films. The most important applications of ultraviolet light are directed at: (1) satisfactory air hygiene through destruction of air-borne organisms; (2) inactivation of microorganisms located on surfaces or suspended in liquids, but accessible to UV; and (3) protection and disinfection of many products of unstable composition which cannot be treated by conventional methods (Shechmeister, 1977).

At present, there is an increasing concern over chemical fumigants, pesticides and food additives. The food industry is in search of a suitable technology for cold sterilization. It is anticipated that UV light will be useful, especially in the surface applications on foods, packaging materials and equipment. Though much work is

being directed towards the use of ionizing radiation for food preservation, there is a small but growing awareness of the benefits that UV light may provide for this purpose.

Consequently, this is the most appropriate time to explore the potential benefits of UV light which, although having, applications limited to the near surfaces region of most solid foods, may provide a safer technique when compared to ionizing radiation. This research was focused on the areas of microbiology, sensory evaluation and detoxification.

Our objectives included the following:

(1) To calibrate the Flashblast apparatus with respect to the amount of energy crossing a unit area of space normal to the direction of propagation of a beam of light (fluence) under varying conditions of distance and input energies.

(2) To determine the effectiveness of Flashblast light to inactivate various food-borne microorganisms (vegetative cells and spores) and to investigate the mechanism of inactivation through electron microscopy studies.

(3) To evaluate the effect of Flashblast light on food surface microbial growth and the resultant effects on flavor profiles and shelf-life of selected foods stored at $4^{\circ}C$ for 16 days.

(4) To examine the susceptibilities of eight aflatoxins to Flashblast light using thin layer chromatography.

CHAPTER 2

REVIEW OF LITERATURE

2.1 ELECTROMAGNATIC RADIATION AND ULTRAVIOLET SPECTRUM

The spectrum of electromagnetic (EMR) includes in order of decreasing energy: gamma; X; UV; Visible; IR; Radar; and Radio. Electromagnetic radiation energy is stored in quantitized photons which are emitted from various sources. The photon energy increases with increasing frequency and decreasing wavelength. The ultraviolet portion of the spectrum includes all wavelengths from 15 to 390 nm with those near 265 nm having the highest bactericidal efficiency. John Jagger (1985) has divided the UV spectrum into these wavelengths: 320-400 nm (near UV or UV-A); 290-320 nm (mid UV or UV-B) and 190-290 nm (far UV or UV-C). Solar UV (290-400 nm) includes the near UV and the mid UV.

Light must interact with matter to cause alteration in susceptible molecules. All interactions are expressed as absorption, and only the absorbed light is responsible for the photoinactivation and alteration which occurs in microorganisms and matter. Davis (1970) reported that the amount of light absorbed by a material is proportional to its absorbency and thickness and to the product of the intensity and duration of the exposure (dose). The selection of a suitable source is an important consideration

in UV treatment. Basic parameters are the emitted spectrum, duration of exposure and spectrum intensity. Source geometry (the distance from the source to the sample) is also an important factor. Theoretically, the intensity from an infinite line source will decrease as the inverse first power of the distance, and the intensity from a point source will decrease as the inverse square of the distance.

2.2 FLASHBLAST APPARATUS

Flashblast is a pulsed power light apparatus developed by Maxwell Laboratories, Inc., San Diego, California. It can be described as an electronic device that transforms electrical energy into high intensity, short duration pulses of light enegy (Hidalgo, 1985). The Flashblast apparatus is capable of generating very high voltage pulses in comparatively small size of equipment by employing complex state-of-the-art electronic circuits and electrical components. It consists of three capacitors, each having a capacitance of 400 microfarads. The number of capacitors in the apparatus can be adjusted in order to obtain a required magnitude of input energy. The spectrum of the emitted light can be varied by changing input energy and voltage adjustments in the equipment. The capacitor bank stores the electrical energy until a trigger mechanism discharges the capacitors through a flashlamp (Hidalgo, 1985). The light pulse is discharged within a 1.5 to 2.5 millisecond time interval. Consequently, the exposure time is short when

compared to conventional surface sterilization and detoxification methods. The limited Flashblast exposure time should prevent some of the problems usually associated with alternative methods. These would include: undesirable odors and flavors; formation of toxic compounds, as free radicals; and physical properties.

Treatment is performed in a polyphenolic chamber (20"x20"x36"). Flashblast utilizes Xenon flashlamps as the light source. The flashlamp used in these studies has a 6" arc length, 9" physical length and 7 mm bore and is filled at 450 Torr in a fused quartz envelope. The flashlamp was housed in an aluminium reflector of size 11.5"x2"x1.75" (see diagram in Appendix F). The flashlamp/reflector assembly can be moved 70 cm vertically with the help of an adjustable handle. This feature provides a convenience to change fluence on the object which is to be treated. Hidalgo (1985) has reviewed some of the surface applications of the Flashblast treatment.

The Flashblast apparatus employes inexpensive contemporary technology, capacitors, electronic circuits, and flashlamp. In addition, the ability to employ pulsed power technology with the apparatus permits low-cost operation with minimum maintenance. Other surface sterilization and detoxification processes, as thermal processing, chemical treatments, and electromagnetic radiation have more expensive equipment and operating costs.

From economical and cost competitive perspectives, Flashblast could become a contemporary technology before the twenty-first century.

2.3 XENON FLASHLAMPS

High-pressure Xenon lamps are widely used to obtain ultraviolet light. Because of the high filling pressure, very high ignition voltages and pulses delivering tens of thousands of volts are required (Phillips, 1983). Phillips (1983) further described the characteristics of Xenon gas and flashlamps. He reported that Xenon has the lowest ionization energy and the lowest thermal conductivity among all the inert gases that are commomly used in the filling of discharge lamps. It is also the most efficient in converting electrical energy to light (Hoyt and McCormick, 1950, Elenbaas, 1972). A Xenon arc lamp provides a relatively smooth continuous spectrum. Xenon arcs are very stable and easy to use, and the lamps have relatively long lifetimes depending on the conditions of operation (Jagger, 1985).

The full spectrum light from a Xenon flashlamp consists of varying amounts of ultraviolet, visible and infrared light depending on the conditions of operation. The photobiological and photochemical effects are primarily due to the UV portion of the light. While the visible light may play some role in thermal effects, the contribution of the infrared portion of the light is rather non-significant.

CHAPTER 3

CALIBRATION OF FLASHBLAST APPARATUS

3.1 INTRODUCTION

The Flashblast apparatus was calibrated with respect to the energy density distributions along the X, Y and Z axes at different input energies as measured with a calorimeter. The energy density distribution was obtained through three dimensional space measurements below the lamphead. The magnitude of input energy was changed by varying both the capacitance and charging voltage. The values were found to be 171 J, 406 J and 684 J with a single capacitor when the voltage adjustments were 30%, 45% and 58% (full) respectively. Input energies with three capacitors were 513 J, 1218 J and 2053 J with similar voltage adjustments.

MATERIALS AND METHODS

A point in the center of the shadow beneath the flashlamp was chosen to be (0, 0, 0) in the Cartesian coordinate system. The X-axis was aligned parallel to the length of the flashlamp with the Y-axis perpendicular to the lamp width from the center. The positive Z-axis increased as the flashlamp was moved in a vertical plane away from the calorimeter head as shown in Appendix H.

The energy distribution along the Z-axis was measured by varying the distance between the calorimeter and lamp head from 5 to 55 cm. The calorimeter head remained at the center during the entire scanning procedure.

In order to evaluate the spatial fluence distribution at the target, calorimeter measurements were also recorded at different distances along the X and Y axes.

The energy density along the Y-axis was measured by displacing the calorimeter head from the center along the Y-axis at $\pm$3, $\pm$6 and $\pm$9 cm. The energy distribution along the X-axis was obtained similarly by displacing the calorimeter along the X-axis at $\pm$5, $\pm$10 and $\pm$15 cm from the center. All calorimeter absorptions were measured as peak heights on an oscilloscope. The peaks obtained from each Flashblast exposure were photographed on Polaroid 612 film by an oscilloscope camera (see Figure 2 in Appendix G).

Flashlamp output is a function of charging voltage and capacitance, therefore, separate curves must be generated for each variance of charging voltage and capacitance. flashlamp energy fluence was obtained by observing the energy distribution at 30%, 45% and 58% (full) voltage adjustments with one and three capacitors. Each capacitor had a capacitance of 400 microfarads.

The input energy, expressed in Joules, was calculated by the following formula:

$$E = 1/2\ C*V^2$$

where E is the input energy in Joules, C is the capacitance in microfarads, and V is the charging voltage in volts.

The absorbed energy in J/cm^2 was determined as follows:

(1) Peak height was multiplied by Channel 2 (CH2) volts/divisions setting on the oscilloscope.

(2) This value was divided by the calorimeter calibration (10.31 volts/J).

(3) The value obtained above is further divided by an area of calorimeter working surface (3.8 cm^2) to determine the absorbed energy in terms of J/cm^2.

In all cases, a single was applied.

RESULTS AND DISCUSSION

Z-AXIS SCAN

Figures 1 and 2 show the absorbed energies at different voltages as a function of the distance between the calorimeter head and the lamphead with one and three capacitors respectively. Both graphs exhibit calibration curves with a similar shape but having different energy values. At distances greater than 30 cm, the energy density remains fairly constant along the Z-axis. The energy density slowly increases as the distance along the Z-axis is decreased from 30 cm to 15 cm. Therefore, irradiance was found to be inversely proportional to the distance within this range.

At distances less than 15 cm, the flashlamp behaves like a line source. There is a sharp increase in the energy density when the fluence is inversely proportional to the square of the distance. All the curves show an identical rectangular hyperbolic behavior. It is evident that at higher charging voltages and capacitances, a greater fluence could be attained at the same distance along the Z-axis. However, the lamp spectrum characteristics change as the power-input settings are altered.

Y-AXIS SCAN

The calorimeter absorptions for the positive and negative displacements were found to be fairly symmetrical. Therefore, each curve is represented in terms of the positive displacements along a particular axis.

Figures 3-5 show the curves of energy density as a function of the displacements along the Y-axis when input energies were adjusted to 171 J, 406 J and 684 J respectively with a single capacitor. Figures 6-8 represent energy densities at 513 J, 1218 J and 2053 J respectively using three capacitors. Because of a displacement limitation along the Y-axis due to the flashlamp cabinet configuration, the distance was confined to a range from 0 to 9 cm. The x value remained at 0 and the calorimeter absorptions were measured along the Y-axis at z values ranging from 5 cm to 45 cm.

At z values greater than 25 cm, the energy density remained fairly constant against displacements along the Y-axis. This effect occurs when the lamp behaved like a point source. At a distance as low as 5 cm on the Z-axis, the flashlamp behaved like a line source. A sharp decrease in the energy density was observed when the calorimeter was displaced from the center at this height.

X-AXIS SCAN

Figures 9-11 contain the curves of energy density as a function of the displacement along the X-axis when the input energies were adjusted to 171 J, 406 J and 684 J respectively using a single capacitor. Figures 12-14 represent energy densities at 513 J, 1218 J and 2053 J respectively when three capacitors were employed.

The Z-axis scan was similar to the Y-axis scan in that the energy densities remained fairly constant at z values higher than 25 cm. There was a significant decrease in the energy density along X-axis at a z value of 5 cm. However, the decrease was not as great as the Y-axis displacements because the displacements were along the length of the flashlamp.

The microbial inactivation data in these experiments were obtained by the spread plate and microdrop plating techniques. It is important to consider the target geometry and dimensions in order to account for a variability in the absorbed energy densities along the X and Y axes. The Petri

plate has a diameter of 9 cm. When the inactivation data are collected at a distance of 5 cm on the Z-axis, it is likely that the microorganisms on the peripheral part of the Petri plate will absorb a lesser amount of than those residing near the center. Again, the microorganisms aligned along the X-axis may have received a relatively uniform incident energy while those aligned along the Y-axis may have received greater variability in energies.

It is observed from the calibration curves that at z = 15 cm, there was less variability in the energy densities along the X and Y axes. At distances greater than 15 cm, one may assume a nonsignificant variability in the absorbed energy under similar experimental conditions. When the microdrop plating technique was used, the microorganisms were plated within a one inch wide area along the X-axis. This procedure maintained a fairly uniform energy density even at the smallest Z-axis distance of 5 cm.

Since most experiments were performed at input energies of 513 J, 1218 J and 2053 J, an attempt was made to calculate a maximum variability in the Petri plate incident energy when the shortest Z-axis distance of 5 cm was used. It was found that at an input energy of 513 J, reductions of 21.5% and 76.5% in the absorbed energy occured along the X and Y axes respectively from the center to the periphery of

the Petri plate. At an input energy of 1218 J, energy density reductions of 23.7% and 76.6% occured along the X and Y axes respectively. At the highest capacitance (3 capacitors) and 58% charging voltage (input energy of 2053 J), a significant variation in the energy density was observed. There were reductions of 44.4% and 81.9% in the absorbed energy along the X and Y axes respectively when the distance on Z-axis was as low as 5 cm.

This variability in absorbed energy indicates that the variability along the X and Y axes was highly significant at a distance of 5 cm between the flashlamp and the Petri plate. At a distance of 15 cm and higher, reductions in the absorbed energies were found to be less than 7%. In the photoinactivation experiments, the 5 cm distance was used only with the microdrop plating technique. Spread plates were not treated at a distance less than 10 cm. Under these conditions, the occurence of variability in the energy density was minimized to some extent.

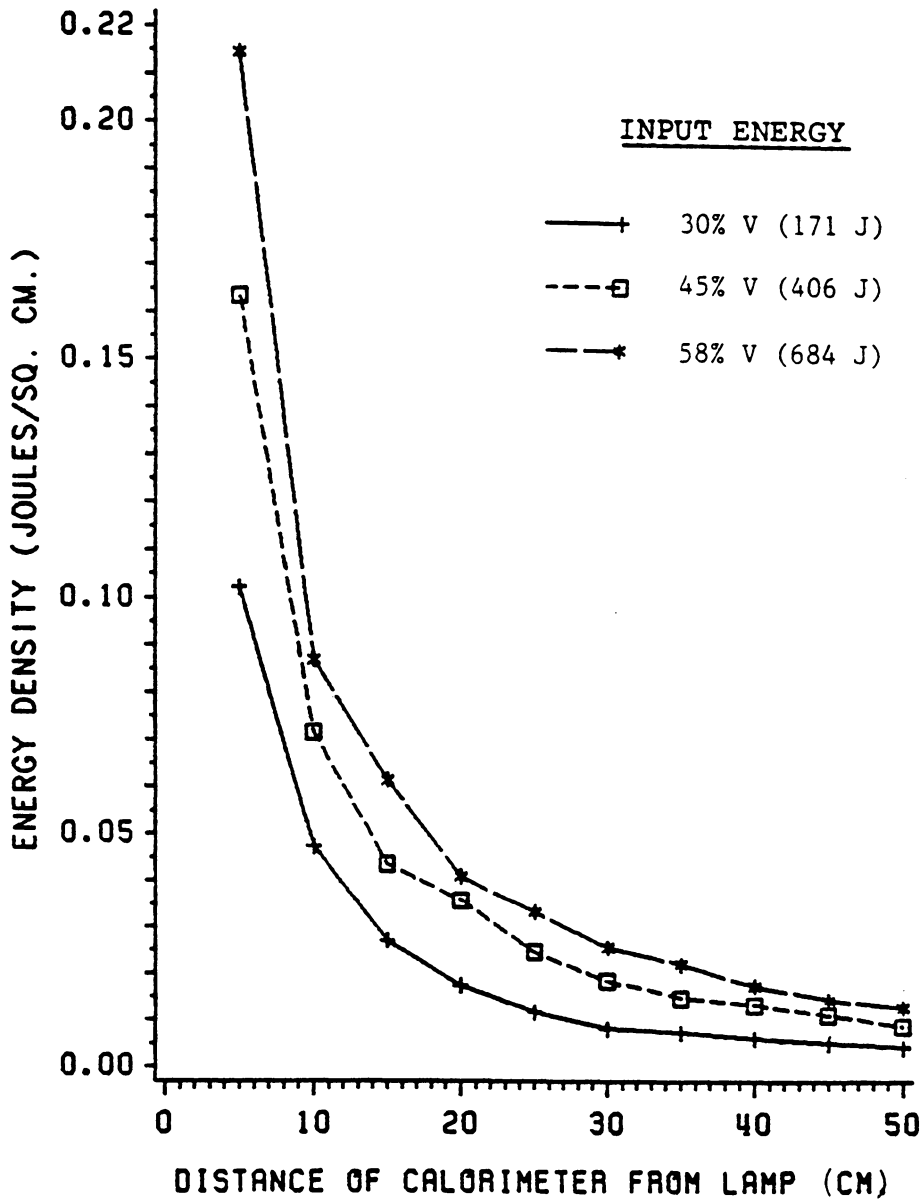

FIG. 1. Energy density scan on the Z-axis

The calorimeter head was located in the center and the measurements were taken at three voltage adjustments using one capacitor.

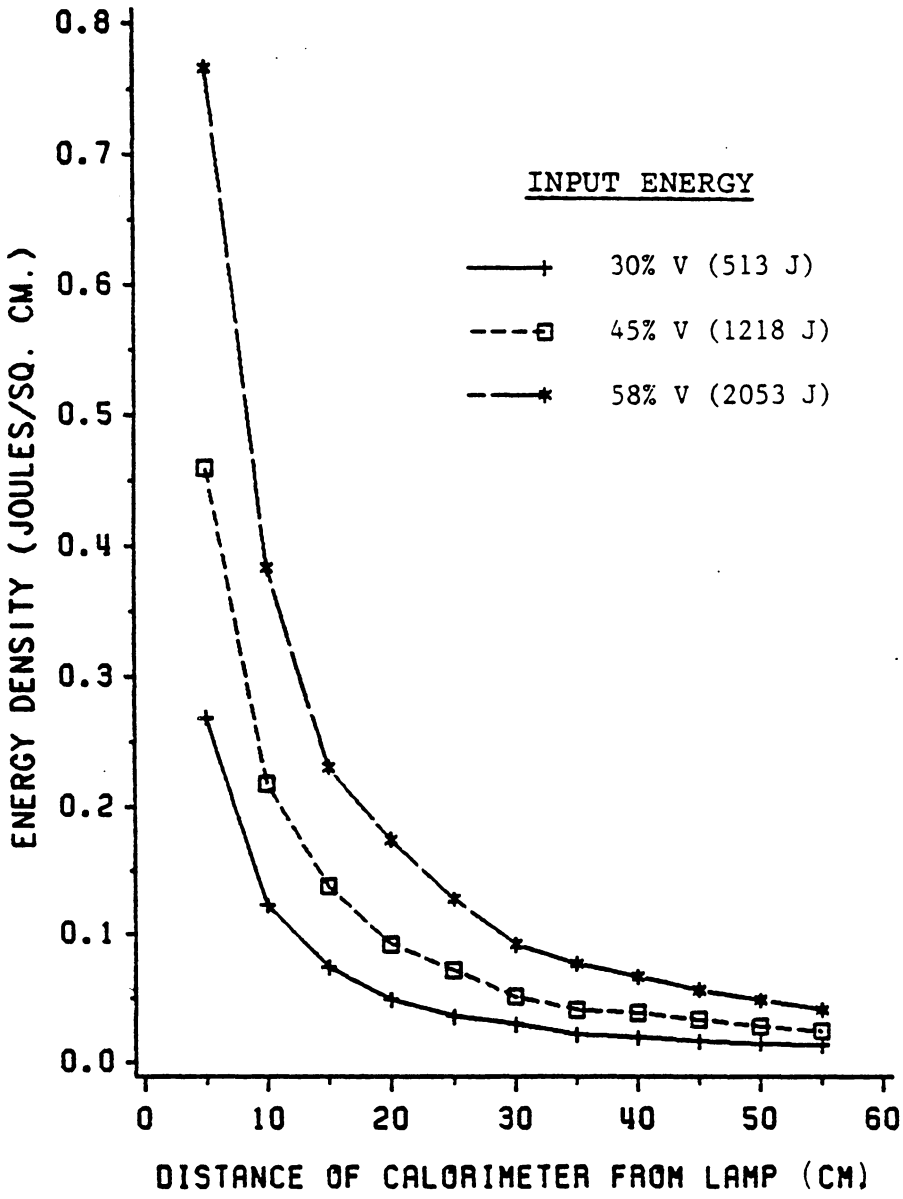

FIG. 2. Energy density scan on the Z-axis

The calorimeter head was located in the center and the measurements were taken at three voltage adjustments using three capacitors.

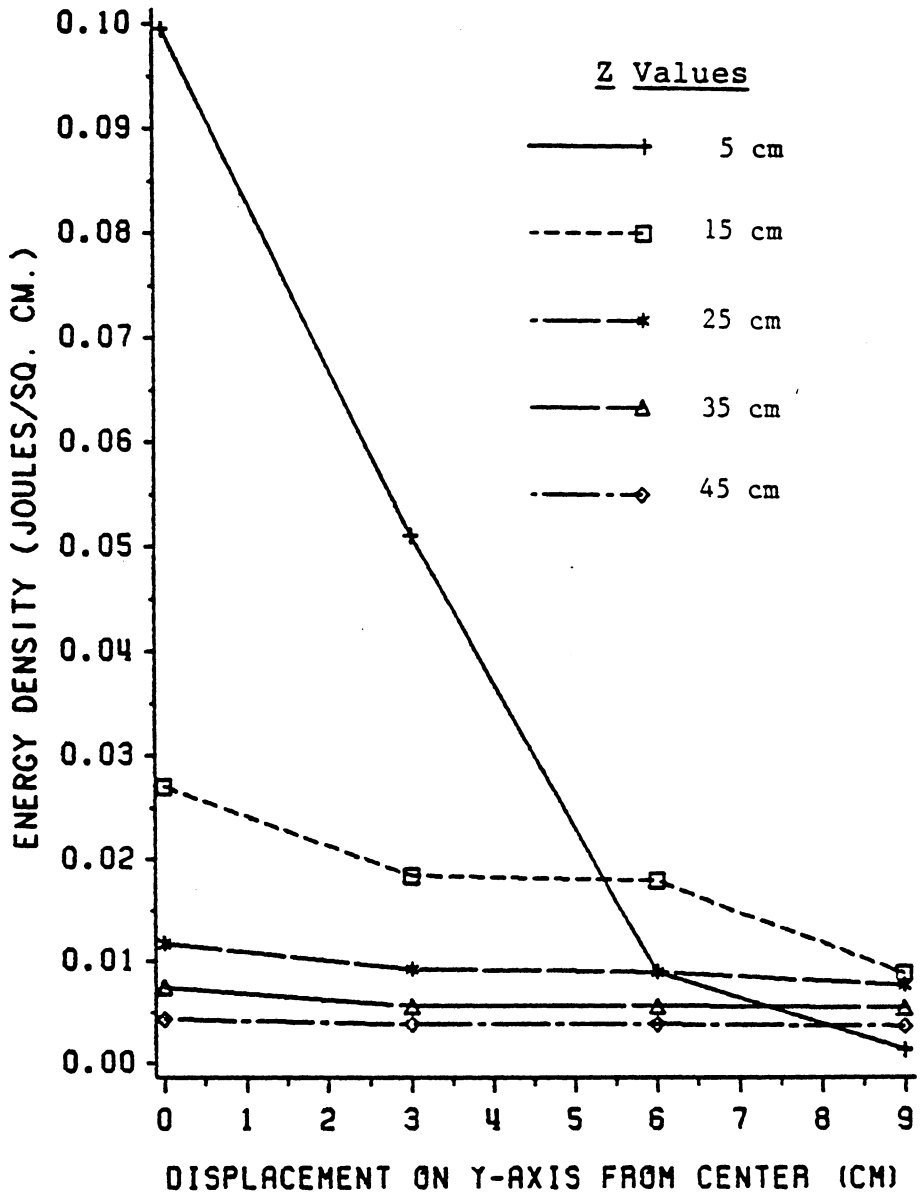

FIG. 3. Energy density scan on the Y-axis

The calorimeter absorptions were measured at an input energy of 171 Joules. The distance between the calorimeter head and Flashlamp varied from 5 cm to 45 cm along the Z-axis.

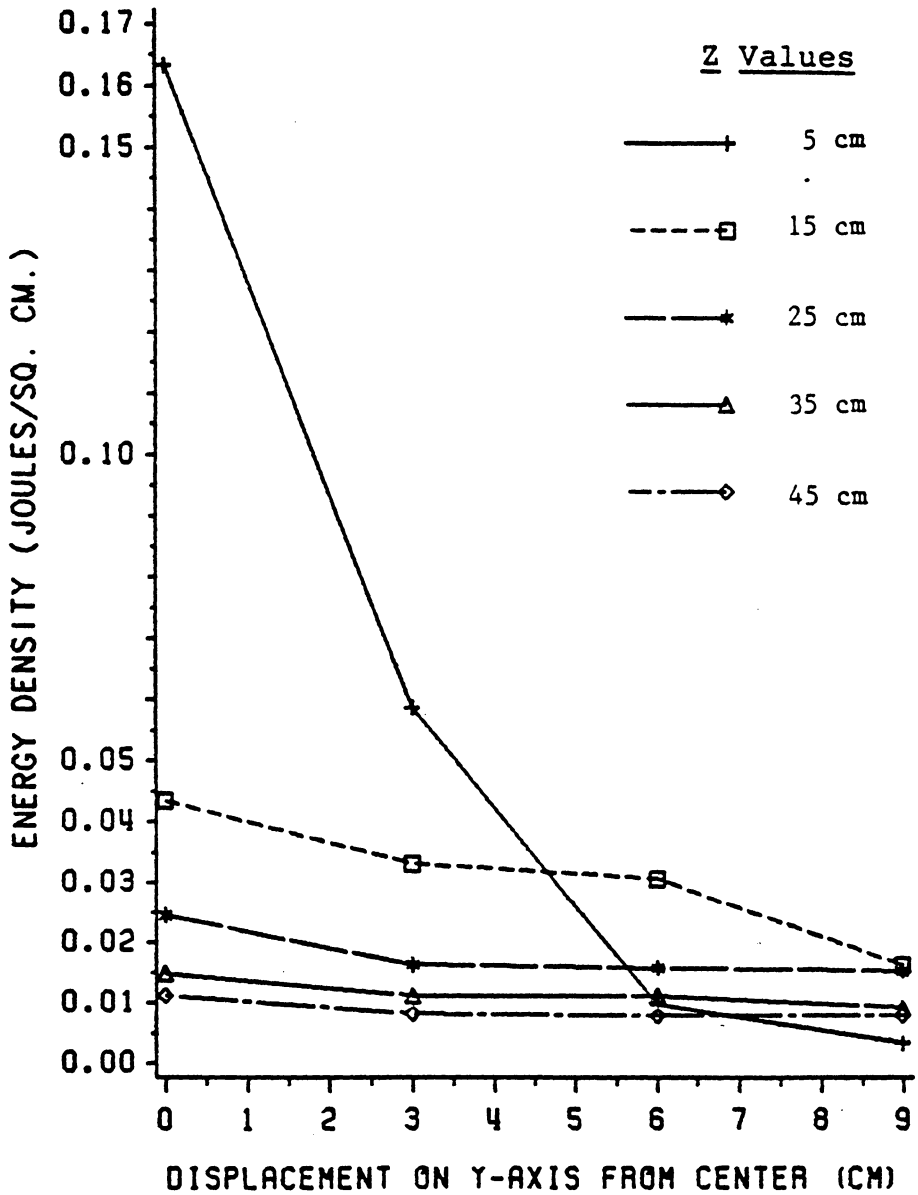

FIG. 4. Energy density scan on the Y-axis

The calorimeter absorptions were measured at an input energy of 406 Joules. The distance between the calorimeter head and Flashlamp varied from 5 cm to 45 cm along the Z-axis.

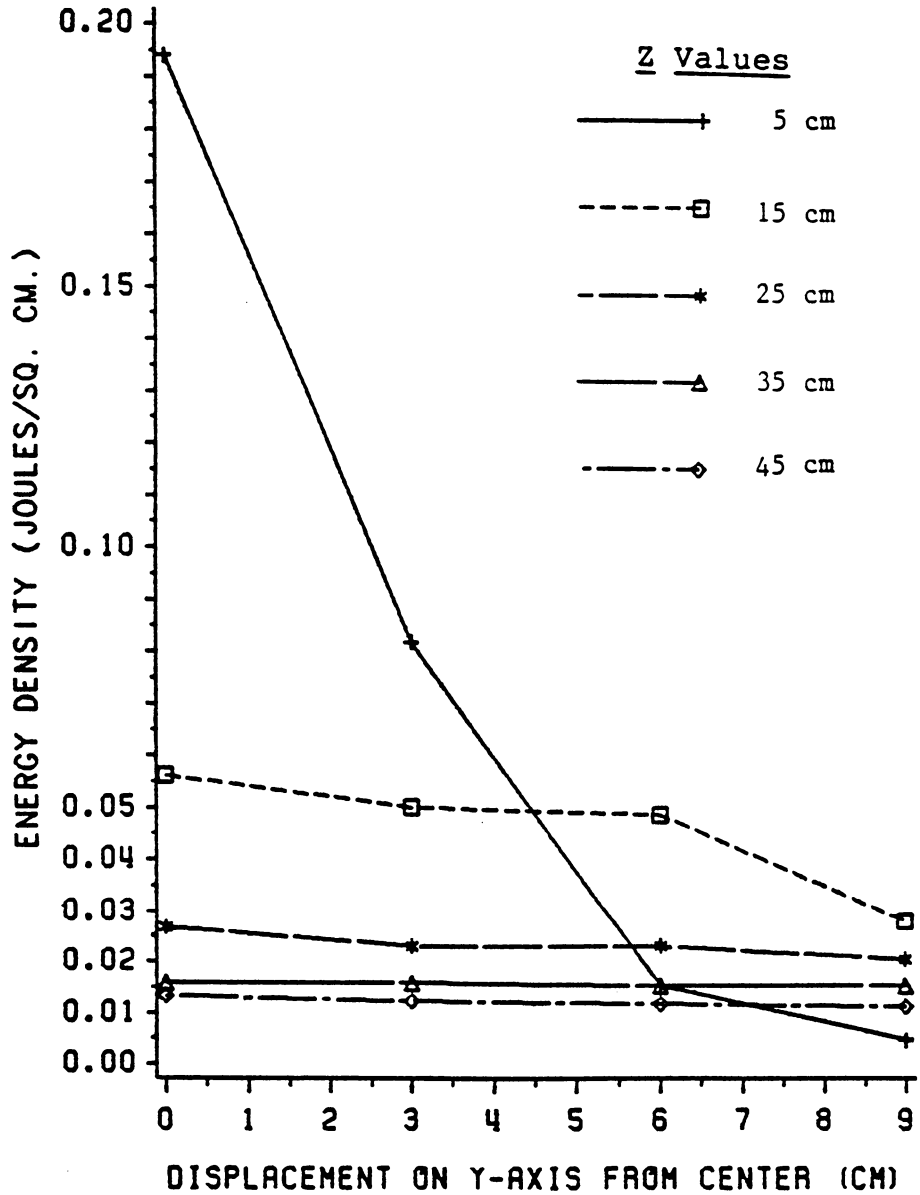

FIG. 5. Energy density scan on the Y-axis

The calorimeter absorptions were measured at an input energy of 684 Joules. The distance between the calorimeter head and Flashlamp varied from 5 cm to 45 cm along the Z-axis.

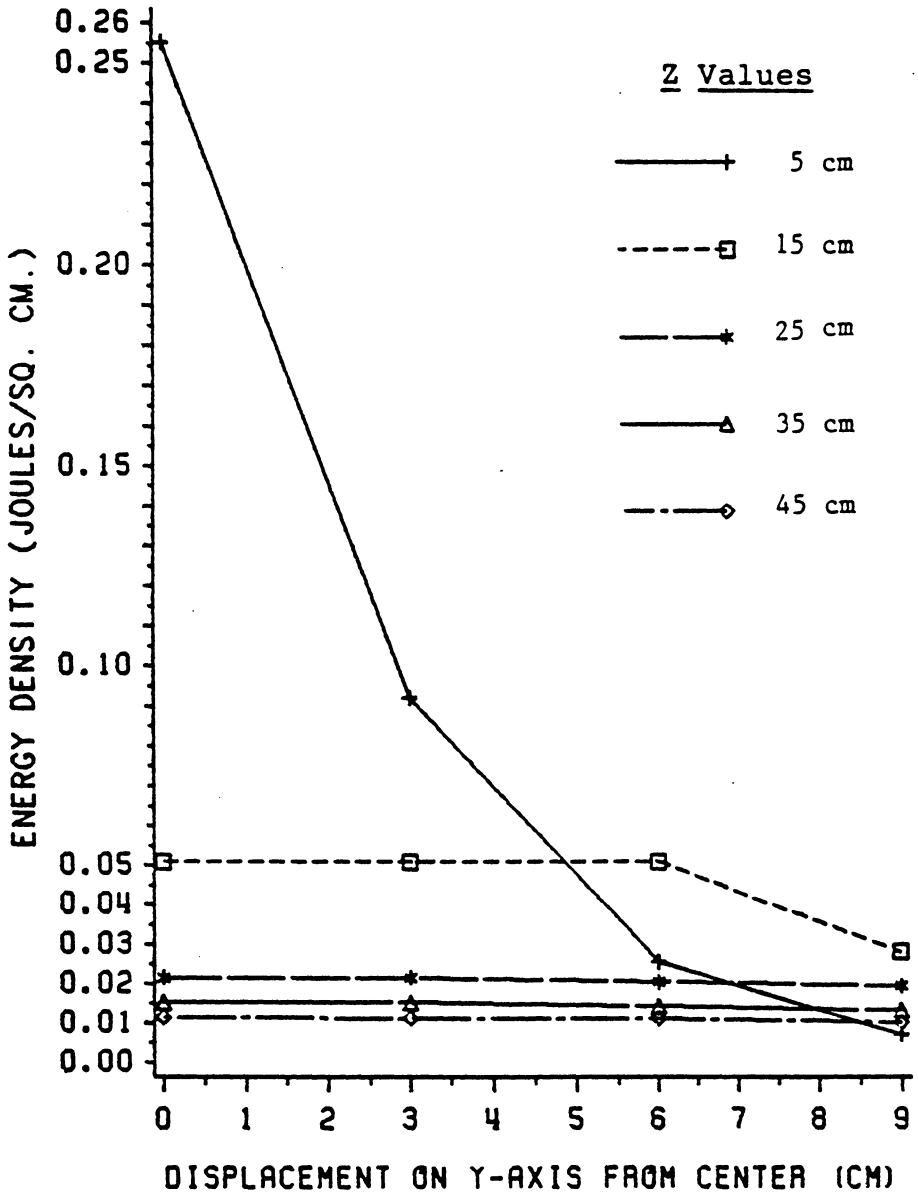

FIG. 6. Energy density scan on the Y-axis

The calorimeter absorptions were measured at an input energy of 513 Joules. The distance between the calorimeter head and Flashlamp varied from 5 cm to 45 cm along the Z-axis.

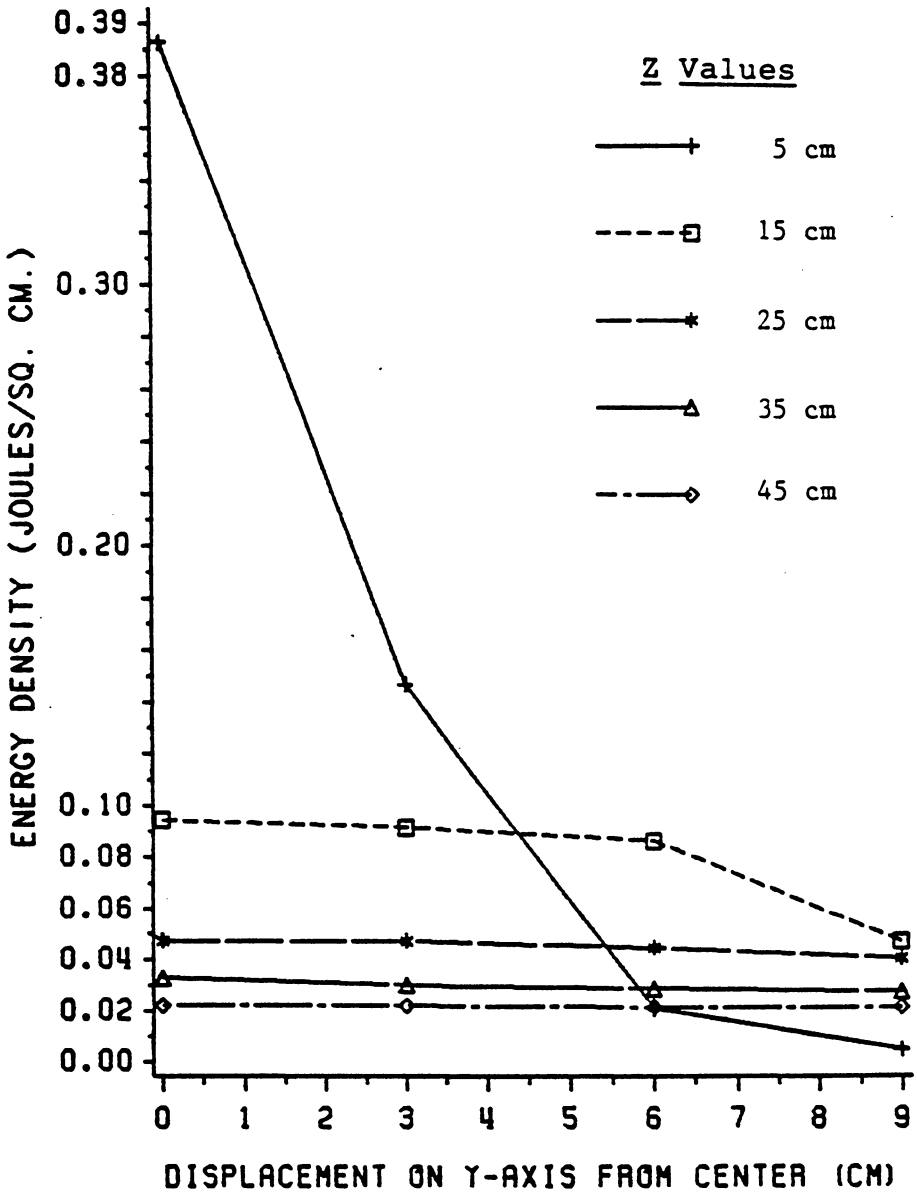

FIG. 7. Energy density scan on the Y-axis

The calorimeter absorptions were measured at an input energy of 1218 Joules. The distance between the calorimeter head and Flashlamp varied from 5 cm to 45 cm along the Z-axis.

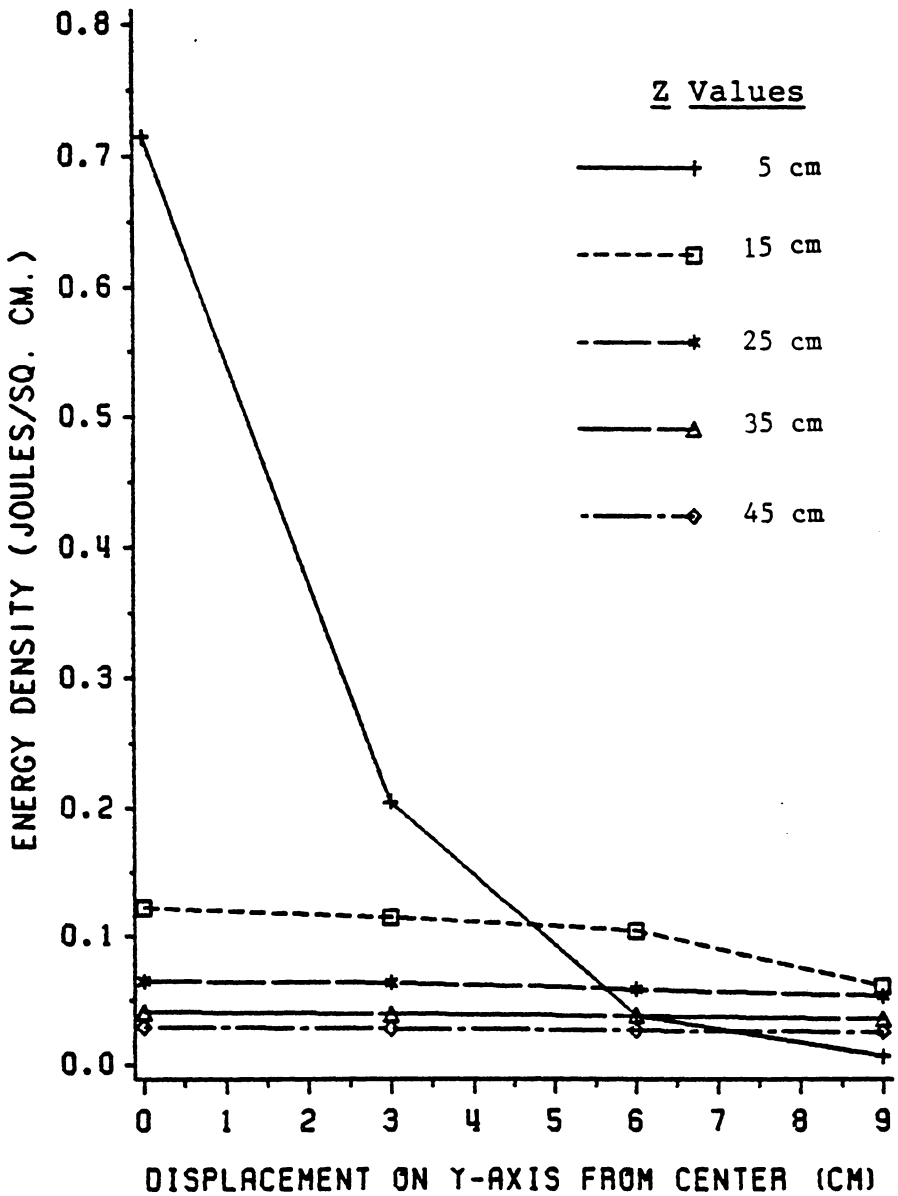

FIG. 8. Energy density scan on the Y-axis

The calorimeter absorptions were measured at an input energy of 2053 Joules. The distance between the calorimeter head and Flashlamp varied from 5 cm to 45 cm along the Z-axis.

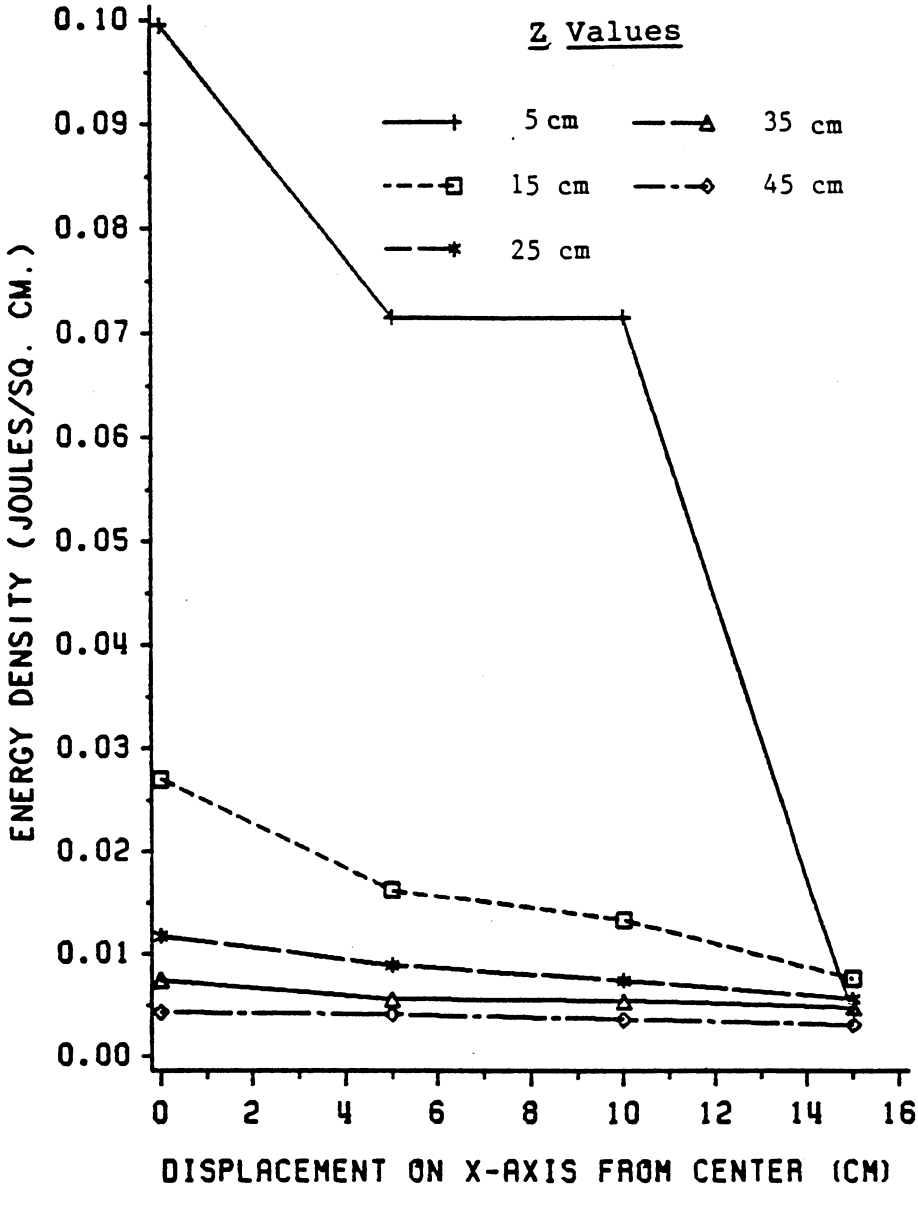

FIG. 9. Energy density scan on the X-axis

The calorimeter absorptions were measured at an input energy of 171 Joules. The distance between the calorimeter head and Flashlamp varied from 5 cm to 45 cm along the Z-axis.

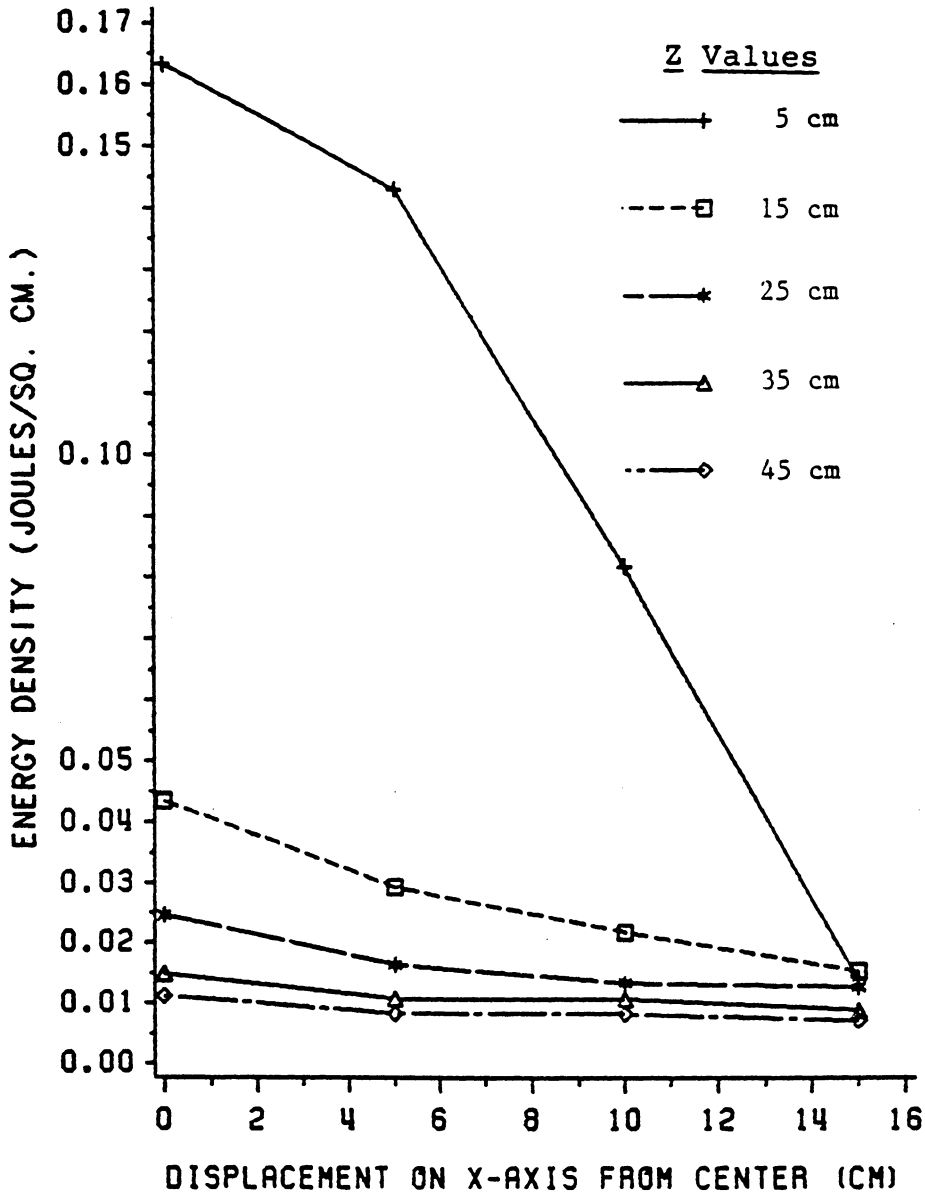

FIG. 10. Energy density scan on the X-axis

The calorimeter absorptions were measured at an input energy of 406 Joules. The distance between the calorimeter head and Flashlamp varied from 5 cm to 45 cm along the Z-axis.

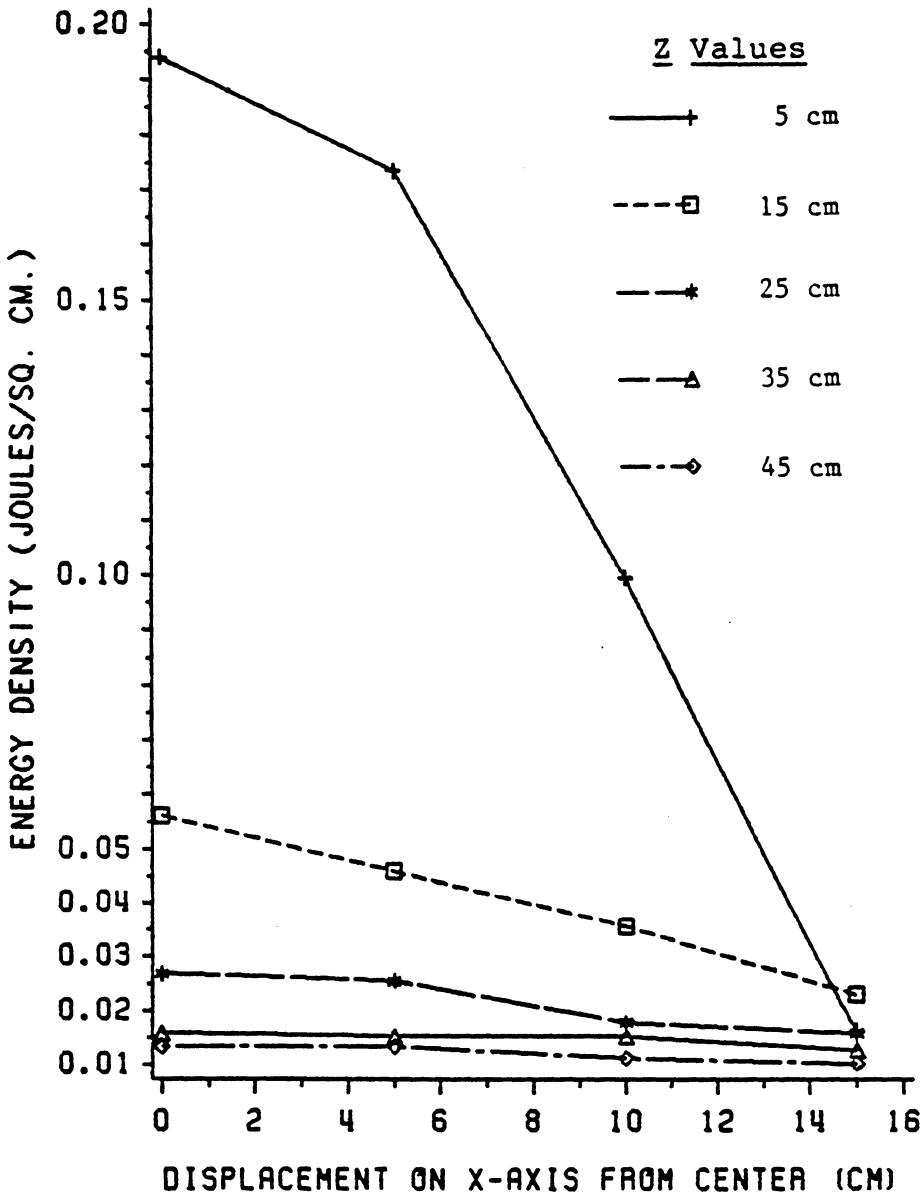

FIG. 11. Energy density scan on the X-axis

The calorimeter absorptions were measured at an input energy of 684 Joules. The distance between the calorimeter head and Flashlamp varied from 5 cm to 45 cm along the Z-axis.

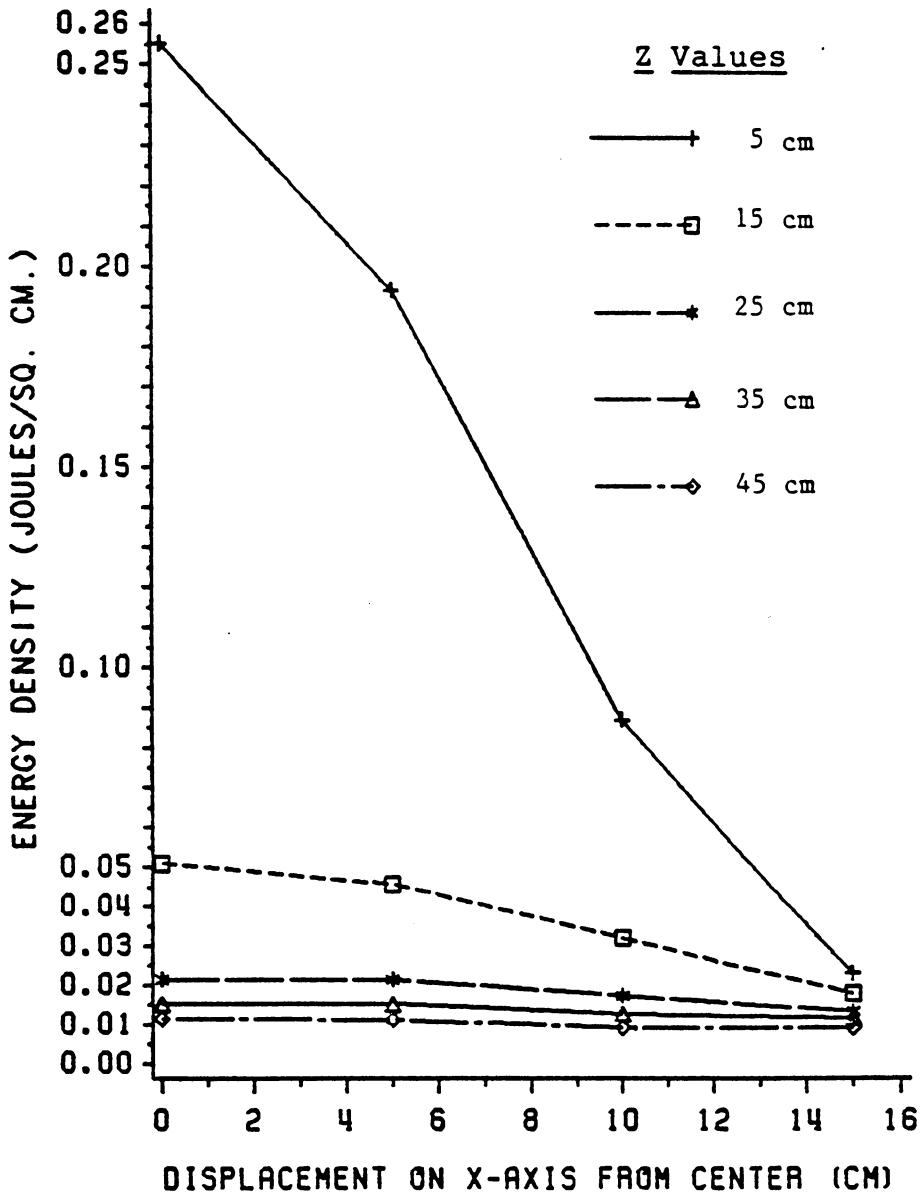

FIG. 12. Energy density scan on the X-axis

The calorimeter absorptions were measured at an input energy of 513 Joules. The distance between the calorimeter head and Flashlamp varied from 5 cm to 45 cm along the Z-axis.

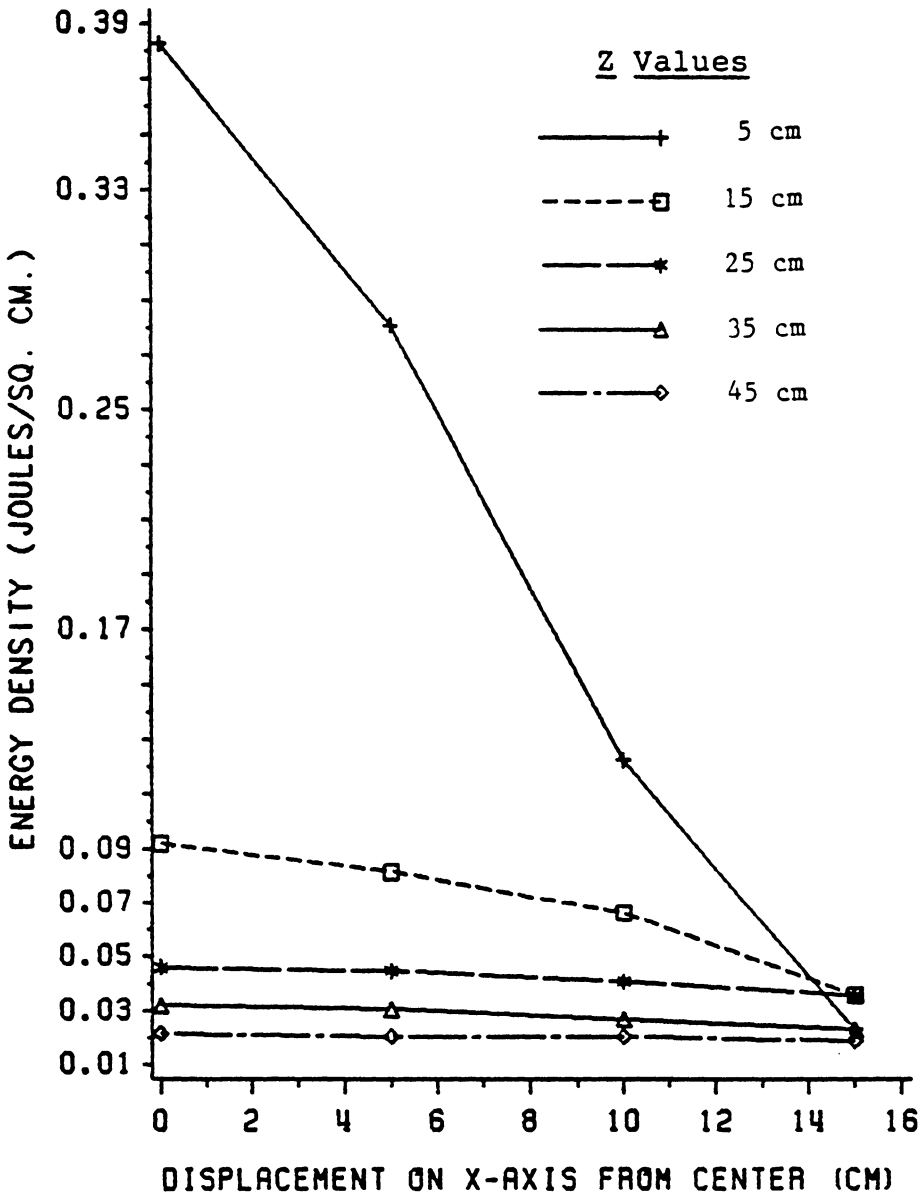

FIG. 13. Energy density scan on the X-axis

The calorimeter absorptions were measured at an input energy of 1218 Joules. The distance between the calorimeter head and Flashlamp varied from 5 cm to 45 cm along the Z-axis.

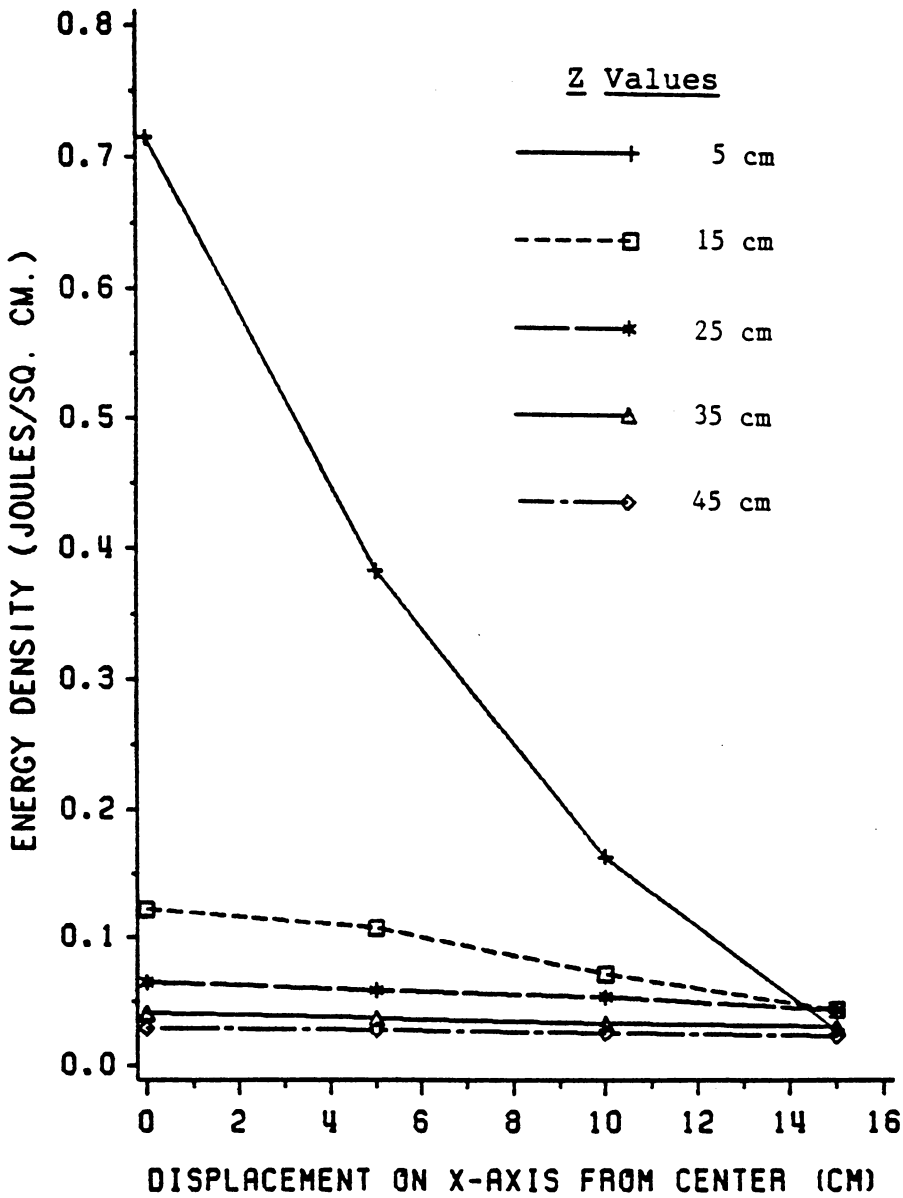

FIG. 14. Energy density scan on the X-axis

The calorimeter absorptions were measured at an input energy of 2053 Joules. The distance between the calorimeter head and Flashlamp varied from 5 cm to 45 cm along the Z-axis.

CHAPTER 4

SUSCEPTIBILITY OF MICROORGANISMS TO HIGH INTENSITY FLASHBLAST LIGHT

4.1 INTRODUCTION

(a) UV inactivation of microorganisms

The most pronounced effect of UV treatment on the vegetative cells and spores of microorganisms is inactivation, that is, a loss of their ability to reproduce. In populations of microorganisms, (like bacteria, yeasts and molds, exposed to increasing fluences of UV light), inactivation is experimentally recognized by a decreasing percentage of survivors capable of producing colony forming units on Nutrient Agar. Many researchers have investigated the susceptibility of different microorganisms to photoinactivation.

Sharp (1939) reported the lethal action of short ultraviolet rays on several common pathogenic bacteria. He determined the relative resistance of several pathogens such as Staphylococcus albus, Escherichia coli and Serratia marcescens to the unfiltered rays of a low-pressure mercury glow lamp of the type used for air sterilization in operating rooms. McCulloch (1945) discovered that gram negative rods were the organisms most easily killed by UV light, Staphylococci and Streptococci requiring about 5-10

times, bacterial spores about 10 times, and mold spores 50 times as much treatment dosage for destruction. At low UV doses, the dose ratio at the same survival for spores and vegetative cells of B. subtilis was about 20-40.

Chang et al., (1985) measured the survival of several species of bacteria and spores as a function of germicidal UV light and found that the doses of UV light necessary for 99.9% inactivation of the cultured vegetative microorganisms were comparable. However, viruses, bacterial spores and amoebic cysts required about 3 to 4 times, 9 times, and 15 times respectively, the dose required for E. coli. Butler et al., (1987) investigated the susceptibility of two enteric pathogens, Campylobacter jejuni and Yersinia enterocolitica together with E. coli to UV treatment at 254 nm and found that C. jejuni and Y. enterocolitica are more sensitive to UV than any of the common pathogens and can be easily inactivated in most commercially available UV reactors.

Shepherd (1962) and Maruyama (1963) reported a decreased conidia viability in Aspergillus niger and Peronospora tabacina when treated with UV light. Sussman and Halvorson (1966) demonstrated that fungal spores with darker pigmentation have greater resistance to UV treatment than those with light colored pigmentation.

(b) Studies on the mechanism of photoinactivation

The lethal effects of sunlight on bacteria were first observed by Downes and Blunt (1877). Gates (1928) obtained action spectra of monochromatic ultraviolet light at different wavelengths and found that the relative effectiveness of bacteria destruction by different wavelengths paralleled the absorption spectrum of nucleic acid. Short wave UV, between 200 and 300 nm, is germicidal with maximum cellular damage at 265 nm (Gates, 1929). The principal mechanism for microorganism death by UV light was suggested to be direct damage to cellular nucleic acids.

Beukers and Berends (1960) discovered UV induced thymine dimers in DNA. Haynes (1964) found that UV acts on cellular DNA primarily by producing linkages between adjacent thymine residues in the same strand. The cyclo-butane type thymine dimers thus formed may prevent DNA from replicating which results in cell death.

Harm (1980) reported that the main types of photoproducts in irradiated DNA are: (a) cyclobutyle type dimers; (b) pyrimidine adducts; (c) the 'Spore Photoproduct formed only under special conditions; (d) pyrimidine hydrates; and (e) DNA-protein crosslinks. Other UV induced lesions of possible biological significance are strand breakage and interstrand crosslinkages.

The spores have a much higher resistance against UV

treatment when compared to the vegetative cells of different microorganism species. Variation in bound water, electrolyte concentration, antigenically altered proteins and many other factors have been suggested to account for the differences in radiation resistance of spores and vegetative cells. Leif and Herbert (1960) found that dipicolinic acid (DPA) and its chelates absorb strongly in the most lethal portion of the UV spectrum and consiquently have been assciated with the resistance of spores to UV treatment. Grecz et al., (1972) studied photoprotection by dipicolinate against inactivation of Bacillus cereus spores with ultraviolet light. Munakata and Rupert (1972) reported the mechanism of UV sensitivity of Bacillus subtilis spores. Their results confirmed that the UV resistance of bacterial spores is determined by the genetically controlled removal of UV induced spore photoproducts from spore DNA.

It is important to know that under certain conditions, such as presence of visible light and buffering solvents, a reversal of damage may occur through photorepair and photorecovery mechanisms. Smith and Hanawalt (1969) has described in detail various mechanisms of repair, e.g. (1) spontaneous decay of photoproducts to the original undamaged state, (2) direct reversal of pyrimidine dimers and (3) enzyme-catalyzed photoreactivation.

4.2 THE BACTERIA SUSCEPTIBILITY TO HIGH INTENSITY FLASHBLAST LIGHT

MATERIALS AND METHODS

An evaluation of bacteria susceptibility to high intensity light with Flashblast was initiated. The objective of this study was to determine the effects of Flashblast capacitor number, distance between the sample and the flash lamp, and Flashblast voltage on four microorganisms.

The microorganisms used in the study were:

(1) E. coli

(2) S. aureus

(3) B. cereus (Vegetative cells)

(4) B. subtilis (Vegetative cells)

The experiments were performed with one and three capacitors for each microorganism. The two voltage adjustments used were: 30% and 45%, corresponding to input energies of 171 J and 406 J at a capacitance of 400 microfarads and 513 J and 1218 J at a capacitance of 1200 microfarads respectively. The distance between the spread plate containing bacteria and the lamp was varied from 60 cm to 10 cm in order to obtain a gradual increase in radiant energy.

Flashblast calibration data along the Z-axis indicated that under these parameters, the surface fluence varied from 0.0043 J/cm^2 to 0.0715 J/cm^2 with one capacitor and from 0.0143 J/cm^2 to 0.2169 J/cm^2 with three capacitors.

An equal number of microorganisms were subjected to

both the 30% and 45% voltage adjustments so that the initial microbial population number would not be a dependent variable while comparing the survival at different input energies with the same capacitance. In all cases, a single flash was applied.

The microorganism cultures were supplied by Dr. Joseph Dunn, Maxwell Laboratories, Inc. Four vegetative bacteria cell suspensions were obtained by placing 10 ml of Difco Trypticase Soy Broth solution into test tubes 48 hours prior to plating. Serial dilutions were made in phosphate buffer (pH 7.0). A dilution that gave a countable number of microbial populations (usually 100 to 300) in a 0.1 ml aliquot was selected for the spread plates. A 0.1 ml sample of this dilution was pipetted onto the spread plates (Tryptic Soy Agar, Difco) and uniformly spread with a glass hockey stick on the entire surface of the solidified agar. Four replicates of each microorganism were retained as controls to determine the initial microbial population number. The other plates with microorganisms were placed in the center of the X and Y-axis under the flashlamp and exposed to different illumination conditions by varying Flashblast parameters of capacitance, voltage and distance between the Petri plate and the lamphead. Both the control and treated plates were then incubated at 37^{o}C for 24 - 48 hours. The number of survivors was determined for each microorganism and treatment condition.

RESULTS AND DISCUSSION

Figures 1-4 show the survival curves of four microorganisms for Flashblast treatment at different input energies. The surviving fraction (N/No) is plotted against absorbed energy (fluence) on a semilog axes. The logarithm of survival number (N) of each microorganism is plotted against the fluence on a linear scale in Figures 1-4 of the Appendix C). Table 3 of Appendix A contains LD_{90} values (fluence required to obtain a one log cycle reduction in the initial population) of each microorganism. The reduction in microbial population was observed at all input energies. A complete log cycle reduction was not possible even at the nearest distance when using one capacitor and the 30% voltage adjustment (input energy 171 J). The surviving fraction decreased sharply at higher input energies. The slopes of the curves representing the treatment with one capacitor (input energies of 171 J and 406 J) had higher values when compared to the curves with three capacitors (input energies of 513 J and 1218 J). This suggests that the treatment with one capacitor requires shorter distances between the lamp and the Petri plate (hence, a higher fluence) than the distances required for three capacitors in order to achieve an equivalent lethality.

Input energies at three capacitors yielded a treatment spectrum with a higher proportion of ultraviolet light which is responsible for inactivation or destruction of

microorganisms. In most cases, a complete inactivation was obtained at 1218 J when the distance between the lamp and the Petri plate was 30 cm. These data show promising results for the feasibility of Flashblast treatment to destroy or inactivate different microorganisms.

4.3 SUSCEPTIBILITY OF BACILLUS AND ASPERGILLUS SPORES TO HIGH INTENSITY FLASHBLAST LIGHT

MATERIALS AND METHODS

The susceptibility of B. cereus, B. subtilis and A. niger spores to high intensity Flashblast light was evaluated. Preliminary experiments with one capacitor and 58% (full) voltage adjustment produced a limited reduction in the initial spore population. Hence, for this study, the Flashblast parameters were adjusted to provide higher input energies. The experiments were performed with three capacitors and the following three voltage adjustments: 30%; 45%; and 58% (full) which corresponded to input energies of 513 J, 1218 J and 2053 J respectively. The distance between the spread plate containing the spores and the lamp was progressively reduced from 60 cm to 10 cm in order to vary the light fluence on the Petri plate surface.

In order to obtain Bacilli spores, the vegetative cells were grown in TYG broth and surface plated on TYG agar plates. The plates were evaluated for the presence of spores by using a wet mount sample preparation with a phase

contrast microscope after 24, 48, and 72 hours incubation at 30°C. After 72 hours, approximately 90% of the culture were found to be spores. The plates were then refrigerated for 24 - 48 hours to induce further sporulation and prevent germination.

The spores were harvested from the plates using cold sterile deionized distilled water at 4°C and repeatedly centrifuged (10,000 g, 10 min.) to eliminate vegetative cells. A suspension of a suitable concentration of the spores was prepared in sterile distilled water and stored in a freezer. The spores were activated by heating at 80°C for 15 minutes immediately prior to plating.

A suspension containing a countable spore number was spread on Triptic Soy Agar plates and exposed to different fluences. Three replicates per treatment and four controls were prepared. The control and treated plates were incubated at 37°C for 18 - 36 hours and the colony forming units were counted on each Petri plate.

Aspergillus niger spores were obtained by growing the culture on a Difco Yeast Morphology Agar plate at room temperature (25°C) for 5 - 6 days. A sterile 0.1% Tergitol 7 Anionic solution was used to harvest the spores. The Tergitol/spore suspension thus obtained was subsequently serially diluted. A suitable dilution was used for the preparation of spread plates so that a countable number of colonies could be obtained on the control plates.

A. niger spores were exposed to Flashblast light on the surface of Yeast Morphology Agar plates containing 0.05% Rose Bengal to inhibit the colony spreading. The control and treated plates were incubated in the dark at room temperature for 3 - 5 days and the number of survivors in the treated plates was compared with the control plates for each treatment.

RESULTS AND DISCUSSION

Figures 5-7 show survival curves of three spore species at input energies of 513 J, 1218 J and 2053 J respectively. The spores of B. cereus and B. subtilis behaved similarly in terms of susceptibility to Flashblast treatment under identical experimental conditions. A differential reduction in the initial populations of the spores was observed at all three input energies when the distance from the lamp head was progressively reduced from 60 cm to 10 cm.

A 30% voltage treatment (input energy 513 J) could not achieve a complete spore log cycle reduction even at the lowest used distance from the lamp head. At the input energy of 1218 J with a 45% voltage adjustment, Bacilli spores exhibited a complete log cycle reduction at a distance of 10 cm from the lamp head when the surface fluence was 0.2169 J/cm^2. However a complete inactivation of the initial population was not attained at this fluence. The 58% (full) voltage adjustment (input energy 2053 J) was

found to be most efficient among the three input energy adjustments. A complete inactivation of the initial population was obtained at a distance of 10 cm from the lamp head with the 58% (full) voltage adjustment. Consequently, a very high fluence was required to obtain a one log cycle reduction in the initial Bacilli spore population using a single flash. It is important to note that under similar conditions of maximum intensity, experiments with the vegetative cells of B. cereus and B. subtilis exhibited a significantly higher susceptibility to Flashblast treatment.

The susceptibilities of Bacilli vegetative cells and the spores to Flashblast treatment at input energies of 513 J and 1218 J are compared in Figures 8 and 9 respectively. In the case of Bacilli vegetative cells, the slopes of the survival curves are significantly higher than those for the spores. The Bacilli spores show a greater resistance to Flashblast treatment as compared to the vegetative cells of the same bacteria at input energies of 513 J and 1218 J (compare LD_{90} values in Table 3 of Appendix A). A treatment with an input energy of 2053 J was required to destroy or inactivate Bacilli spores.

In the case of A. niger spores, treatment at an input energy of 513 J did not produce any reduction in the number of survivors even at the closest possible distance from the lamp head. An input energy of 1218 J inactivated about half the initial mold spore population at the shortest distance

of 10 cm. However a greater destruction was obtained only when the highest input energy of 2053 J was used under similar conditions. At this input energy, an approximate one log cycle reduction was obtained at a distance of 10 cm from the lamp head when the surface fluence was 0.38 J/cm^2. This indicated that the full capacity of the Flashblast apparatus was required to obtain a one log cycle reduction of the initial A. niger spore populations using one flash. The LD_{90} values (Table 3, Appendix A) indicate that the resistance of A. niger spores to Flashblast treatment is at least 3 to 4 times higher as compared to Bacilli spores.

4.4 MICRODROP INACTIVATION OF THE VEGETATIVE CELLS AND SPORES OF MICROORGANISMS WITH FLASHBLAST LIGHT

MATERIALS AND METHODS

Although the spread plate technique successfully demonstrated a reduction in microbial populations at input energies of 513 J and 1218 J with variable distances between the lamp head and Petri plates, the procedure could not be used to evaluate the lethality of an initial population with an excessive number of microorganisms. In order to subject the entire surface of each Petri plate to treatment, the distance between the Petri plate and the flash lamp could not be reduced to less than 10 cm.

These limitations were overcome to some extent by performing similar experiments with a modified microdrop

plating method. This technique involved plating microdrops containing several logarithmic microbial dilutions within a defined area paralleling the flashlamp axis (see Figure 1 in Appendix G). Treatment fluences were varied in a similar mannner as the spread plate experiments by changing the voltage percentages and the distances from the lamphead.

The objectives of this study were:

1. To determine the ability of Flashblast treatment to destroy or inactivate the microorganisms contained within a confined area.

2. To estimate the number of log cycle reductions by varying both the treatment fluence and the initial population of each microorganism.

The microorganisms used in the study were:

(1) Escherichia coli

(2) Staphylococcus aureus

(3) Bacillus cereus (Vegetative cells)

(4) Bacillus subtilis (Vegetative cells)

(5) Bacillus cereus (Spores)

(6) Bacillus subtilis (Spores)

(7) Aspergillus niger (Spores)

Suspensions of all microorganism species were prepared in a manner similar to the spread plate method described in the previous study. A suspension of each microorganism was adjusted to an approximate concentration of 10^8 organisms per ml so that a comparable evaluation of microorganism

inactivation or destruction could be obtained. The suspensions were then serially diluted in a sterile phosphate buffer (pH 7.0) solution to obtain a 6 to 7 logarithmic dilution. Twenty-five microliters of each vegetative cell and spore suspension were pipetted onto an area bounded by two lines paralleling the lamp axis.

For A. niger spores, the treatments and plating procedures were identical to those used for bacteria except that the serial dilutions were made in a Tergitol solution. Yeast Morphology Agar plates containing 0.05% Rose Bengal were used to inhibit the spread of colonies and to facilitate counting of the colony forming units. Each microdrop was carefully pipetted on the solidified agar such that it occupied approximately 1 cm^2 of surface area.

Three replicates per treatment and four controls were employed. The control and treated plates were incubated at $37^{\circ}C$ for 18 - 36 hours and colony forming units were counted within each microdrop on the Petri plate. The experiments were performed with three capacitors for each microorganism species. The three voltage adjustments used were: 30%, 45%, and 58% (full) and corresponded to input energies of 513 J, 1218 J and 2053 J respectively. The distance between the Petri plates containing the microdrops and the flashlamp was progressively reduced from 55 cm to 5 cm for all voltage adjustments. In all studies, one flash was applied.

RESULTS AND DISCUSSION

The results are presented in terms of microorganism survival (Tables 1-7), and number of log cycle reduction (Tables A-G) with different initial populations and various voltage/distance adjustments. The destruction or inactivation pattern of all microorganisms is in accordance with the results previously obtained using the spread plate technique. A lower distance from the lamphead and a higher voltage treatment yielded a greater lethality.

The vegetative cells of all four bacteria exhibited a similar susceptibility to Flashblast treatment under identical distances and voltage adjustment conditions. At a 30% voltage treatment (Input energy 513 J), complete inactivation was obtained only at a distance of 10 cm or lower, provided that the initial populations in the microdrops were in the order of 10^4 or lower. The voltage adjustment at 45% (input energy 1218 J) was found to be more efficient than the 30% adjustment (input energy 513 J). It was possible to inactivate initial microdrop populations of 10^6 at an input energy of 1218 J when the distance between the lamphead and the Petri plate was reduced to the minimum (5 cm), corresponding to a surface energy density of 0.4594 J/cm^2. The input energy of 2053 J provided the greatest inactivation for all microorganisms among the three input energy adjustments in terms of the number of log cycles destroyed or inactivated at greater distances.

The spores of B. cereus and B. subtilis exhibited a significantly higher resistance to Flashblast treatment as compared to their vegetative cells. The complete inactivation of spores was achieved only at the minimum distance (5 cm) between the lamp and the Petri plate eventhough lower initial populations were used than those employed for the vegetative cells under identical experimental conditions. A complete inactivation of the spores could not be achieved with the highest fluence used when the initial population in the microdrop was 10^6 or greater. Under similar conditions, the vegetative cells showed a complete inactivation. In case of the bacterial spores, a complete inactivation was achieved only at the maximum fluence used when the initial microdrop population was on the order of 10^4 or lower.

Aspergillus niger spores showed a slightly greater resistance to Flashblast treatment than the bacterial spores. A 30% voltage adjustment (input energy 513 J) was not found to be germicidal. The 45% voltage treatment (input energy 1218 J) showed some lethality at lower distances with a lower initial population. Complete inactivations were achieved only at the maximum fluence used (58% Voltage and 5 cm distance) when the the initial populations were on the order of 10^4 or lower. This suggests that an input energy of 2503 J and surface energy density of 0.76 J per square centimeter is required to

destroy or inactivate A. niger spores under these conditions when one flash is applied.

The microdrop plating technique enabled the use of higher initial microbial populations. Therefore, it provided an observation of an inactivation greater than a one log cycle at different fluences. A modification of this method as adapted in these studies required plating the microorganisms along a narrow distance under the lamp so that the treatment fluence along X-axis would be constant.

Although this method provides a convenient assay of the susceptibility of microorganisms to Flashblast light, it has several limitations. Care has to be exercised while interpreting microdrop data.

The following points should betaken into consideration while making any inferences from the results obtained by this technique:

(1) The more concentrated spots have some microorganisms overlapping each other creating a situation which provides a protective shield to the microorganisms on the bottom. Consequently, it is easier to destroy or inactivate all the microorganisms in a more dilute location than in a more concentrated location.

(2) The non-uniform appearance of the colonies formed by the surviving microorganisms after the treatment poses a problem of accuracy in counting the number of survivors. Due to a restricted area of approximately 1 sq. cm, some of

the colonies group together to form a large colony while some remain in a characteristic size. An uneven absorption of the microdrop may lead to an increased concentration of the microorganisms in certain areas of the spot which in turn may show a higher resistance to the treatment.

(3) It is not possible to count a number of colony forming units higher than 90 in a microdrop and numbers higher than 50 are counted with less accuracy. This limitation restricts the determination of the intermediate log cycle reductions when higher initial populations are used. At lower fluences, an inactivation occurs which can not be evaluated because the survivors in the microdrop are too numerous to count. However, a gradual decrease in the survivors was visually observed. This indicates the ability of Flashblast light to affect higher initial populations of the microorganisms.

(4) It is very important to interpret these results in terms of the inactivation or destruction of a particular population of microorganisms per unit area. The same microdrop will show a greater susceptibility to Flashblast treatment if spread over a larger area.

(5) A multiple flash treatment under identical conditions may provide a greater destruction or inactivation of Bacillus and Aspergillus spores.

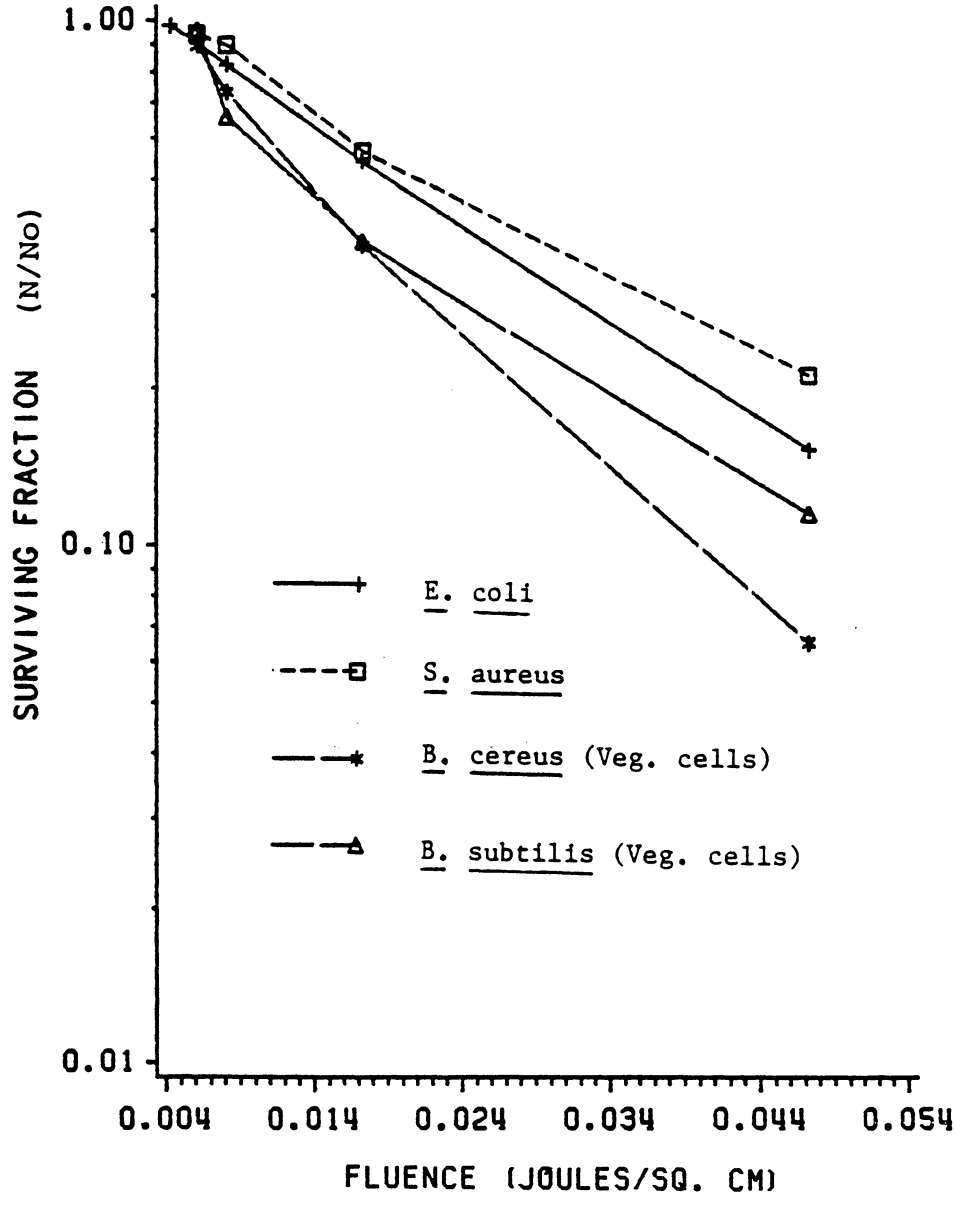

FIG. 1

Survival of four microorganisms at a Flashblast input energy of 171 Joules.

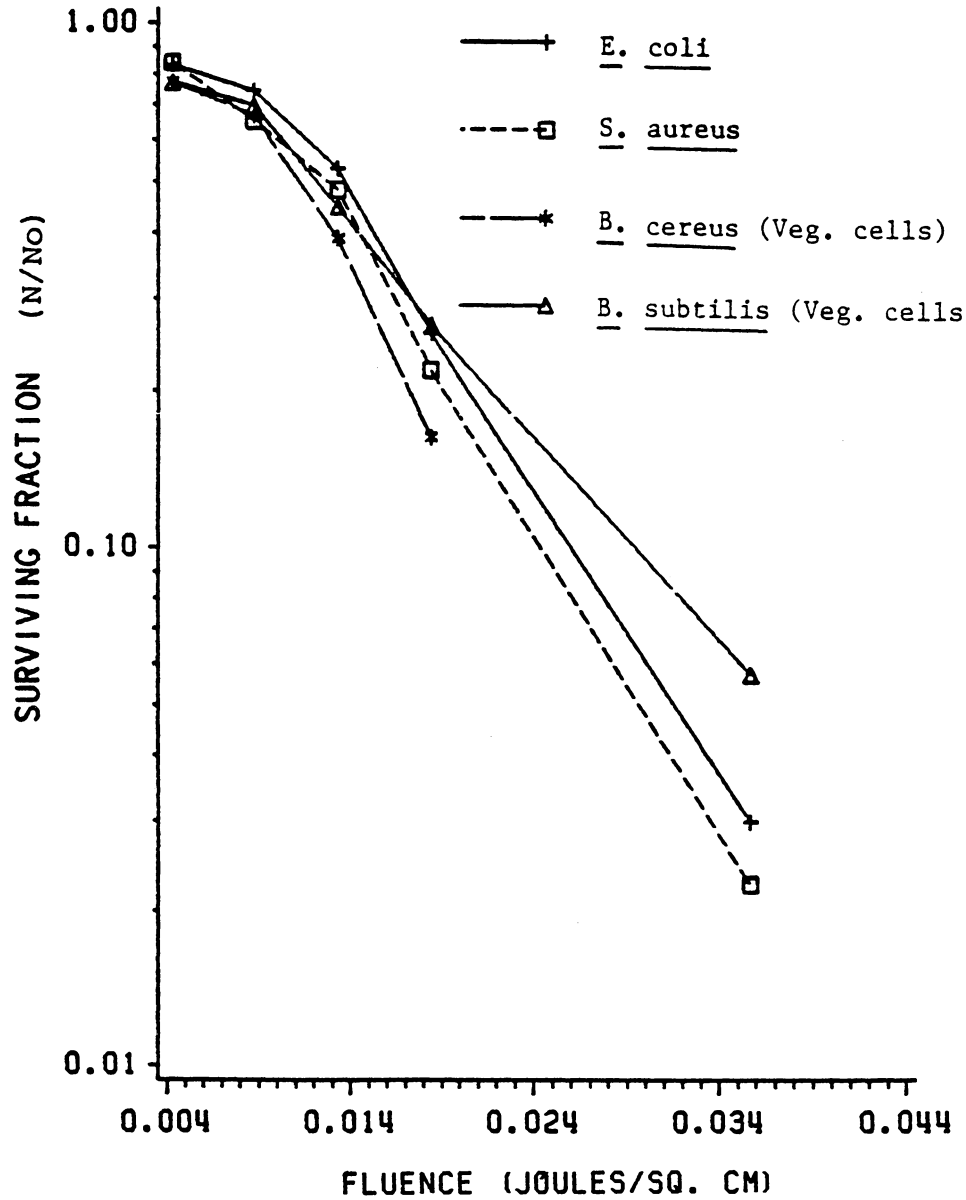

FIG. 2

Survival of four microorganisms at a Flashblast input energy of 406 Joules.

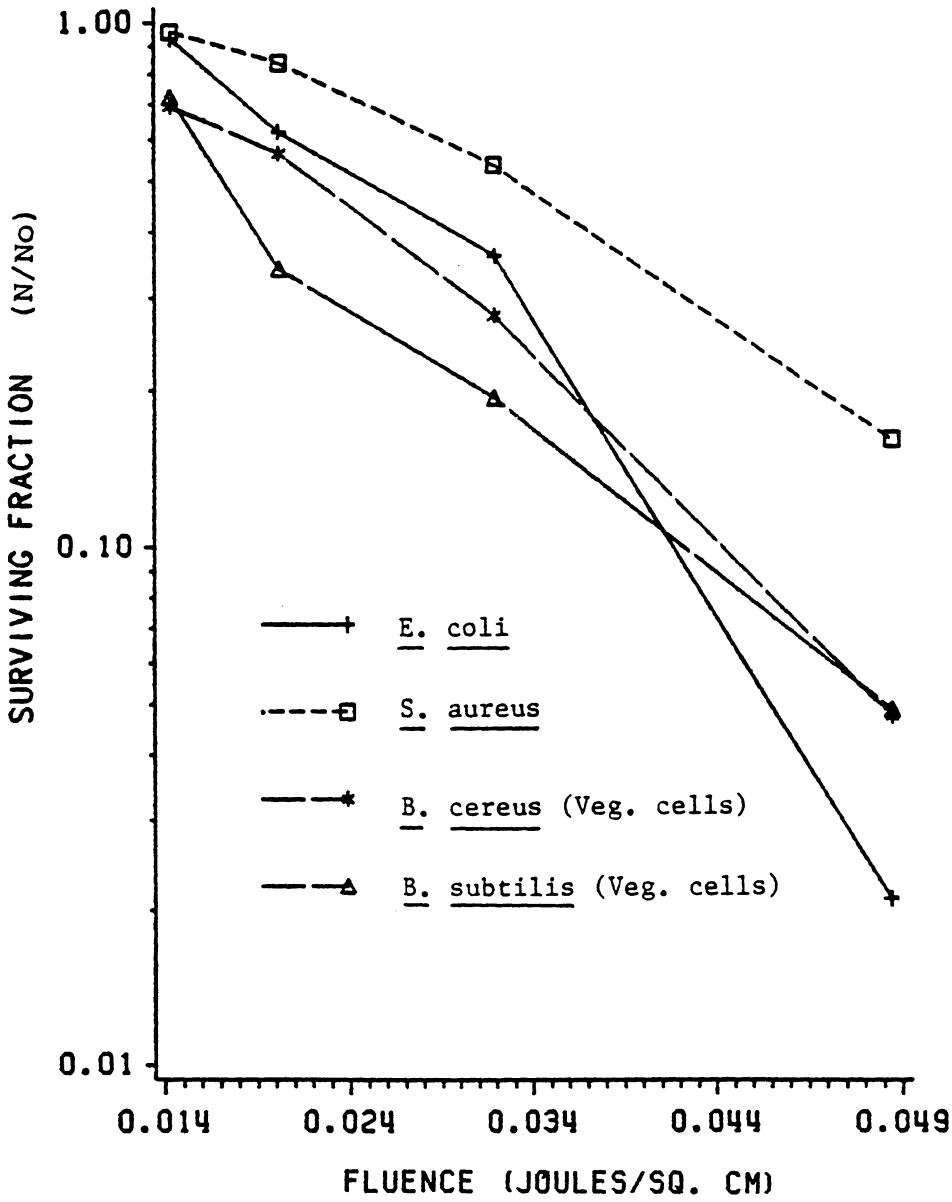

FIG. 3

Survival of four microorganisms at a Flashblast input energy of 513 Joules.

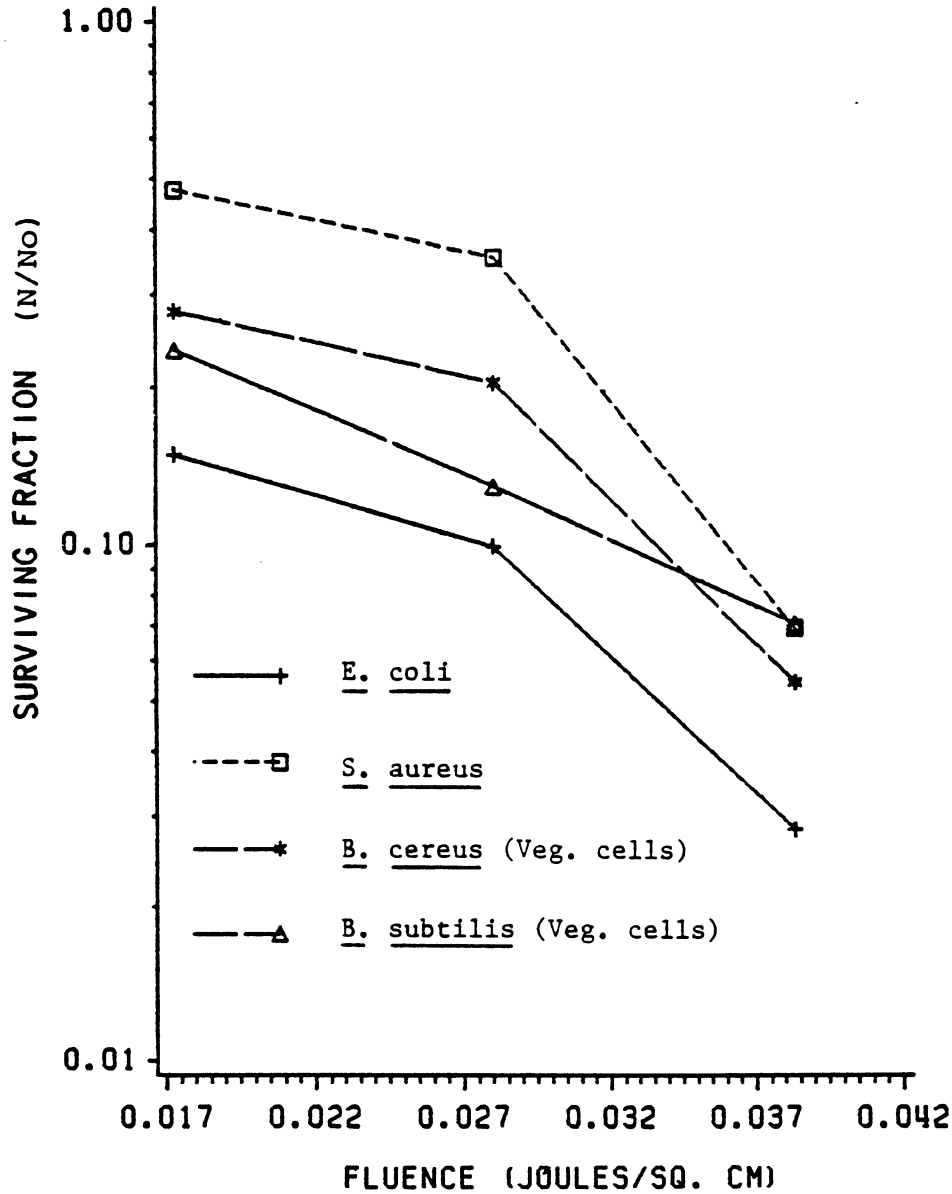

FIG. 4

Survival of four microorganisms at a Flashblast input energy of 1218 Joules.

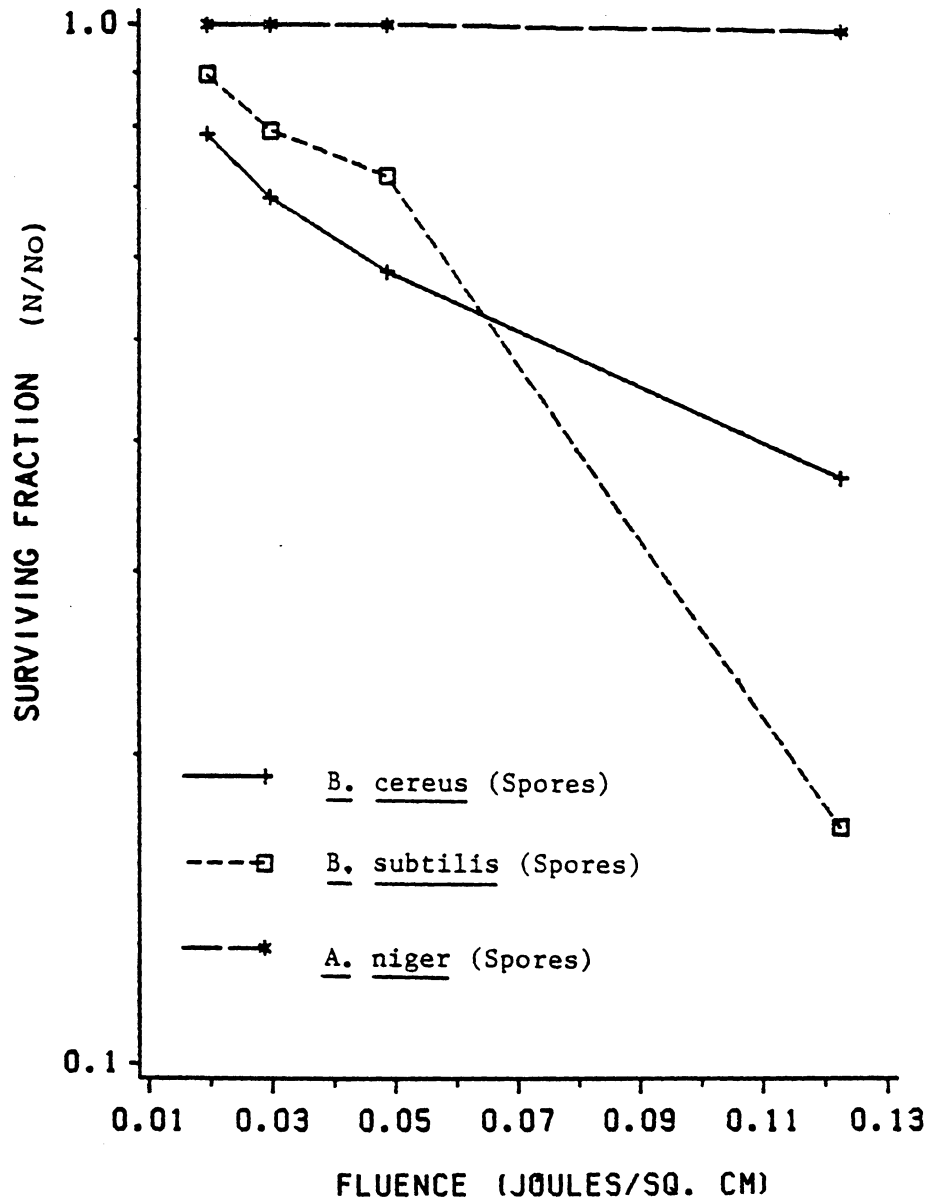

FIG. 5

Survival of three spore species at a Flashblast input energy of 513 Joules.

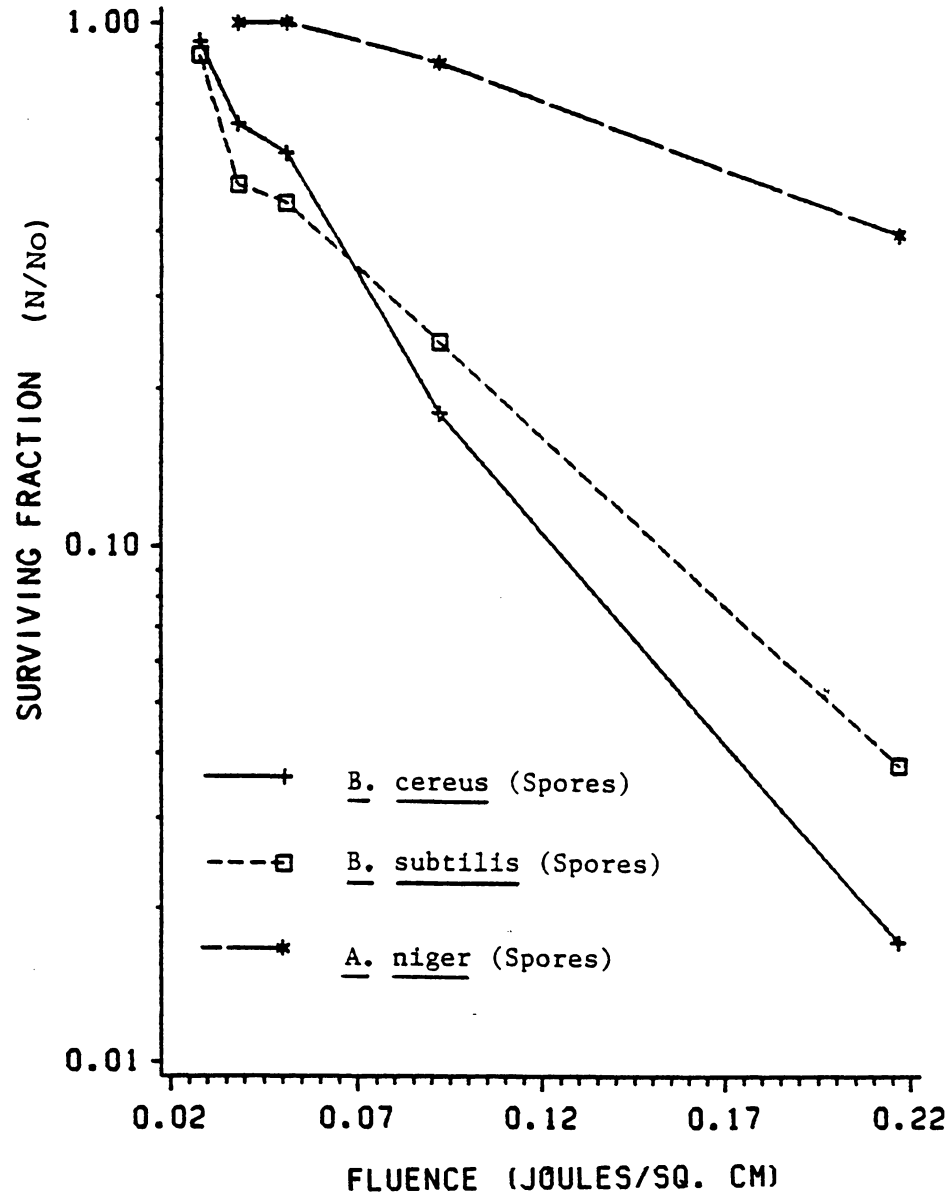

FIG. 6

Survival of three spore species at a Flashblast input energy of 1218 Joules.

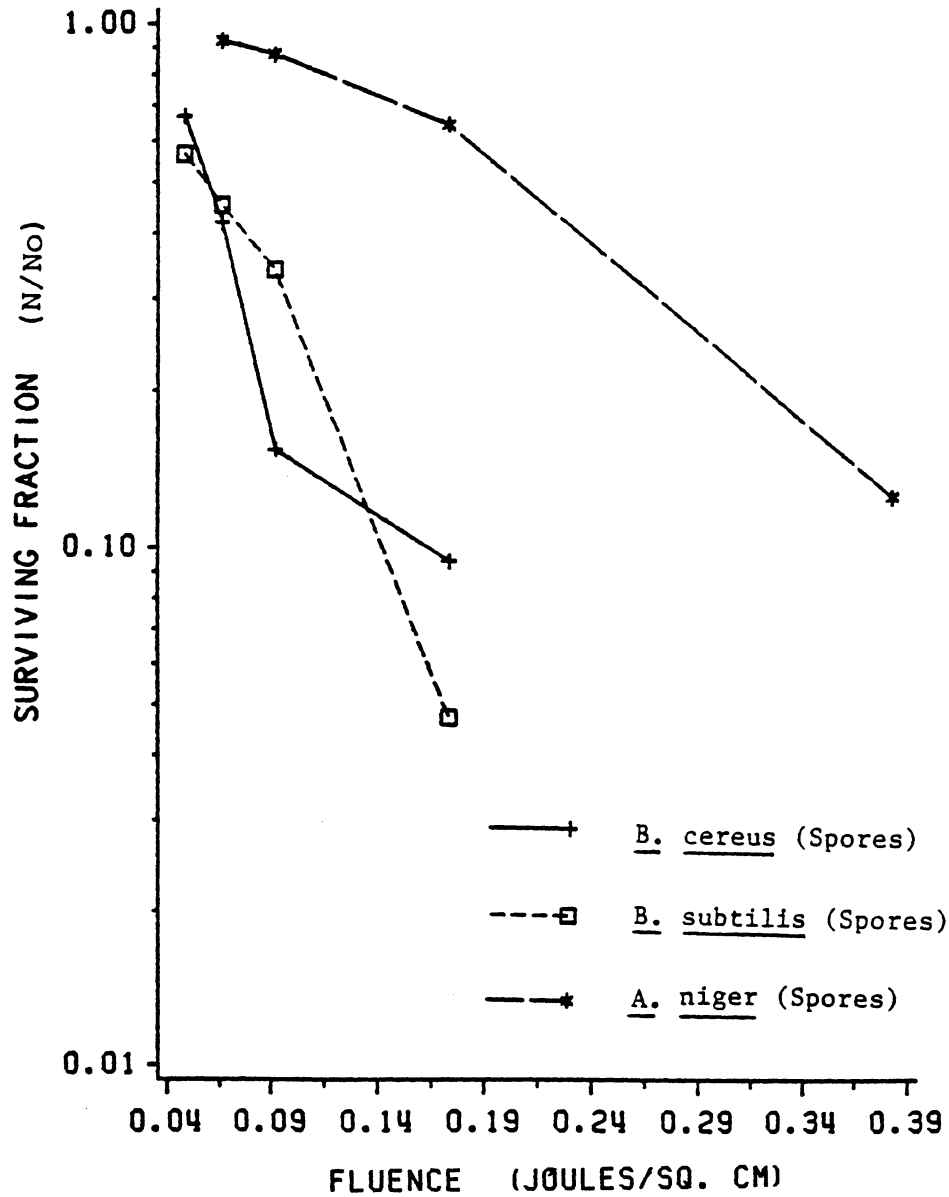

FIG. 7

Survival of three spore species at a Flashblast input energy of 2053 Joules.

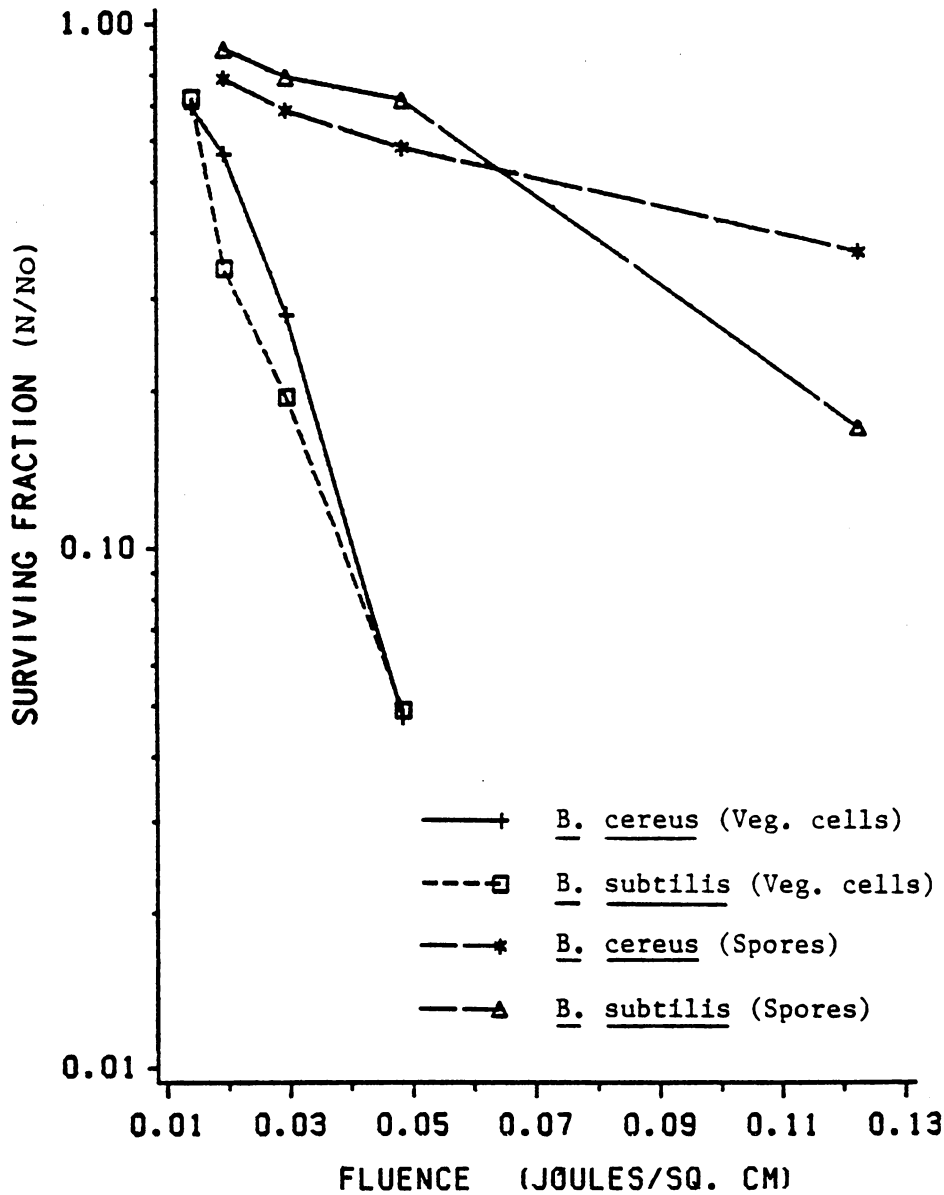

FIG. 8

Survival of Bacilli vegetative cells and spores at a Flashblast input energy of 513 Joules.

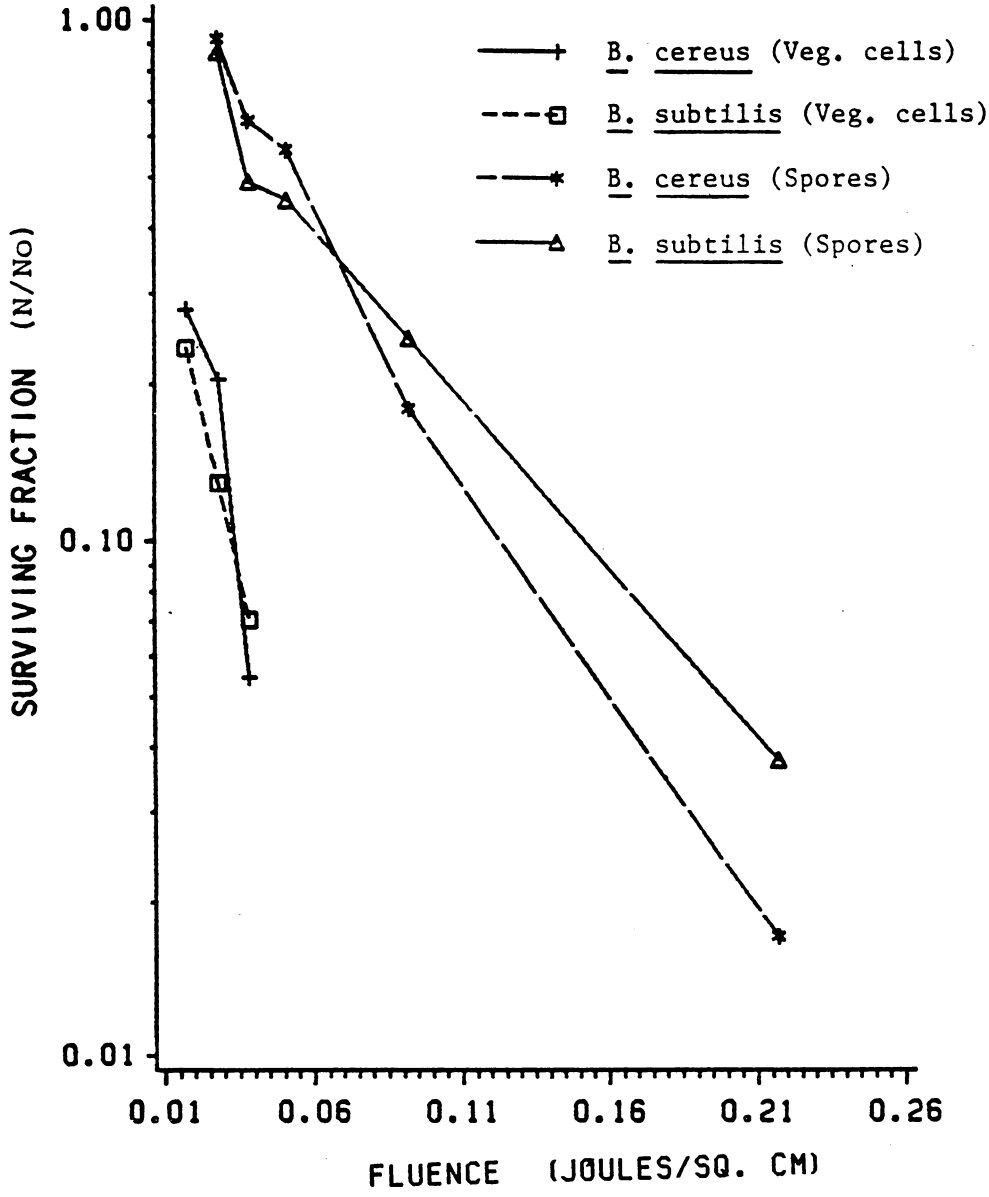

FIG. 9

Survival of Bacilli vegetative cells and spores at a Flashblast input energy of 1218 Joules.

TABLE 1. Microdrop Inactivation Data for E. coli

Number of survivors at different input energies after treatment with Flashblast light using three capacitors.

Input Energy (J)	Dist. (cm)	Absorbed Energy (J/cm^2)	Initial Populations In 25 micro-liters $6x10^6$	$6x10^5$	$6x10^4$	$6x10^3$	$6x10^2$	$6x10^1$
513	55	0.0133	TNTC	TNTC	TNTC	TNTC	TNTC	60
513	40	0.0194	TNTC	TNTC	TNTC	TNTC	TNTC	60
513	25	0.0357	TNTC	TNTC	TNTC	TNTC	TNTC	16
513	10	0.1225	18	<10	<10	<5	0	0
513	5	0.2680	<10	<10	<5	<5	0	0
1218	55	0.0242	TNTC	TNTC	TNTC	TNTC	90	11
1218	40	0.0383	TNTC	TNTC	TNTC	TNTC	29	<5
1218	25	0.0715	49	15	<10	<5	0	0
1218	10	0.2169	<10	<10	<5	0	0	0
1218	5	0.4594	0	0	0	0	0	0
2053	55	0.0408	TNTC	TNTC	TNTC	20	<10	0
2053	40	0.0664	76	15	<5	0	0	0
2053	25	0.1276	17	10	<5	0	0	0
2053	10	0.3828	<5	0	0	0	0	0
2053	5	0.7656	0	0	0	0	0	0

TNTC = Too Numerous To Count

TABLE 2. Microdrop Inactivation Data for S. aureus

Number of survivors at different input energies after treatment with Flashblast light using three capacitors.

Input Energy (J)	Dist. (cm)	Absorbed Energy (J/cm^2)	Initial Populations In 25 micro-liters $4x10^6$	$4x10^5$	$4x10^4$	$4x10^3$	$4x10^2$	$4x10^1$
513	55	0.0133	TNTC	TNTC	TNTC	TNTC	TNTC	40
513	40	0.0194	TNTC	TNTC	TNTC	TNTC	TNTC	32
513	25	0.0357	TNTC	TNTC	TNTC	TNTC	24	18
513	10	0.1225	TNTC	TNTC	TNTC	TNTC	19	<5
513	5	0.2680	10	<10	<5	<5	0	0
1218	55	0.0242	TNTC	TNTC	TNTC	TNTC	TNTC	27
1218	40	0.0383	TNTC	TNTC	TNTC	TNTC	53	<10
1218	25	0.0715	TNTC	29	<10	0	0	0
1218	10	0.2169	17	<10	<5	0	0	0
1218	5	0.4594	11	<10	<5	0	0	0
2053	55	0.0408	TNTC	TNTC	TNTC	49	<10	0
2053	40	0.0664	74	13	<5	0	0	0
2053	25	0.1276	22	<10	<5	0	0	0
2053	10	0.3828	<5	<5	0	0	0	0
2053	5	0.7656	0	0	0	0	0	0

TNTC = Too Numerous To Count

TABLE 3. Microdrop Inactivation Data for B. cereus (Vegetative cells)

Number of survivors at different input energies after treatment with Flashblast light using three capacitors.

Input Energy (J)	Dist. (cm)	Absorbed Energy (J/cm^2)	Initial Populations In 25 micro-liters $6x10^6$	$6x10^5$	$6x10^4$	$6x10^3$	$6x10^2$	$6x10^1$
513	55	0.0133	TNTC	TNTC	TNTC	TNTC	TNTC	32
513	40	0.0194	TNTC	TNTC	TNTC	TNTC	TNTC	15
513	25	0.0357	TNTC	TNTC	TNTC	TNTC	30	10
513	10	0.1225	TNTC	20	<10	<5	0	0
513	5	0.2680	20	<10	0	0	0	0
1218	55	0.0242	TNTC	TNTC	TNTC	TNTC	36	10
1218	40	0.0383	TNTC	TNTC	TNTC	TNTC	20	<10
1218	25	0.0715	TNTC	TNTC	19	<5	<5	0
1218	10	0.2169	17	<5	0	0	0	0
1218	5	0.4594	<10	0	0	0	0	0
2053	55	0.0408	TNTC	TNTC	TNTC	35	16	<5
2053	40	0.0664	TNTC	TNTC	17	<10	0	0
2053	25	0.1276	22	<5	<5	0	0	0
2053	10	0.3828	<5	0	0	0	0	0
2053	5	0.7656	0	0	0	0	0	0

TNTC = Too Numerous To Count

TABLE 4. Microdrop Inactivation Data for B. subtilis (Vegetative cells)

Number of survivors at different input energies after treatment with Flashblast light using three capacitors.

Input Energy (J)	Dist. (cm)	Absorbed Energy (J/cm^2)	Initial Populations In 25 micro-liters $9x10^6$	$9x10^5$	$9x10^4$	$9x10^3$	$9x10^2$	$9x10^1$
513	55	0.0133	TNTC	TNTC	TNTC	TNTC	TNTC	29
513	40	0.0194	TNTC	TNTC	TNTC	TNTC	TNTC	18
513	25	0.0357	TNTC	TNTC	TNTC	TNTC	12	<5
513	10	0.1225	TNTC	25	<10	<5	0	0
513	5	0.2680	<10	0	0	0	0	0
1218	55	0.0242	TNTC	TNTC	TNTC	TNTC	TNTC	12
1218	40	0.0383	TNTC	TNTC	TNTC	TNTC	14	<10
1218	25	0.0715	TNTC	TNTC	27	<10	0	0
1218	10	0.2169	<10	0	0	0	0	0
1218	5	0.4594	0	0	0	0	0	0
2053	55	0.0408	TNTC	TNTC	TNTC	35	<10	0
2053	40	0.0664	TNTC	TNTC	19	<10	<5	0
2053	25	0.1276	32	<5	0	0	0	0
2053	10	0.3828	<10	0	0	0	0	0
2053	5	0.7656	0	0	0	0	0	0

TNTC = Too Numerous To Count

TABLE 5. Microdrop Inactivation Data for B. cereus (Spores)

Number of survivors at different input energies after treatment with Flashblast light using three capacitors.

Input Energy (J)	Dist. (cm)	Absorbed Energy (J/cm^2)	Initial Populations In 25 micro-liters $3x10^6$	$3x10^5$	$3x10^4$	$3x10^3$	$3x10^2$	$3x10^1$
513	55	0.0133	TNTC	TNTC	TNTC	TNTC	TNTC	30
513	40	0.0194	TNTC	TNTC	TNTC	TNTC	TNTC	18
513	25	0.0357	TNTC	TNTC	TNTC	TNTC	TNTC	11
513	10	0.1225	TNTC	TNTC	TNTC	30	14	3
513	5	0.2680	TNTC	TNTC	24	<10	<5	0
1218	55	0.0242	TNTC	TNTC	TNTC	TNTC	40	22
1218	40	0.0383	TNTC	TNTC	TNTC	TNTC	38	20
1218	25	0.0715	TNTC	TNTC	TNTC	TNTC	34	13
1218	10	0.2169	TNTC	TNTC	40	10	<10	<5
1218	5	0.4594	TNTC	21	0	0	0	0
2053	55	0.0408	TNTC	TNTC	TNTC	TNTC	38	18
2053	40	0.0664	TNTC	TNTC	TNTC	TNTC	28	10
2053	25	0.1276	TNTC	TNTC	TNTC	44	22	6
2053	10	0.3828	TNTC	14	26	<10	0	0
2053	5	0.7656	12	<10	0	0	0	0

TNTC = Too Numerous To Count

TABLE 6. Microdrop Inactivation Data for B. subtilis (Spores)

Number of survivors at different input energies after treatment with Flashblast light using three capacitors.

Input Energy (J)	Dist. (cm)	Absorbed Energy (J/cm^2)	Initial Populations In 25 micro-liters $5x10^6$	$5x10^5$	$5x10^4$	$5x10^3$	$5x10^2$	$5x10^1$
513	55	0.0133	TNTC	TNTC	TNTC	TNTC	TNTC	42
513	40	0.0194	TNTC	TNTC	TNTC	TNTC	TNTC	30
513	25	0.0357	TNTC	TNTC	TNTC	TNTC	TNTC	22
513	10	0.1225	TNTC	TNTC	TNTC	TNTC	46	<10
513	5	0.2680	TNTC	TNTC	TNTC	42	<5	0
1218	55	0.0242	TNTC	TNTC	TNTC	TNTC	TNTC	32
1218	40	0.0383	TNTC	TNTC	TNTC	TNTC	TNTC	19
1218	25	0.0715	TNTC	TNTC	TNTC	TNTC	48	10
1218	10	0.2169	TNTC	TNTC	TNTC	36	<5	<5
1218	5	0.4594	TNTC	42	28	<5	0	0
2053	55	0.0408	TNTC	TNTC	TNTC	TNTC	TNTC	24
2053	40	0.0664	TNTC	TNTC	TNTC	TNTC	62	11
2053	25	0.1276	TNTC	TNTC	TNTC	TNTC	17	<5
2053	10	0.3828	TNTC	36	<10	<5	0	0
2053	5	0.7656	18	<5	0	0	0	0

TNTC = Too Numerous To Count

TABLE 7. Microdrop Inactivation Data for A. niger (Spores)

Number of survivors at different input energies after treatment with Flashblast light using three capacitors.

Input Energy (J)	Dist. (cm)	Absorbed Energy (J/cm^2)	Initial Populations In 25 micro-liters $3x10^6$	$3x10^5$	$3x10^4$	$3x10^3$	$3x10^2$	$3x10^1$
513	55	0.0133	TNTC	TNTC	TNTC	TNTC	TNTC	30
513	40	0.0194	TNTC	TNTC	TNTC	TNTC	TNTC	30
513	25	0.0357	TNTC	TNTC	TNTC	TNTC	TNTC	30
513	10	0.1225	TNTC	TNTC	TNTC	TNTC	TNTC	12
513	5	0.2680	TNTC	TNTC	TNTC	TNTC	40	10
1218	55	0.0242	TNTC	TNTC	TNTC	TNTC	TNTC	30
1218	40	0.0383	TNTC	TNTC	TNTC	TNTC	TNTC	21
1218	25	0.0715	TNTC	TNTC	TNTC	TNTC	35	12
1218	10	0.2169	TNTC	TNTC	TNTC	30	<10	<5
1218	5	0.4594	TNTC	35	<10	<5	<5	0
2053	55	0.0408	TNTC	TNTC	TNTC	TNTC	TNTC	22
2053	40	0.0664	TNTC	TNTC	TNTC	TNTC	32	12
2053	25	0.1276	TNTC	TNTC	28	15	<5	0
2053	10	0.3828	TNTC	18	<5	<5	0	0
2053	5	0.7656	TNTC	<5	0	0	0	0

TNTC = Too Numerous To Count

TABLE A. Microdrop Inactivation Data for E. coli

Number of log cycles reduced at different input energies after treatment with Flashblast light using three capacitors.

Input Energy (J)	Dist. (cm)	Absorbed Energy (J/cm^2)	Initial Populations In 25 micro-liters $6x10^6$	$6x10^5$	$6x10^4$	$6x10^3$	$6x10^2$	$6x10^1$
513	55	0.0133	TNTC	TNTC	TNTC	TNTC	TNTC	<1
513	40	0.0194	TNTC	TNTC	TNTC	TNTC	TNTC	<1
513	25	0.0357	TNTC	TNTC	TNTC	TNTC	TNTC	<1
513	10	0.1225	5	4	3	3	*	*
513	5	0.2680	5	4	4	3	*	*
1218	55	0.0242	TNTC	TNTC	TNTC	TNTC	<1	<1
1218	40	0.0383	TNTC	TNTC	TNTC	TNTC	1	1
1218	25	0.0715	5	4	3	3	*	*
1218	10	0.2169	5	4	4	*	*	*
1218	5	0.4594	*	*	*	*	*	*
2053	55	0.0408	TNTC	TNTC	TNTC	2	1	*
2053	40	0.0664	4	4	4	*	*	*
2053	25	0.1276	5	4	4	*	*	*
2053	10	0.3828	6	*	*	*	*	*
2053	5	0.7656	*	*	*	*	*	*

TNTC = Too Numerous To Count
* = Total Inactivation or Death

TABLE B. Microdrop Inactivation Data for S. aureus

Number of log cycles reduced at different input energies after treatment with Flashblast light using three capacitors.

Input Energy (J)	Dist. (cm)	Absorbed Energy (J/cm^2)	Initial Populations In 25 micro-liters $4x10^6$	$4x10^5$	$4x10^4$	$4x10^3$	$4x10^2$	$4x10^1$
513	55	0.0133	TNTC	TNTC	TNTC	TNTC	TNTC	<1
513	40	0.0194	TNTC	TNTC	TNTC	TNTC	TNTC	<1
513	25	0.0357	TNTC	TNTC	TNTC	TNTC	1	<1
513	10	0.1225	TNTC	TNTC	TNTC	TNTC	1	1
513	5	0.2680	5	4	4	3	*	*
1218	55	0.0242	TNTC	TNTC	TNTC	TNTC	TNTC	<1
1218	40	0.0383	TNTC	TNTC	TNTC	TNTC	<1	<1
1218	25	0.0715	TNTC	4	3	*	*	*
1218	10	0.2169	5	4	4	*	*	*
1218	5	0.4594	5	4	4	*	*	*
2053	55	0.0408	TNTC	TNTC	TNTC	1	1	*
2053	40	0.0664	4	4	4	*	*	*
2053	25	0.1276	5	4	4	*	*	*
2053	10	0.3828	6	5	*	*	*	*
2053	5	0.7656	*	*	*	*	*	*

TNTC = Too Numerous To Count
* = Total Inactivation or Death

TABLE C. Microdrop Inactivation Data for B. cereus (Vegetative cells)

Number of log cycles reduced at different input energies after treatment with Flashblast light using three capacitors.

Input Energy (J)	Dist. (cm)	Absorbed Energy (J/cm^2)	Initial Populations In 25 micro-liters $6x10^6$	$6x10^5$	$6x10^4$	$6x10^3$	$6x10^2$	$6x10^1$
513	55	0.0133	TNTC	TNTC	TNTC	TNTC	TNTC	<1
513	40	0.0194	TNTC	TNTC	TNTC	TNTC	TNTC	<1
513	25	0.0357	TNTC	TNTC	TNTC	TNTC	1	<1
513	10	0.1225	TNTC	4	3	3	*	*
513	5	0.2680	5	4	*	*	*	*
1218	55	0.0242	TNTC	TNTC	TNTC	TNTC	1	<1
1218	40	0.0383	TNTC	TNTC	TNTC	TNTC	1	<1
1218	25	0.0715	TNTC	TNTC	3	3	2	*
1218	10	0.2169	5	5	*	*	*	*
1218	5	0.4594	5	*	*	*	*	*
2053	55	0.0408	TNTC	TNTC	TNTC	2	1	1
2053	40	0.0664	TNTC	TNTC	3	2	*	*
2053	25	0.1276	5	5	4	*	*	*
2053	10	0.3828	6	*	*	*	*	*
2053	5	0.7656	*	*	*	*	*	*

TNTC = Too Numerous To Count
* = Total Inactivation or Death

TABLE D. Microdrop Inactivation Data for B. subtilis (Vegetative cells)

Number of log cycles reduced at different input energies after treatment with Flashblast light using three capacitors.

Input Energy (J)	Dist. (cm)	Absorbed Energy (J/cm^2)	Initial Populations In 25 micro-liters $9x10^6$	$9x10^5$	$9x10^4$	$9x10^3$	$9x10^2$	$9x10^1$
513	55	0.0133	TNTC	TNTC	TNTC	TNTC	TNTC	<1
513	40	0.0194	TNTC	TNTC	TNTC	TNTC	TNTC	<1
513	25	0.0357	TNTC	TNTC	TNTC	TNTC	1	1
513	10	0.1225	TNTC	4	4	3	*	*
513	5	0.2680	5	*	*	*	*	*
1218	55	0.0242	TNTC	TNTC	TNTC	TNTC	TNTC	<1
1218	40	0.0383	TNTC	TNTC	TNTC	TNTC	1	1
1218	25	0.0715	TNTC	TNTC	3	3	*	*
1218	10	0.2169	6	*	*	*	*	*
1218	5	0.4594	*	*	*	*	*	*
2053	55	0.0408	TNTC	TNTC	TNTC	2	1	*
2053	40	0.0664	TNTC	TNTC	3	3	2	*
2053	25	0.1276	5	5	*	*	*	*
2053	10	0.3828	6	*	*	*	*	*
2053	5	0.7656	*	*	*	*	*	*

TNTC = Too Numerous To Count
* = Total Inactivation or Death

TABLE E. Microdrop Inactivation Data for B. cereus (Spores)

Number of log cycles reduced at different input energies after treatment with Flashblast light using three capacitors.

Input Energy (J)	Dist. (cm)	Absorbed Energy (J/cm^2)	Initial Populations In 25 micro-liters $3x10^6$	$3x10^5$	$3x10^4$	$3x10^3$	$3x10^2$	$3x10^1$
513	55	0.0133	TNTC	TNTC	TNTC	TNTC	TNTC	<1
513	40	0.0194	TNTC	TNTC	TNTC	TNTC	TNTC	<1
513	25	0.0357	TNTC	TNTC	TNTC	TNTC	TNTC	<1
513	10	0.1225	TNTC	TNTC	TNTC	2	1	<1
513	5	0.2680	TNTC	TNTC	3	2	1	*
1218	55	0.0242	TNTC	TNTC	TNTC	TNTC	<1	<1
1218	40	0.0383	TNTC	TNTC	TNTC	TNTC	<1	<1
1218	25	0.0715	TNTC	TNTC	TNTC	TNTC	<1	<1
1218	10	0.2169	TNTC	TNTC	3	2	1	<1
1218	5	0.4594	TNTC	4	*	*	*	*
2053	55	0.0408	TNTC	TNTC	TNTC	TNTC	<1	<1
2053	40	0.0664	TNTC	TNTC	TNTC	TNTC	1	<1
2053	25	0.1276	TNTC	TNTC	TNTC	1	1	<1
2053	10	0.3828	TNTC	4	3	2	*	*
2053	5	0.7656	5	4	*	*	*	*

TNTC = Too Numerous To Count
* = Total Inactivation or Death

TABLE F. Microdrop Inactivation Data for B. subtilis (Spores)

Number of log cycles reduced at different input energies after treatment with Flashblast light using three capacitors.

Input Energy (J)	Dist. (cm)	Absorbed Energy (J/cm^2)	Initial Populations In 25 micro-liters $5x10^6$	$5x10^5$	$5x10^4$	$5x10^3$	$5x10^2$	$5x10^1$
513	55	0.0133	TNTC	TNTC	TNTC	TNTC	TNTC	<1
513	40	0.0194	TNTC	TNTC	TNTC	TNTC	TNTC	<1
513	25	0.0357	TNTC	TNTC	TNTC	TNTC	TNTC	<1
513	10	0.1225	TNTC	TNTC	TNTC	TNTC	1	<1
513	5	0.2680	TNTC	TNTC	TNTC	2	2	*
1218	55	0.0242	TNTC	TNTC	TNTC	TNTC	TNTC	<1
1218	40	0.0383	TNTC	TNTC	TNTC	TNTC	TNTC	<1
1218	25	0.0715	TNTC	TNTC	TNTC	TNTC	1	<1
1218	10	0.2169	TNTC	TNTC	TNTC	2	2	1
1218	5	0.4594	TNTC	4	3	3	*	*
2053	55	0.0408	TNTC	TNTC	TNTC	TNTC	TNTC	<1
2053	40	0.0664	TNTC	TNTC	TNTC	TNTC	<1	<1
2053	25	0.1276	TNTC	TNTC	TNTC	TNTC	1	1
2053	10	0.3828	TNTC	4	3	3	*	*
2053	5	0.7656	5	5	*	*	*	*

TNTC = Too Numerous To Count
* = Total Inactivation or Death

TABLE G. Microdrop Inactivation Data for A. niger (Spores)

Number of log cycles reduced at different input energies after treatment with Flashblast light using three capacitors.

Input Energy (J)	Dist. (cm)	Absorbed Energy (J/cm^2)	Initial Populations In 25 micro-liters $3x10^6$	$3x10^5$	$3x10^4$	$3x10^3$	$3x10^2$	$3x10^1$
513	55	0.0133	TNTC	TNTC	TNTC	TNTC	TNTC	<1
513	40	0.0194	TNTC	TNTC	TNTC	TNTC	TNTC	<1
513	25	0.0357	TNTC	TNTC	TNTC	TNTC	TNTC	<1
513	10	0.1225	TNTC	TNTC	TNTC	TNTC	TNTC	<1
513	5	0.2680	TNTC	TNTC	TNTC	TNTC	<1	<1
1218	55	0.0242	TNTC	TNTC	TNTC	TNTC	TNTC	<1
1218	40	0.0383	TNTC	TNTC	TNTC	TNTC	TNTC	<1
1218	25	0.0715	TNTC	TNTC	TNTC	TNTC	<1	<1
1218	10	0.2169	TNTC	TNTC	TNTC	2	1	<1
1218	5	0.4594	TNTC	4	3	2	1	*
2053	55	0.0408	TNTC	TNTC	TNTC	TNTC	TNTC	<1
2053	40	0.0664	TNTC	TNTC	TNTC	TNTC	<1	<1
2053	25	0.1276	TNTC	TNTC	3	2	1	*
2053	10	0.3828	TNTC	4	3	2	*	*
2053	5	0.7656	TNTC	4	*	*	*	*

TNTC = Too Numerous To Count
* = Total Inactivation or Death

CHAPTER 5

EFFECT OF FLASHBLAST LIGHT ON MICROORGANISM ULTRASTRUCTURE

5.1 INTRODUCTION

The targets for the inactivation or destruction of microorganisms would primarily be identified as the cell wall, cytoplasmic membrane, and cytoplasm. Targets in the cytoplasm include the membrane itself and membrane associated enzymes. Within the cytoplasm, targets include ribosomes, nucleic acids, cytoplasmic enzymes and the cytoplasm as a whole, which may be destroyed unselectively by coagulation. DNA is found to be the most selective target for photoinactivation of cells under most cicumstances.

John Jagger (1985) investigated near-UV membrane effects and reported that at near-UV fluences just barely sublethal (~ 50 J/cm^2 at 366 nm) effects on membranes and membrane functions do not appear to result from actions on DNA or cytoplasmic components, but rather from direct effects on the membranes themselves. While the lethal action of near-UV appears to involve DNA as the primary target, the membrane transport effects appear to be independent of DNA damage eventhough they occur in the same fluence range. After a dose of only (10^{-4} J/cm^2), less than

10% of the cells are able to divide and most cells are observed to form long filaments as cytoplasmic synthesis continues in the absence of division (Smith and Hanawalt, 1969). Gram-negative microorganisms, such as E. coli have outer membranes with a lower amount of peptidoglycan than gram-positive microorganisms having a comparatively thick cell wall with a higher amount of peptidoglycan. Because of a loose and thin outer membrane, gram-negative organisms are found to be more permeable to chemicals, antibiotics and radiation. Russell and Harries (1968) quoted evidence from electron micrographs of ultrathin sections of Staphylococcus aureus supporting the idea that the walls of gram-positive cells are less sensitive to heat than those of gram-negative. Meissel (1955) noted visible changes in the structure of microorganisms after exposure to several hundred thousand reps of X-rays. The earliest changes occured in the protoplasm of irradiated cells of Endomyces magnusii. The first reactions were sharply expressed contractive movements of the protoplasm and increased activity of the vacuole apparatus. There was a pronounced swelling of certain cells and a distinct condensation of the cariosomes within the nucleus with an increase in their dye absorption capabilities.

The ozone production in the microenvironment of microorganisms treated with a high intensity UV light may contribute to photoinactivation. McNair Scott and Lesher

(1963) studied the effects of ozone on E. coli and found that it caused leakage of the cell contents. They proposed that the primary sites of attack were the double bonds of lipids in the cell wall or membrane, with the extent of the reaction determining the amount of leakage or lysis.

The visible portion of the EMR spectrum is usually responsible for the thermal effects on treated microorganisms. There is now considerable evidence that elevated temperatures do damage the cytoplasmic membrane. Morita and Burton (1963) considered that heat induced permeability changes could account for alterations in the activity of malic dehydrogenase in a psychrophylic marine bacterium.

ELECTRON MICROSCOPY

An attempt was made to investigate the mechanism of Flashblast destruction or inactivation of microorganisms with the help of ultrastructural studies performed on both the control and treated microorganisms. The effects of the Flashblast treatment on the morphology of microorganisms were studied by scanning electron microscopy (SEM), while the effects on the cell walls and cellular constituents were observed by transmission electron microscopy (TEM). The SEM experiments were performed on E. coli.

The microorganisms used in the TEM study were:

(1) Escherichia coli

(2) Staphylococcus aureus

(3) Bacillus cereus (Vegetative cells)

(4) Bacillus subtilis (Vegetative cells)

(5) Bacillus cereus (Spores)

(6) Bacillus subtilis (Spores)

(7) Aspergillus niger (Spores)

5.2 SCANNING ELECTRON MICROSCOPY OF FLASHBLAST TREATED E. COLI

MATERIALS AND METHODS

The E. coli culture was supplied by Dr. Joseph Dunn of Maxwell Laboratories, Inc., San Diego, CA. The cells were transferred from slants to Tryptic Soy Broth (Difco) and incubated at 37°C for 48 hours at which time they were observed to be in a late log growth phase by optical density measurements.

A suspension was prepared with a concentration of 10^6 cells per ml and 0.1 ml of the suspension was pipetted onto an area bounded by two parallel lines one inch apart from the diameter of a Difco Tryptic Soy Agar Petri plate. The suspension was gently spread within the defined area with a glass hockey stick and allowed to be absorbed by the agar.

The microorganisms on the surface of the agar were directly exposed to a single shot of Flashblast light with an input energy of 2053 Joules (3 capacitors) at a distance of 5 cm from the flashlamp. This treatment corresponded to a fluence of 0.76 J/cm^2.

The treatment was performed with several inoculated plates in order to obtain a statistical population of the inactivated cells. The treated cells were then harvested from the agar surface with a primary fixative containing 0.5% glutaraldehyde and 10% formaldehyde (Jones et al., 1986) after one hour of room temperature (25°C) incubation. Three replicates were incubated at 37°C for 48 hours to observe survivor microbial growth. The absence of the colony forming units after 48 hours confirmed that the treated cells were unable to multiply. The control E. coli cells were obtained directly through centrifugation and similarly fixed.

After primary fixation of one hour, the bacterial cell suspension was passed through a 0.2 micron Nucleopore filter until an adequate bacterial population ($\sim 10^6$) was obtained on the filter paper surface. Cells were then rinsed in 0.1M cacodylate buffer (pH 6.5) at 4°C, washed with distilled water (4°C) and dehydrated with serial dilutions of 100% ethanol. The dehydrated cells on the filter were critical point dried (Ladd Critical Point Dryer) and placed on a stainless steel SEM stub. Gold-palladium sputter coating was performed with a Hummer 10 Sputter Coater (Anatech Ltd) until a coating of 15 nm was obtained on the surface of the dried cells. The specimen was observed in a Philips 505 scanning electron microscope at 30 KV.

RESULTS AND DISCUSSION

Scanning electron micrographs of the control and Flashblast treated E. coli are presented in Plate 1. There is no observable difference between the two specimens with respect to their surface appearance. This indicates that the effect which makes them incapable of reproduction may have occured due to Flashblast treatment on the bacteria genetic material. The cell structure did not disintegrate or shrivel due to the high intensity Flashblast treatment. However, it must be considered that SEM is not capable of revealing internal damage of the cellular constituents.

5.3 TRANSMISSION ELECTRON MICROSCOPY OF FLASHBLAST TREATED MICROORGANISMS

MATERIALS AND METHODS

All the microorganism cultures were obtained from Dr. Joseph Dunn of Maxwell Laboratories, Inc., San Diego, CA. The vegetative cells of all microorganism species were treated with Flashblast light in a similar manner as described in the previous E. coli SEM study.

In order to obtain the Bacilli spores, the vegetative cells were grown in TYG broth and surface plated on TYG agar plates. The plates were evaluated for the presence of spores using a wet mount sample preparation with a phase contrast microscope after 24, 48, and 72 hours incubation at 30°C.

After 72 hours, approximately 90% of the culture population was found to be spores. The plates were then refrigerated for 24 - 48 hours to induce further sporulation and prevent germination. The spores were harvested from the plates using cold sterile deionized distilled water, repeatedly centrifuged (10,000 g, 10 min) and stored at -20°C. The final concentration of the spores in the suspension was adjusted to 10^6 spores per ml. The spores were activated by heating at 80°C for 15 minutes prior to plating. A 0.1 ml suspension of each microorganism was treated with the Flashblast apparatus in a similar manner to the vegetative cells. However, a sequence of three flashes was applied to the spores in order to ensure complete inactivation.

Aspergillus niger conidia spores were obtained by growing the culture on a Yeast Morphology Agar (Difco) plate at room temperature for 5-6 days. A sterile 0.1% Tergitol-7 Anionic solution was used to harvest the mold spores. A suspension of 10^6 spores per ml was obtained for the control and treated A. niger spores. Both suspensions were exposed to Flashblast light on the surface of YMA plates with a sequence of three flashes as were the Bacilli spores.

The control vegetative cells and spores of all the microorganism species were obtained directly through centrifugation. The primary fixation of the control and treated samples was performed in the same manner as the SEM

study. After primary fixation, the cells were rinsed in 0.1 M cacodylate buffer for 24 hours at 4°C.

All trials included a secondary fixation in 1% osmium tetroxide at 20°C (Jones et al., 1986) overnight followed by 90 minutes in 0.5% uranyl acetate, both in cacodylate buffer. The fixed cells were encapsulated in cold melted Bacto Agar (Difco, 4% in water), and subjected to successive dehydration and infiltration steps. A low viscosity Spurr's medium was used for infiltration and embedment of the cells. Silver-Gray sections were stained with 2% uranyl acetate for 30 minutes at 25°C followed by extensive rinsing with a wash bottle containing distilled water. A final staining was performed with a Raynolds lead citrate solution for 5 minutes (Raynolds, 1963).

All samples were fixed, sectioned and stained identically. The ultrastructure of each species was then observed in a Zeiss 10-CA transmission electron microscope.

RESULTS AND DISCUSSION

The electron micrographs of the seven microorganism species are presented on Plates 2-15. Among all the microorganism species, Flashblast treated E. coli showed the most extensive damage. As seen in the micrographs, the control E. coli cells have a uniform distribution of nuclear material and ribosomes in the cytoplasm. The inner and the outer membranes of gram negative E. coli have maintained their integrity. There was no sign of the lysis that

was observed in the entire population of bacteria sections on the grids.

The micrographs of the Flashblast treated E. coli (Plate 3) show a condensation of cytoplasm at the inner membrane. The center becomes less electron dense probably due to the solubilization of the susceptible cytoplasmic constituents. The outer membrane was also damaged and an initiation of lysis was observed. Extensive damage and lysis appears in Figure 3 of Plate 3. The cell membranes have lost their integrity.

A solubilization of cytoplasmic constituents was also observed in the micrographs of the treated cells of gram positive S. aureus (Plate 5). However the initiation of lysis was rarely seen in the entire population of the treated sections on the grids. The resistance in the susceptibility of S. aureus may be due to a thick peptidoglycan layer in the gram positive cell wall.

Ultrastructures of the control vegetative cells of B. cereus and B. subtilis show defined shapes and continuous cell walls. The micrographs of the treated Bacilli vegetative cells indicate cell wall damage and leakage of the electron dense cellular material (Plates 6-9).

The Bacilli spores were found to be in a germinating stage. This may have occured either during the inactivation treatment prior to treatment or during the period between the treatment and primary fixation or during fixation.

The absence of dormant spores was observed by an insufficient cortex development. The difference between the ultrastructures of the control and treated Bacilli spores was found to be significant. The cytoplasmic constituents and nuclear material of the Flashblast treated spores appeared highly disorganized. Fragments of the spore coats and leakage of the cellular material were found in the sections of the treated Bacilli spores. Also, a condensation of cytoplasm was observed as electron dense aggregates in the micrographs (Plates 11 and 13).

The ultrastructure of control A. niger spores conidia indicate a defined mitochondrion and a bundle of microtubules as observed in Plate 14. A damaged spore after Flashblast treatment contained the electron dense fragments of mitochondria and probably portions of the double layered nuclear membrane (Plate 15). This suggests that Flashblast treatment caused a disruption of the mitochondrion and nucleus, a condensation of the cytoplasm, and a dispersion of the spore walls. Fragments of the microtubules appear near the spore wall. A build-up of lipid bodies is also seen which may be due to a malfunction of the damaged mitochondria (Figure 1 of Plate 15).

Ultrastructural observations of the Flashblast treated microorganisms indicate significant cell wall and membrane damage. A disintegration of the characteristic shape and the initiation of lysis may be a consequential

phenomena after biochemical alterations of nucleic acids and the inactivation of functional enzymes. The study suggests that the damage is internal. The absorption of ultraviolet light by DNA leads to the destruction or inactivation of microorganisms. It has been proved that the absorption of ultraviolet light by DNA leads to the formation of cyclo-butane type pyrimidine dimers. This consequently inhibits the translation and transcription processes which are essential for multiplication.

These observations should be carefully interpreted for future studies on the ultrastructure of Flashblast treated microorganisms. There may be a sequence of biochemical changes involved in the destruction or inactivation of the treated microbial cells. The young and the aged cells may have different susceptibilities to treatment and hence a variable extent of damage would be observed. Future experiments should be performed with synchronized cultures to avoid this problem.

The germinating spores of the Bacilli lack a sufficient amount of dipicololinic acid which is reponsible for photoprotection (Leif et al., 1960). Hence, Flashblast treatment will cause more extensive damage in germinating spores when compared with the dormant spores. A very dilute suspension of microorganisms should be treated on a non-nutritive surface in order to ensure a complete inactivation and the absence of an environment favorable for

germination and multiplication. Precautions should be taken to retain the spores in a dormant condition before the treatment. The ultrastructural studies of A. niger should be extended to obtain a large number of sections with different organelles for both the control and treated specimens so that a sound and meaningful interpretation could be obtained.

The Xenon lamp used in the Flashblast apparatus also emits some percentage of infrared and visible light in addition to ultraviolet. Therefore, the damage as observed from the ultrastructural studies may not be entirely due to ultraviolet light. The excessive heat generated from visible light in the microenvironment of the microbial population can probably cause denaturation of the cytoplasmic proteins and hence an initiation of lysis.

PLATE 1. Scanning Electron Micrographs of E. coli.

The control and Flashblast treated E. coli cells were collected on a Nucleopore filter and prepared for scanning electron microscopy.

1. Control E. coli cells (x 11,000).
   Scale bar measures 2 μm.

2. Treated E. coli cells (x 13,500).
   Scale bar measures 2 μm.

There is no observable difference between the control and Flashblast treated E. coli with respect to their three dimensional morphology.

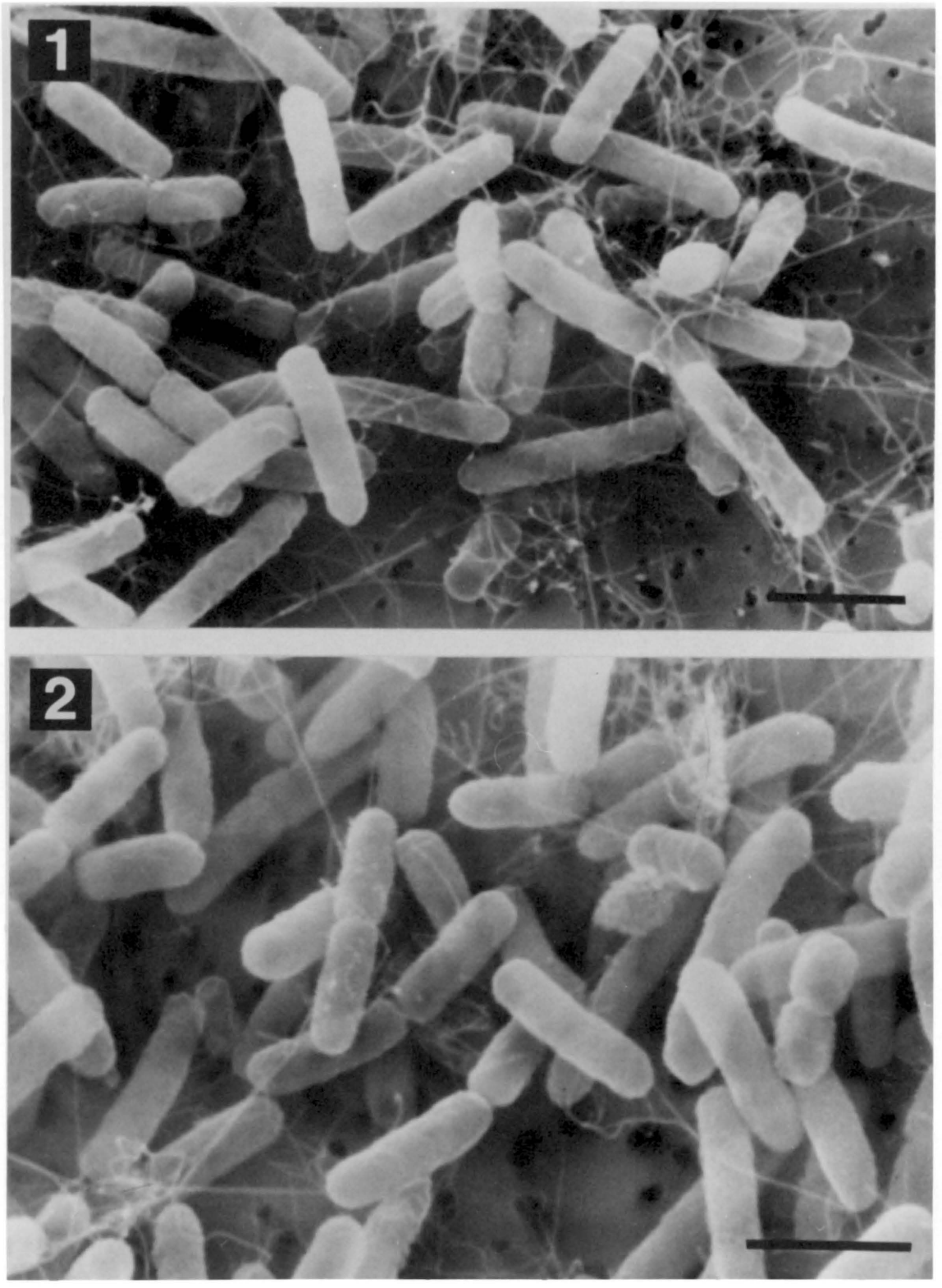
1
2

PLATE 2. Transmission Electron Micrographs of the control *E. coli* cells.

Ultrathin sections of the control *E. coli* cells show the general features of a gram negative microorganism.

OM-Outer membrane, CM-Cytoplasmic membrane, and N-Nuclear material.

1. The untreated control cells (x 49,500) indicate a well defined rod shape with intact outer and cytoplasmic membrane. There is a uniform distribution of nuclear material in the cytoplasm. Scale bar measures 0.5 μm.

2. A control *E. coli* cell (x 125,000) with loose outer and cytoplasmic membranes. Scale bar measures 0.2 μm.

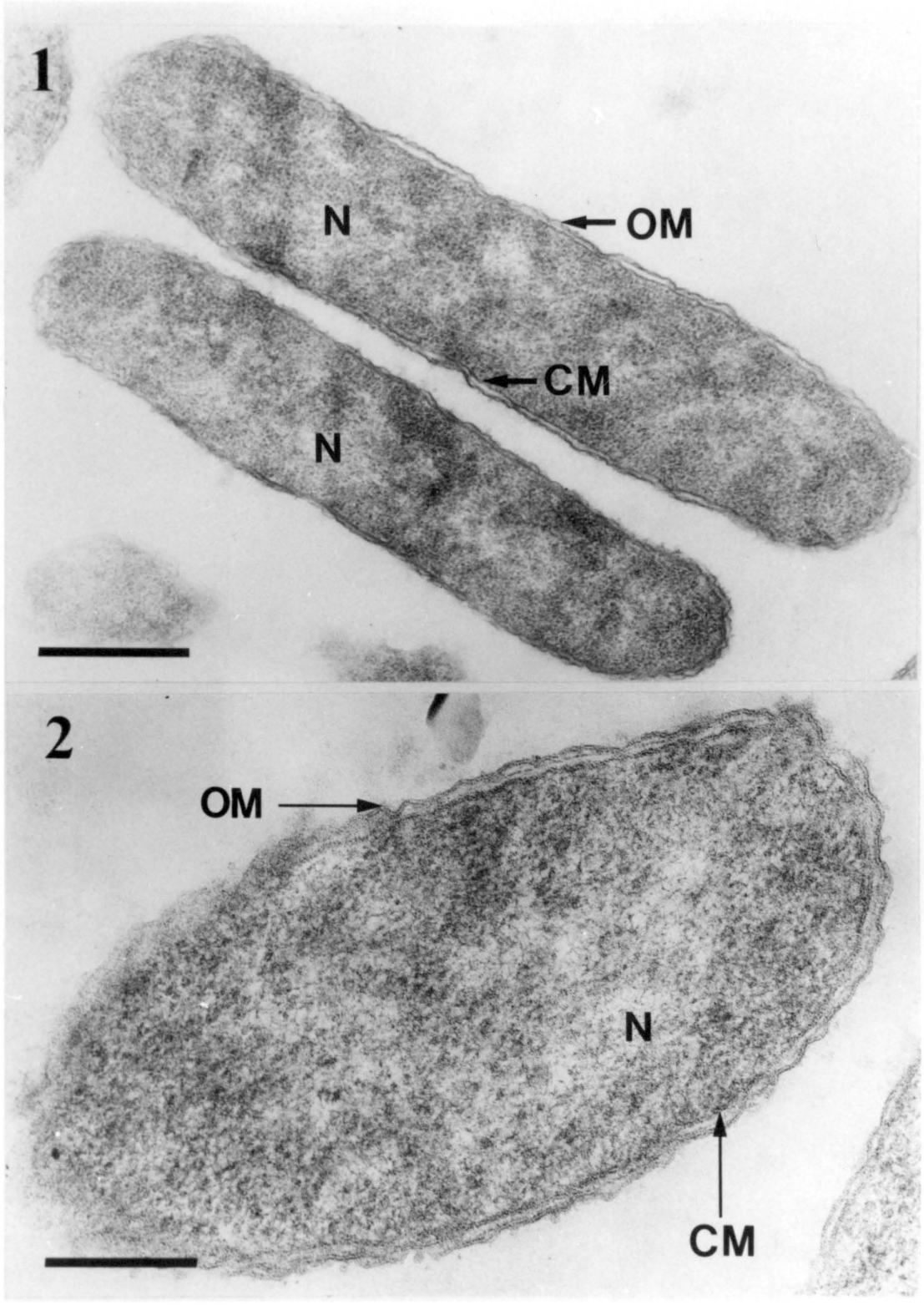
1
N
OM
CM
N
2
OM
N
CM

PLATE 3. Transmission Electron Micrographs of the Flashblast treated E. coli.

Ultrathin sections of Flashblast treated E. coli cells show the effects on cytoplasm and membranes.

CC-Condensed cytoplasm, cm-Cytoplasmic membrane, om-Outer membrane, and mv-Membrane vescicle.

1. The treated E. coli cells (x 15,500) show clumps of condensed cytoplasm.
   Scale bar measures 1 μm.

2. The treated E. coli cells (x 40,000) indicate a dissolution of cytoplasm with electron transparent appearance in the center and condensed cytoplasm accumulation near the cytoplasmic membrane.
   Scale bar measures 0.5 μm.

3. The treated E. coli cells (x 22,000) indicate an extensive damage, disorganization of membranes and an initiation of lysis.
   Scale bar measures 1 μm.

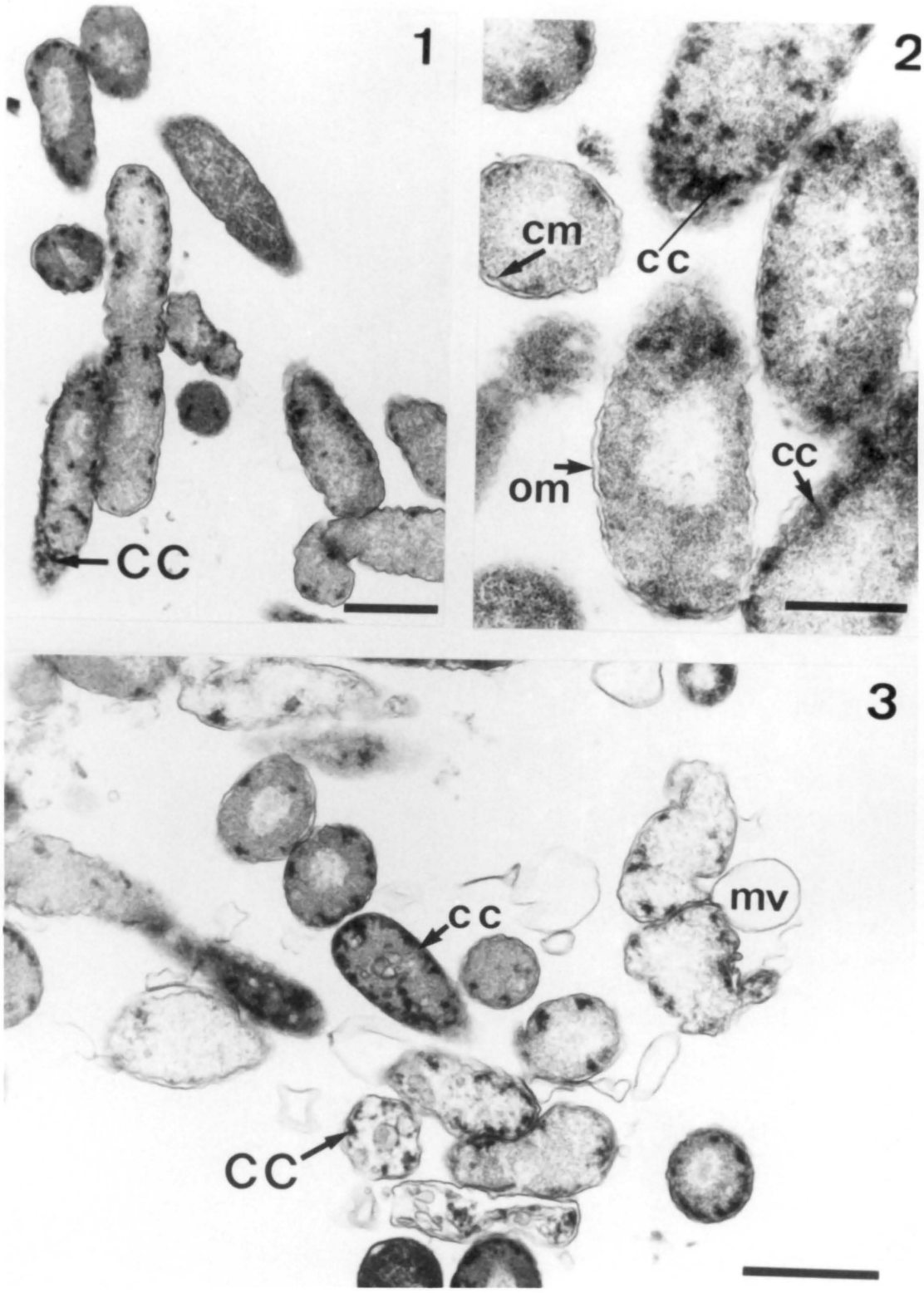
1
cc
2
cm
cc
om
cc
3
cc
mv
cc

PLATE 4. Transmission Electron Micrographs of the control S. aureus cells.

Thin sections of the control S. aureus cells show general features of a gram positive microorganism. A tight and thick cell wall is observed in all the micrographs.

CM-Cytoplasmic membrane, CW-Cell wall and N-Nuclear material.

1. Control S. aureus cell (x 120,000).
   Scale bar measures 0.2 μm.

2. Control S. aureus cells (x 41,500).
   Scale bar measures 0.5 μm.

3. Control S. aureus cells (x 20,500).
   Scale bar measures 1 μm.

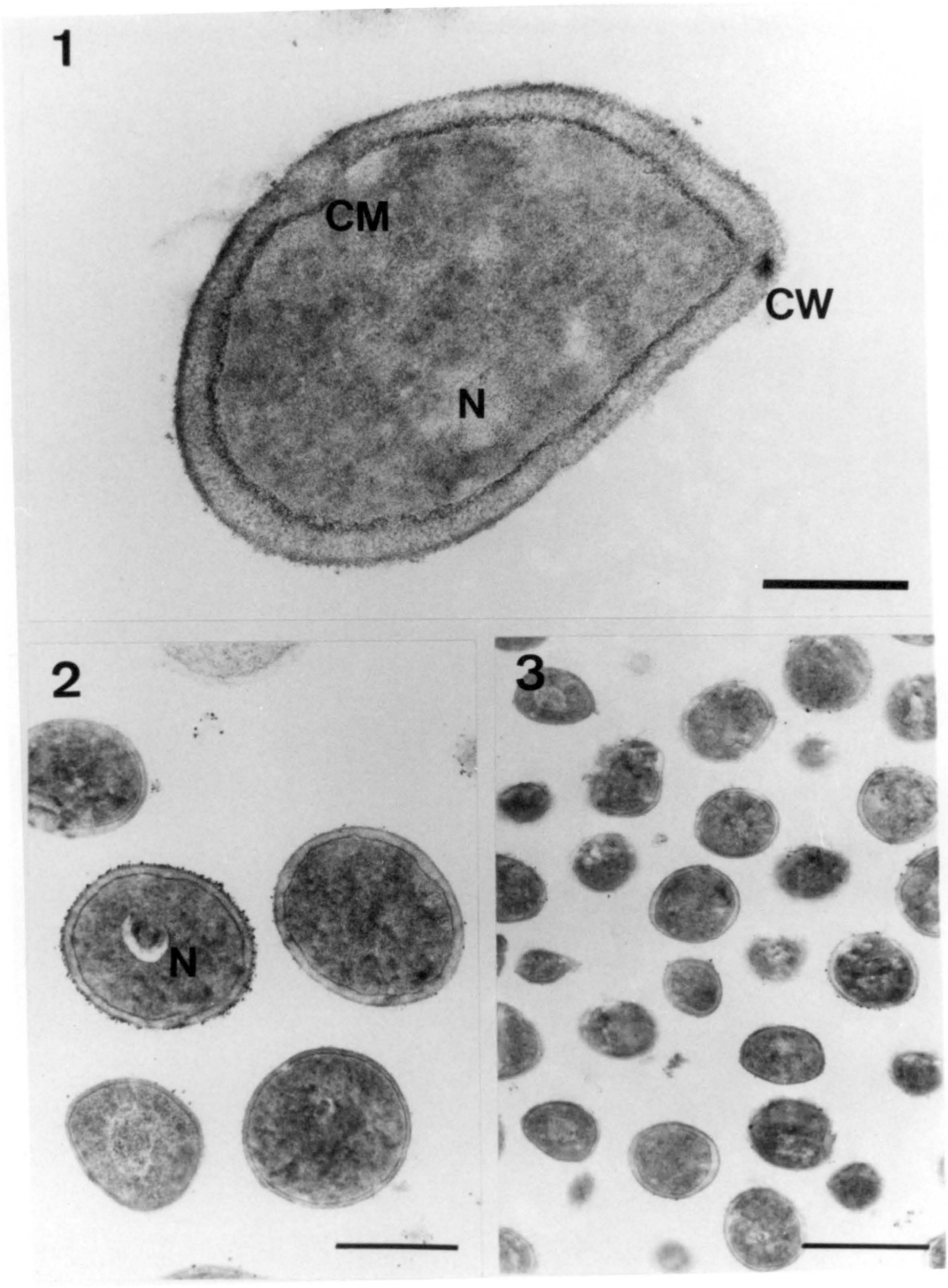
1
CM
CW
N
2
N
3

PLATE 5. Transmission Electron Micrographs of the Flashblast treated S. aureus cells.

The Flashblast treated S. aureus cells indicate intact cell walls in most sections. However, a difference in cytoplasm appearance is observed when compared to the control S. aureus cells.

cm-Cytoplasmic membrane, CW-cell wall,
N,n-Nuclear material and m-Mesosomes.

1. An treated S. aureus cell (x 120,000) with a septum formation.
   Scale bar measures 0.2 μm.

2. A similar cell (x 67,000) with two distinct electron-light regions associated with the division of a nuclear material.
   Scale bar measures 0.5 μm.

3. A group of the treated S. aureus cells (x 20,000) indicating a disorganized state of cytoplasm.
   Scale bar measures 1 μm.

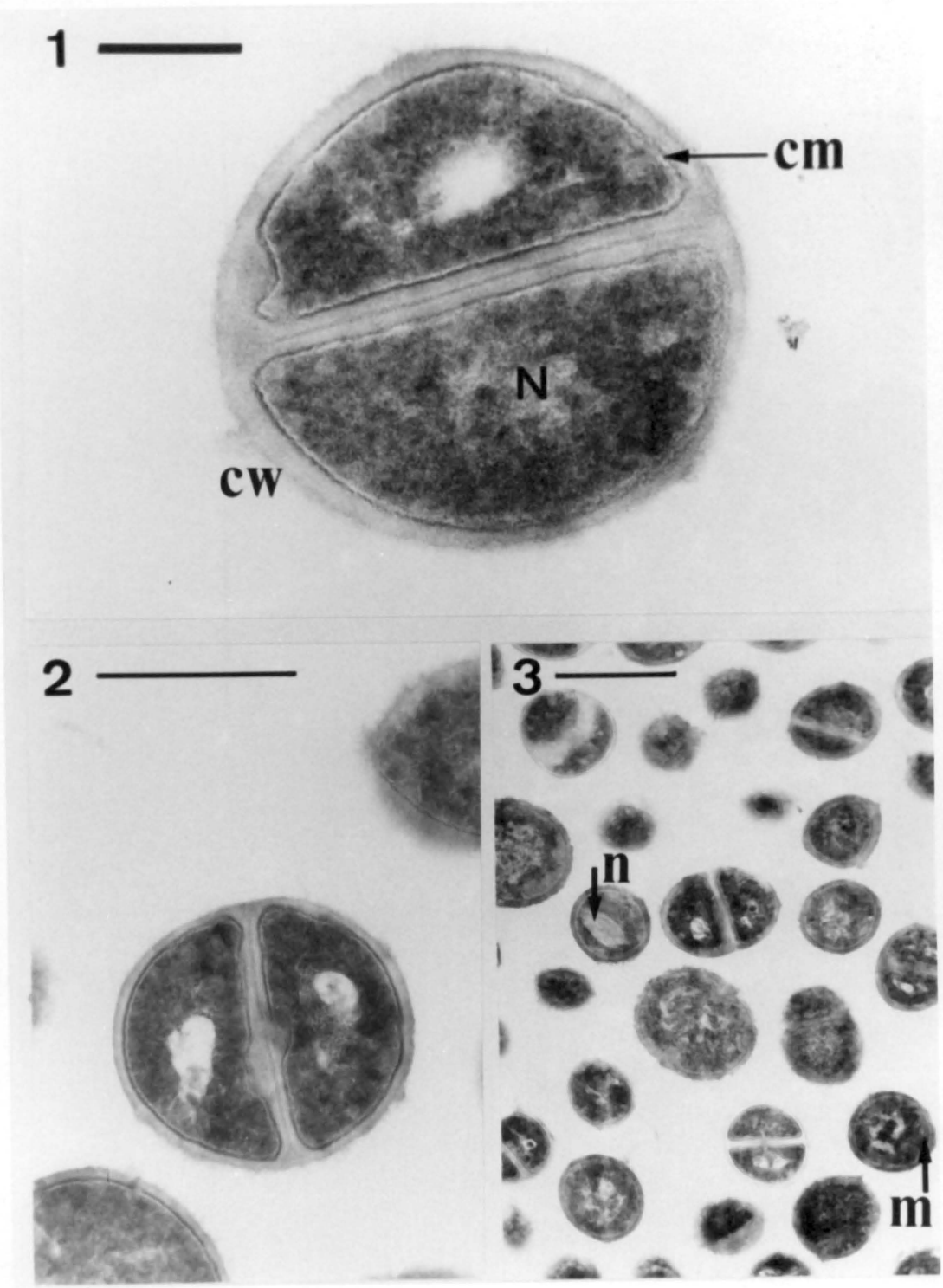
1
cm
N
cw
2
3
n
m

PLATE 6. Transmission Electron Micrographs of the control B. cereus vegetative cells.

Thin sections of control B. cereus vegetative cells show the general features of a gram positive Bacillus microorganism. Electron-light nuclear material is distributed throughout the cytoplasm.

M-Mesosomes, CW-Cell wall, N-Nuclear material and CM-Cytoplasmic membrane.

1. Control B. cereus vegetative cells (x 76,000). Scale bar measures 0.5 μm.

2. Control B. cereus vegetative cells (x 31,500) indicating a development of mesosomes. Scale bar measures 0.5 μm.

3. Control B. cereus vegetative cells (x 41,000) showing blebs. Scale bar measures 0.5 μm.

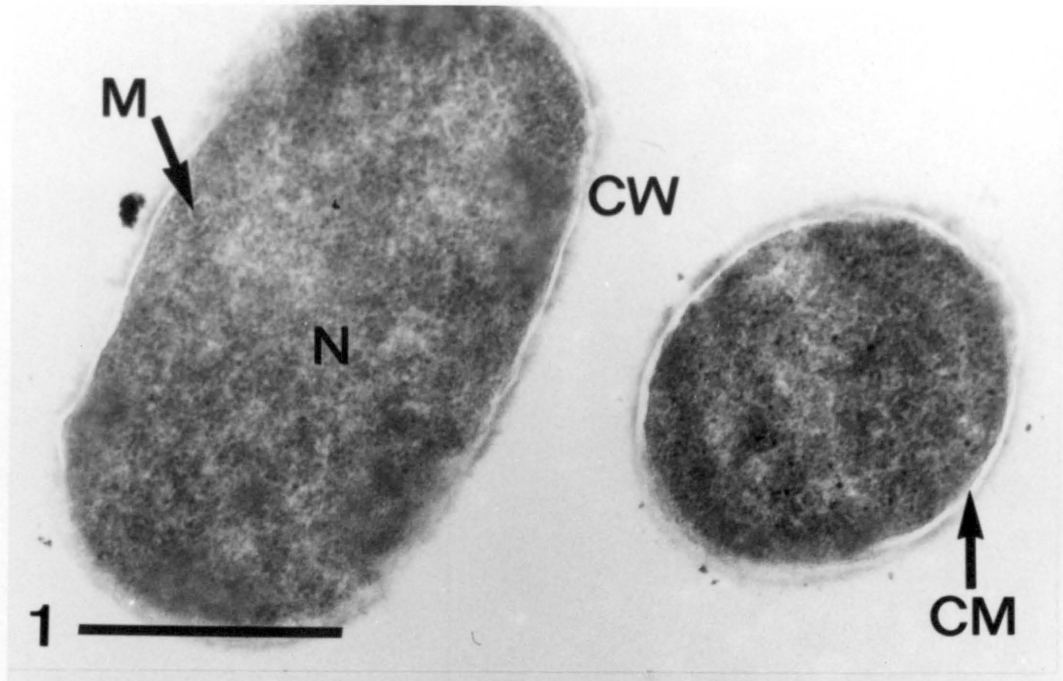
M
CW
N
CM
1

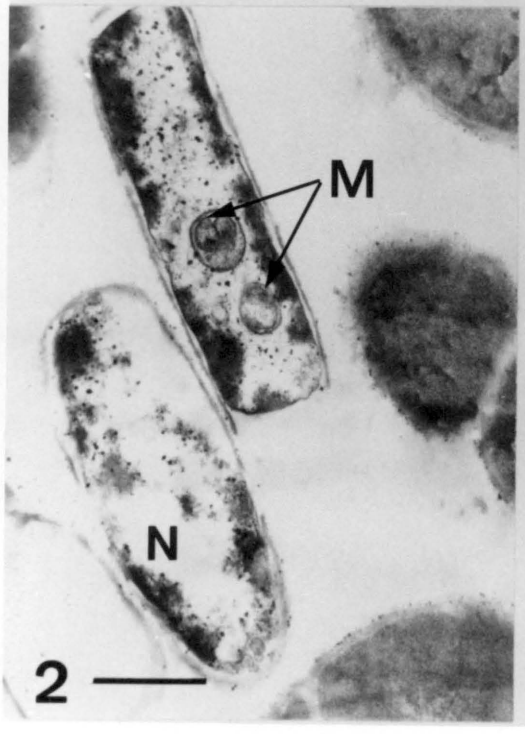
M
N
2

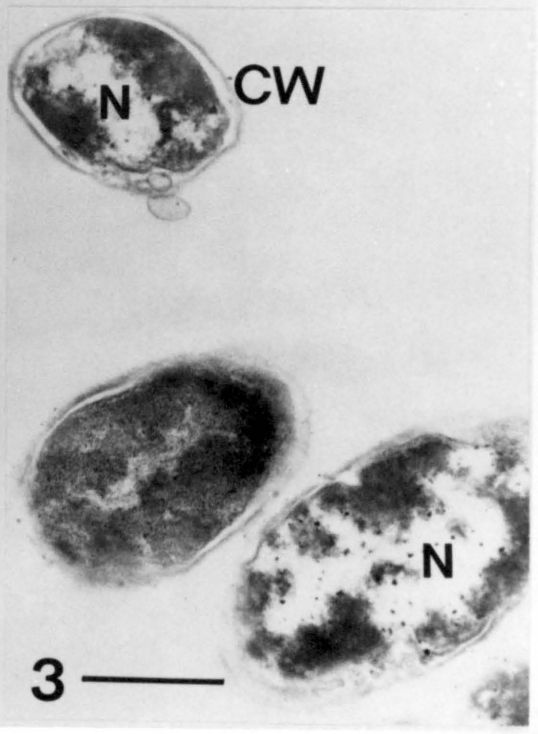
N
CW
N
3

PLATE 7. Transmission Electron Micrographs of the Flashblast treated B. cereus vegetative cells.

Thin sections of treated cells indicating cell wall damage, disorganized cytoplasm and an initiation of lysis.

CM-Cytoplasmic membrane, CW-Cell wall,
N-Nuclear material and wf-Wall fragments.

1. Flashblast treated B. cereus vegetative cells (x 77,000) showing disrupted cell walls. Scale bar measures 0.5 μm.

2. Flashblast treated B. cereus vegetative cells (x 29,000) indicating occurance of lysis. Scale bar measures 1 μm.

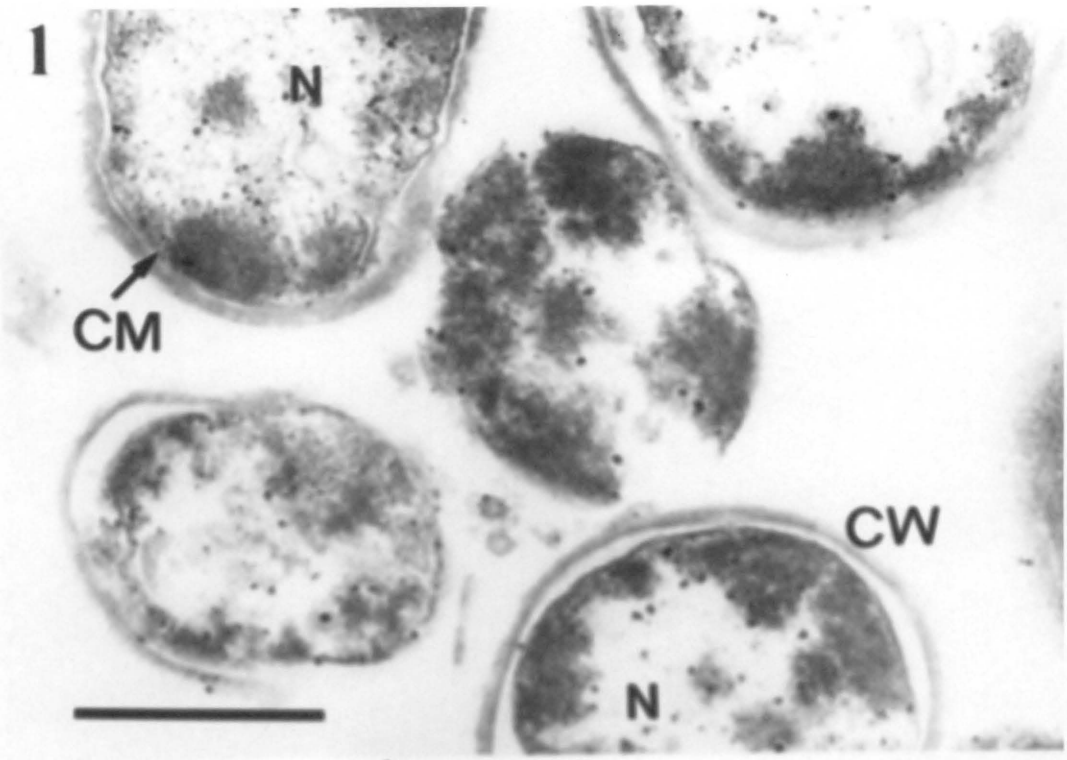
1
N
CM
CW
N

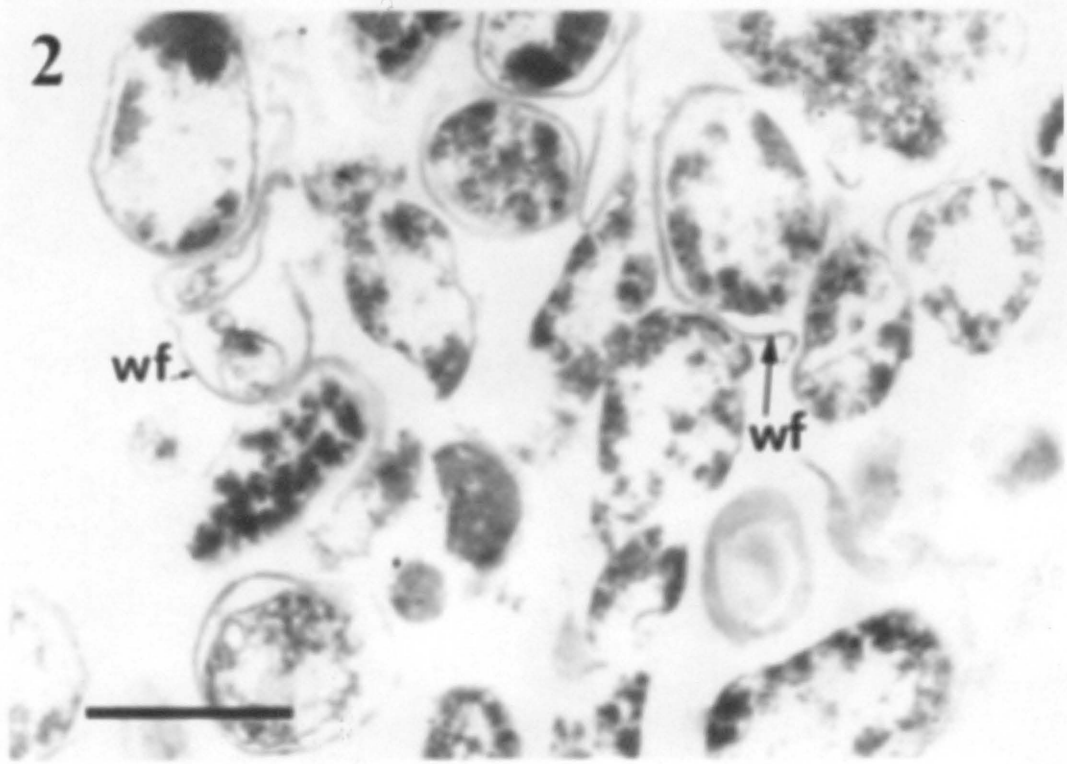
2
wf
wf

PLATE 8. Transmission Electron Micrographs of the control B. subtilis vegetative cells.

Thin sections of control B. subtilis vegetative cells show general features of a gram positive Bacillus microorganism. Intact cell walls are observed in most of the sections and there is no sign of lysis. The particle deposit on the cell walls may have occured as a methodology artifact.

CW-Cell wall, CM,cm-Cytoplasmic membrane and N-Nuclear material.

1. A group of control B. subtilis vegetative cells (x 19,500).
   Scale bar measures 0.5 μm.
2. A control cell (x 66,500) showing a continuous cytoplasmic membrane.
   Scale bar measures 0.5 μm.
3. A control cell (x 34,500) preparing for a cell division.
   Scale bar measures 0.5 μm.
4. Control cells (x 41,500).
   Scale bar measures 0.5 μm.

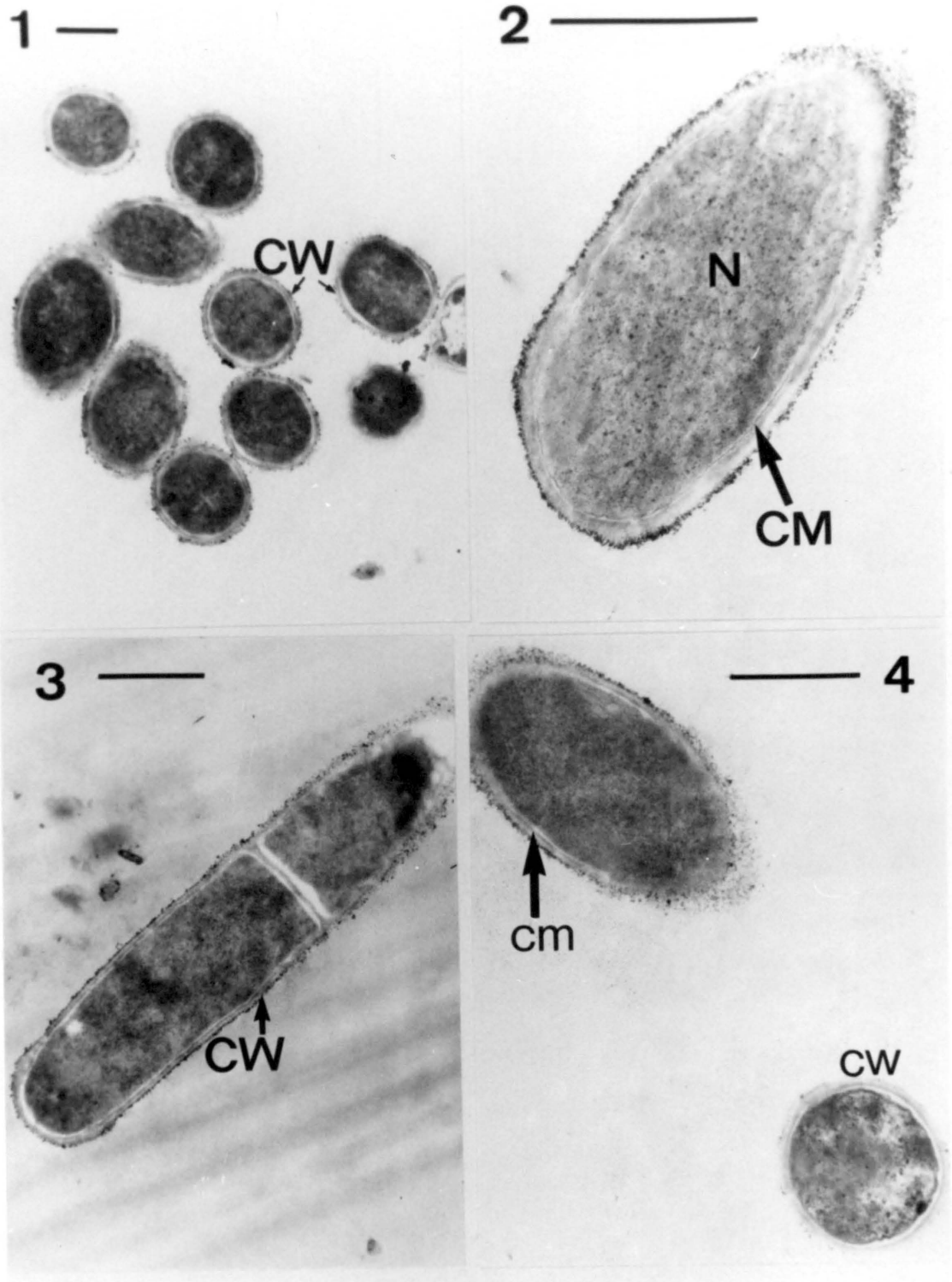
1
CW
2
N
CM
3
CW
4
cm
CW

PLATE 9. Transmission Electron Micrographs of the Flashblast treated B. subtilis vegetative cells.

Thin sections of Flashblast treated B. subtilis vegetative cells indicate a cell wall damage, disorganized cytoplasm and an initiation of lysis. CW-Cell wall, cm-Cytoplasmic membrane, M-Mesosomes and N-Nuclear material.

1. Treated cells (x 46,000) indicating plasmolysis and disruption of cell walls.
   Scale bar measures 0.5 μm.

2. A treated cell (x 70,000) with a broken cell wall.
   Scale bar measures 0.5 μm.

3. A treated cell (x 20,000) preparing to divide indicating a leakage of electron dense aggregates of cytoplasmic constituents.
   Scale bar measures 0.5 μm.

4. Same cell as figure 3 but at a higher magnification (x 55,000) showing the leakage site in detail.
   Scale bar measures 0.5 μm.

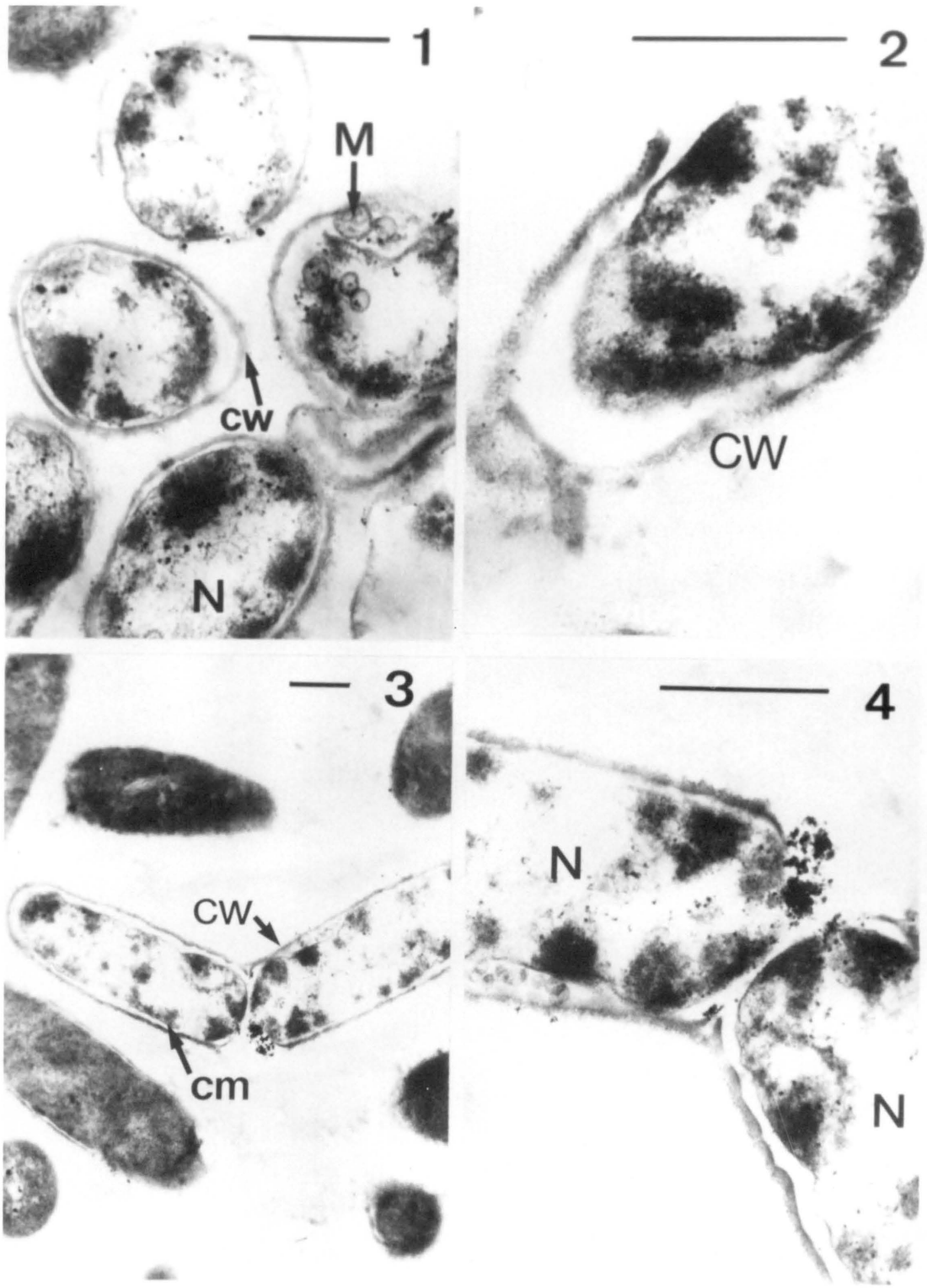
1
M
cw
N
2
CW
3
CW
cm
4
N
N

PLATE 10. Transmission Electron Micrographs of the control B. cereus spores.

Thin sections of Bacillus spores in different stages show a thick outer spore coat, a laminated inner spore coat, a non-staining cortex and a weakly stained inner spore core with its cytoplasmic membrane and germ cell wall.

ex-Exosporium, SC-Spore coat, n-Nuclear material and C-Cortex.

1. Sporulating B. cereus cells (x 22,000) indicating development of spore coats and cortex.
   Scale bar measures 1 μm.

2. A germinating B. cereus spore (x 66,000) with laminated spore coats and a cortex region.
   Scale bar measures 0.5 μm.

3. Germinating B. cereus spore (x 40,000) with a thin cortex region.
   Scale bar measures 0.5 μm.

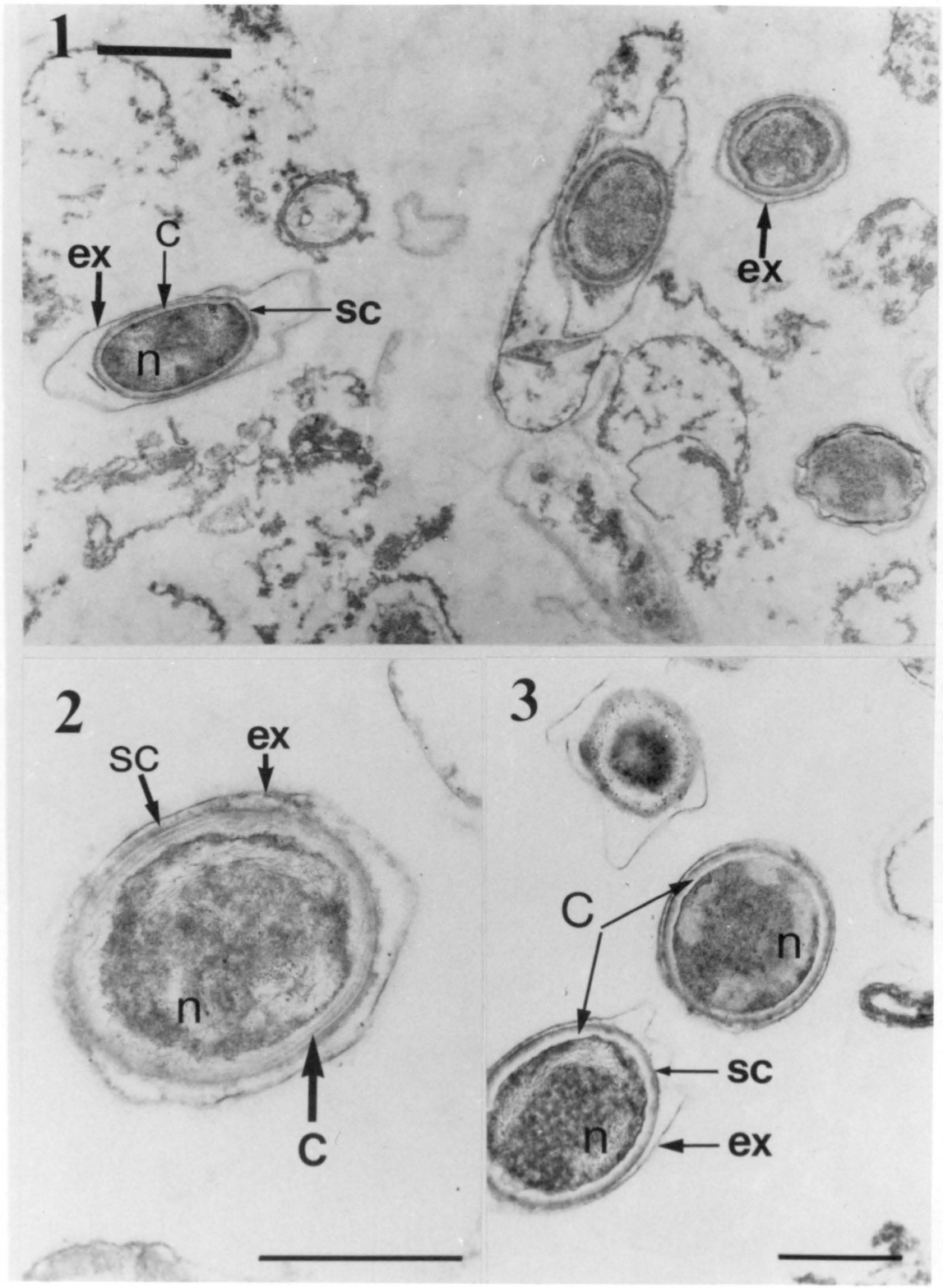
1
ex
C
sc
n
ex
2
SC
ex
n
C
3
C
n
sc
n
ex

PLATE 11. Transmission Electron Micrographs of Flashblast treated B. cereus spores.

Thin sections of Flashblast treated B. cereus spores show disruption of spore coats and lysis.

cyt-Spore cytoplasm, cf-Coat fragments, ex-exosporium, SC-Spore coat, CW-Cell Wall and n-Nucear material.

1. Disrupted spores (x 22,000) indicating coat fragments and electron dense aggregates of the spore protoplast (spore cytoplasm and nucleus). Scale bar measures 1 μm.
2. A convoluted inner membrane is observed in a thin section of germinating spore (x 37,500). Scale bar measures 0.5 μm.
3. A damaged sporulating B. cereus cell (x 27,000) showing a dissolution of forespore cytoplasm and an aggregation of the mother cell cytoplasm. Scale bar measures 0.5 μm.
4. Treated germinating spores (x 32,500) showing coat fragments and cytoplasmic aggregates. Scale bar measures 0.5 μm.

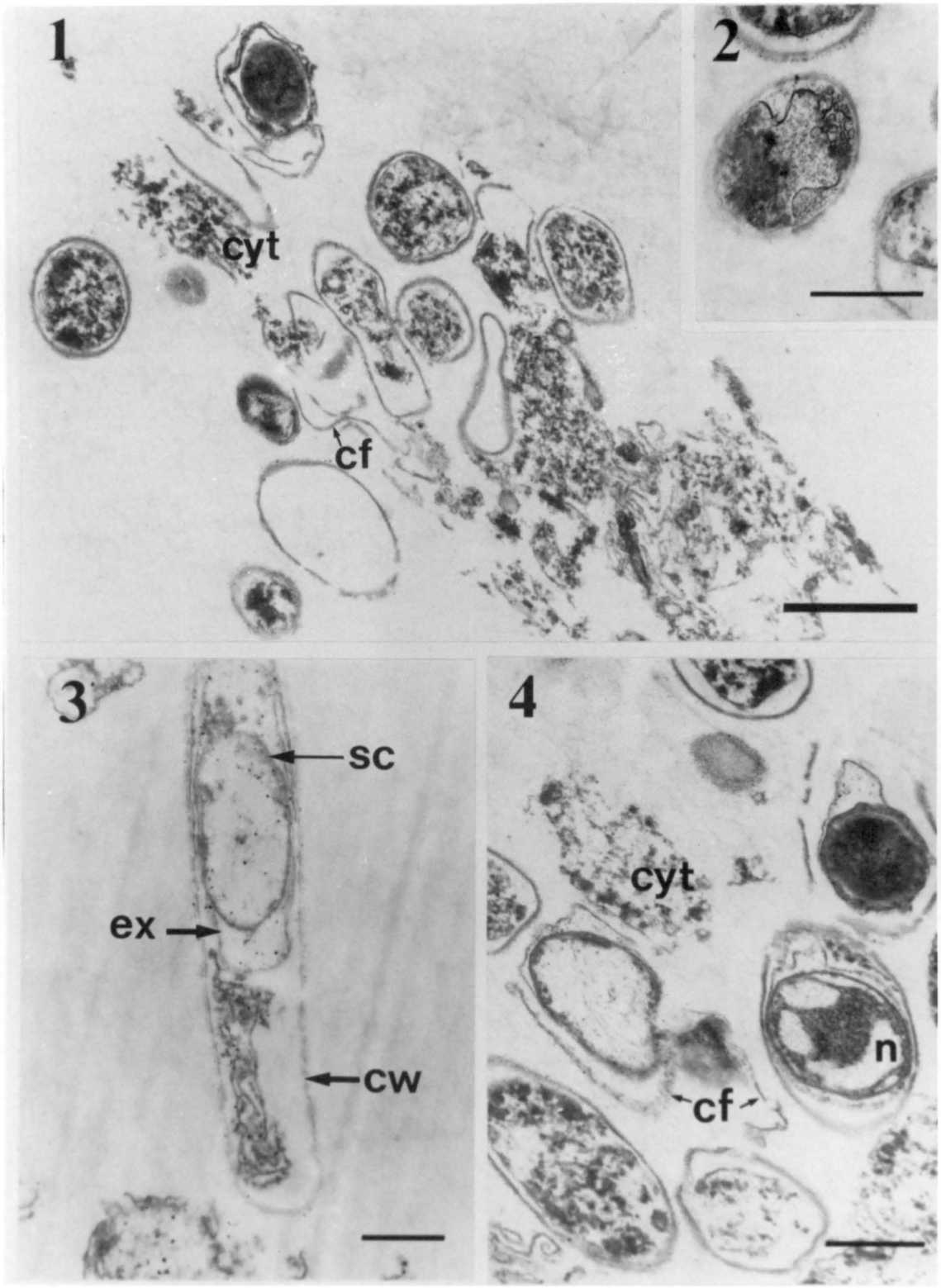
1
cyt
cf
2
3
sc
ex
cw
4
cyt
n
cf

PLATE 12. Transmission Electron Micrographs of the control B. subtilis spores.

Thin sections of germinating and mature B. subtlis spores show general features of a Bacillus spore.

ex-Exosporium, C-Cortex, SC-Spore coat,
N-Spore nucleoid and pm-Protoplasmic membrane.

1. A germinating spore (x 94,000) with a shrunken cortex region.
   Scale bar measures 0.2 μm.

2. A section of a similar spore (x 70,000) with a thickly developed spore coat.
   Scale bar measures 0.2 μm.

3. A mature spore (x 54,500) showing a thick non-staining cortex and a spore coat.
   Scale bar measures 0.2 μm.

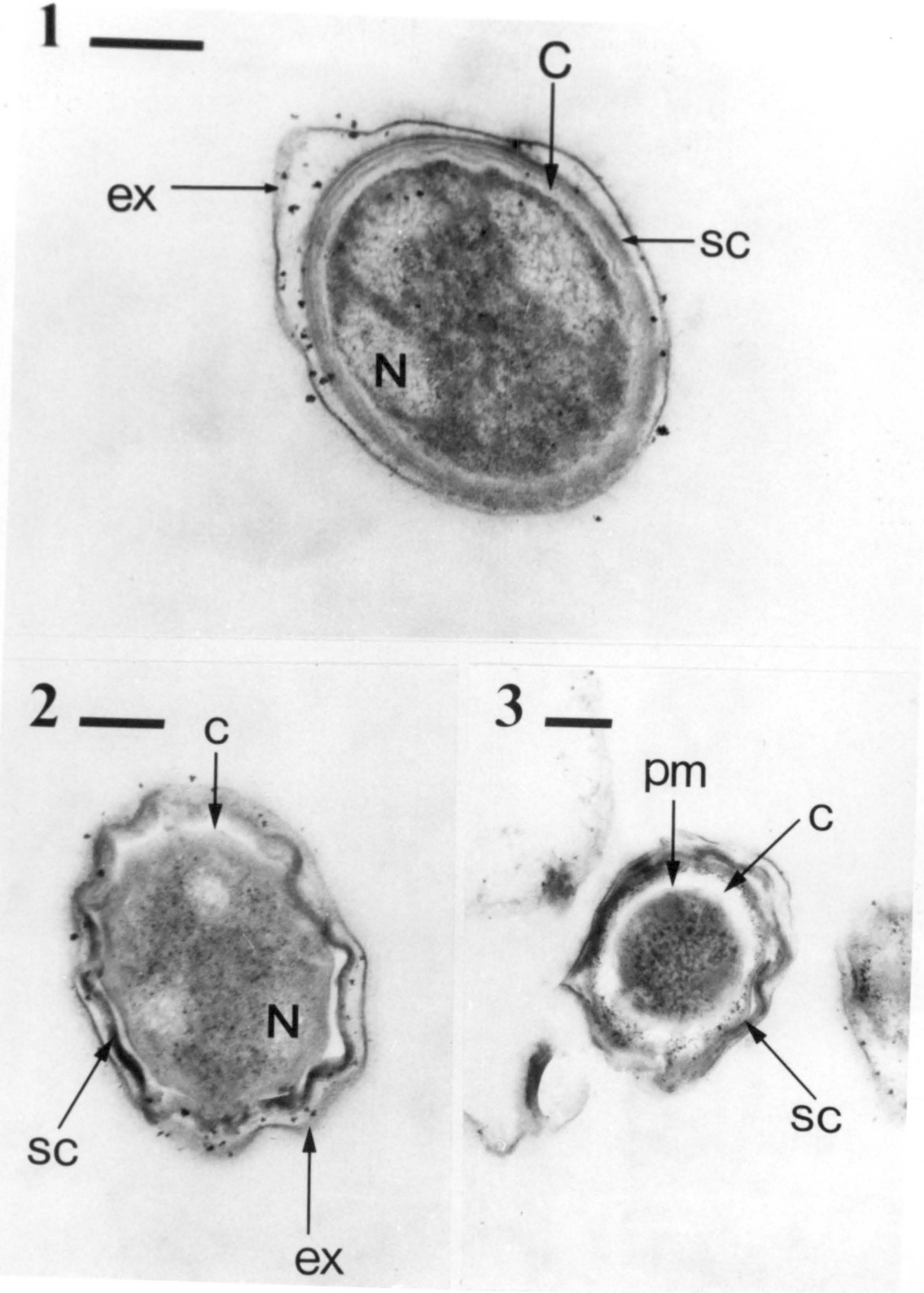
1
C
ex
sc
N
2
c
N
sc
ex
3
pm
c
sc

PLATE 13. Transmission Electron Micrographs of the Flashblast treated B. subtilis spores.

Thin sections of treated spores show disruption of spore coats and lysis.

CW-Cell wall of mother cell, SC-Spore coat, n-Spore nuceoid, C-Cortex, cf-Coat fragments and cyt-Cytoplasmic aggregates.

1. Thin section of a sporulating B. subtilis cell (x 59,500) with a damaged forespore.
   Scale bar measures 0.5 μm.
2. Treated spores (x 41,500) with disrupted and convoluted spore coats.
   Scale bar measures 0.5 μm.
3. Treated spores identical to figure 2 (x 41,000).
   Scale bar measures 0.5 μm.
4. Thin section of damaged spores (x 15,000) indicating a disruption of spore coats, initiation of lysis and an aggregation of electron dense cytoplasm.
   Scale bar measures 1 μm.
5. Damaged spores identical to figure 4 (x 23,500).
   Scale bar measures 1 μm.

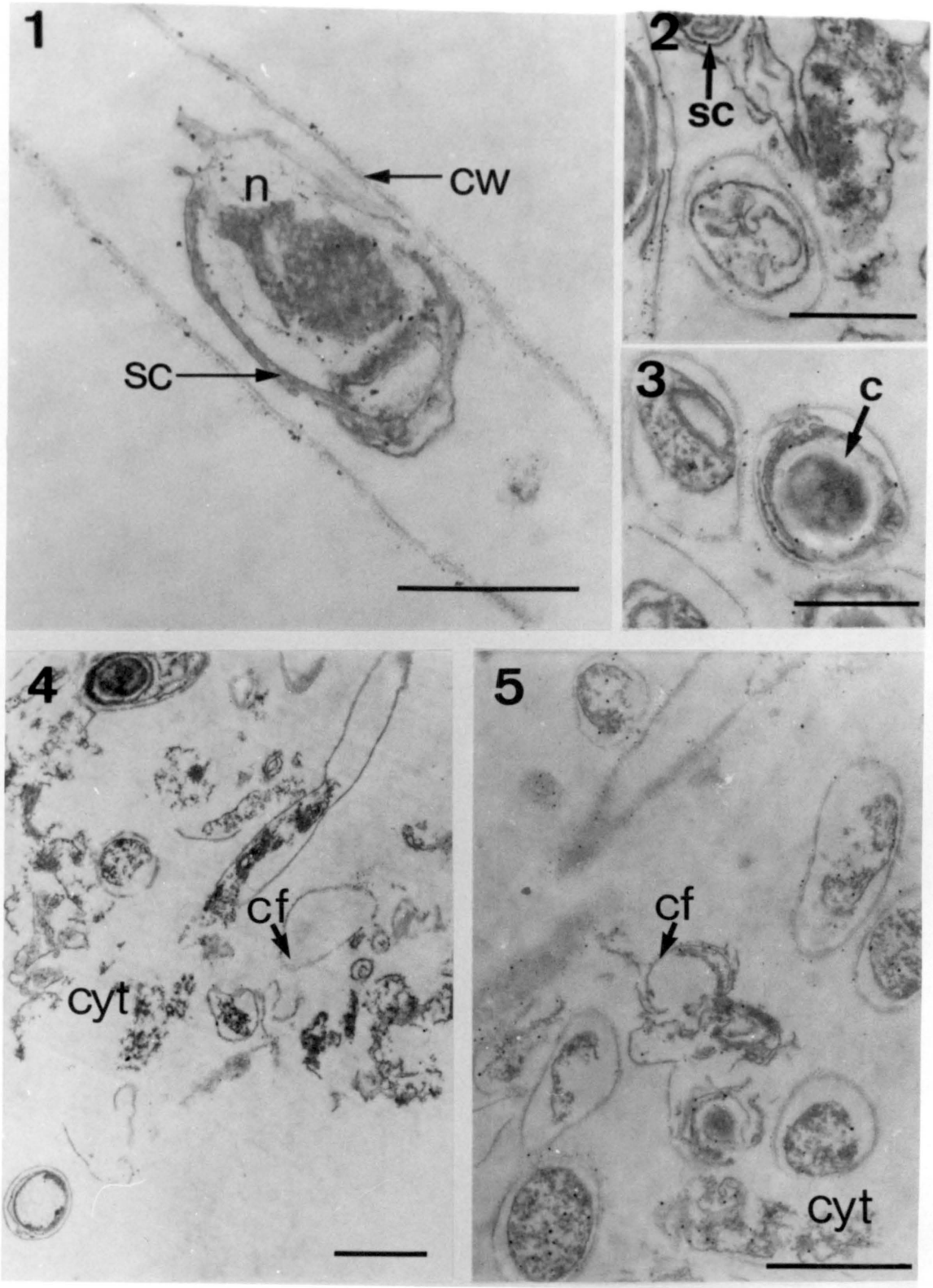
1
n
cw
sc
2
sc
3
c
4
cf
cyt
5
cf
cyt

PLATE 14. Transmission Electron Micrographs of the control A. niger spores.

Thin sections of control A. niger spore show the general features of an Aspergillus mold spore.

OT-Ornamental layer, M-Mitochondrion, SW-Spore wall, MT-Microtubules, PM-Plasm membrane and EB-Electron dense bodies.

1. A control A. niger spore (x 36,500) indicating presence of mitochndrion and microtubules.
   Scale bar measures 0.5 μm.

2. A control spore (x 32,500) showing electron dense bodies.
   Scale bar measures 0.5 μm.

3. A spore similar to figure 2 (x 25,000) with a few electron dense bodies.
   Scale bar measures 0.5 μm.

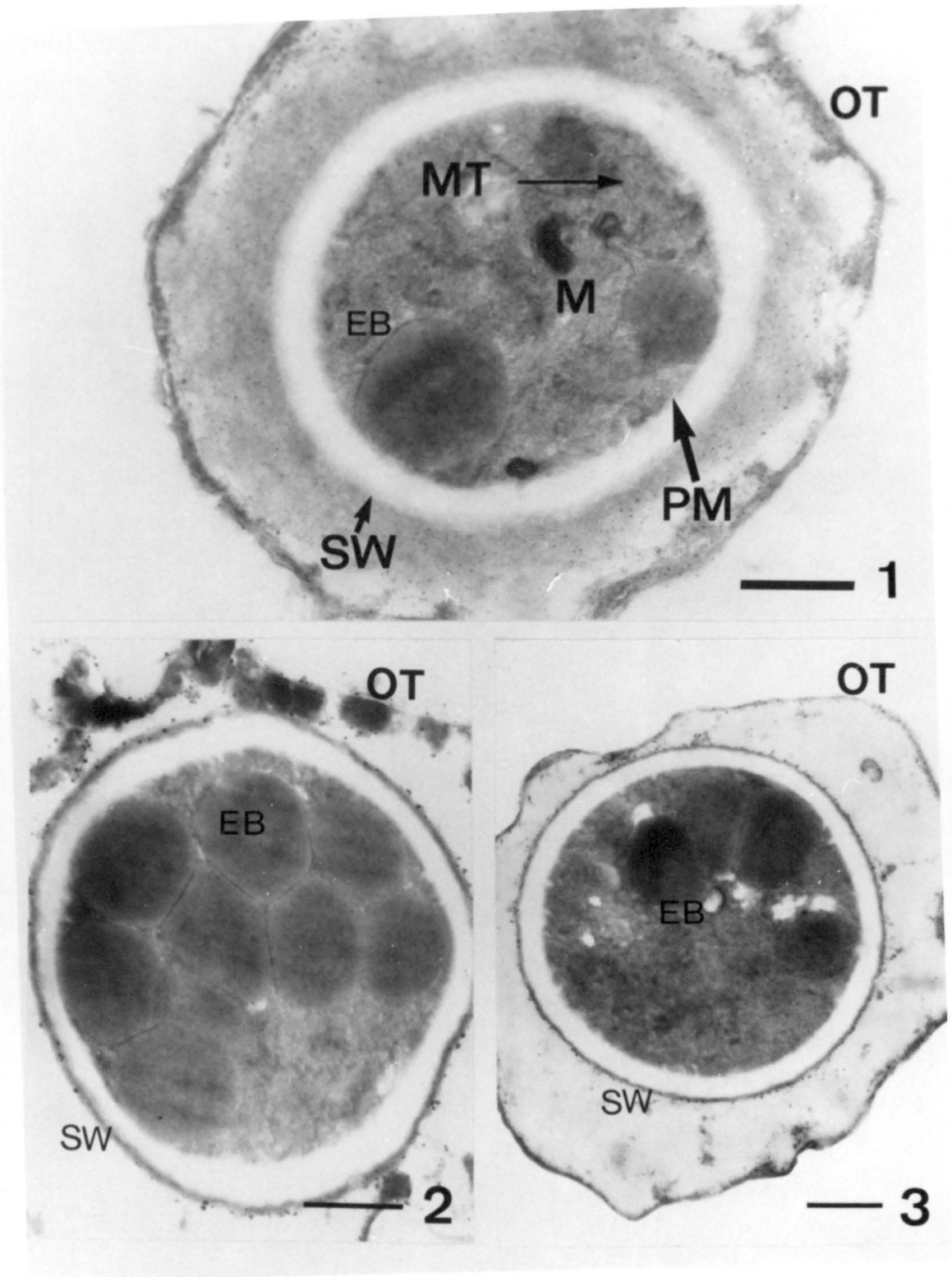
OT
MT
M
EB
PM
SW
1
OT
EB
SW
2
OT
EB
SW
3

PLATE 15. Transmission Electron Micrographs of the Flashblast treated A. niger spores.

Thin sections of treated spores indicate a damage and disruption at different sites.

OT-Ornamental layer, L-Lipid bodies, PM-Plasma membrane, F-Fragments of microtubules, SW-Spore wall, MF-Mitochondrion fragments and DN-Disrupted nuclear membrane.

1. A damaged spore (x 24,000) showing condensed protoplasm with lipid bodies and the dispersed spore walls.
   Scale bar measures 1 μm.
2. Microtubular fragments (x 74,000) near the plasma membrane of an treated spore.
   Scale bar measures 0.5 μm.
3. Ultrathin section of a damaged spore (x 38,000) indicating electron dense fragments of mitochondrion and disrupted nucleus.
   Scale bar measures 0.5 μm.
4. Same section as figure 3, photographed at a higher magnification (x 89,000) showing a detailed disruption of double-layered nuclear membrane.
   Scale bar measures 0.2 μm.

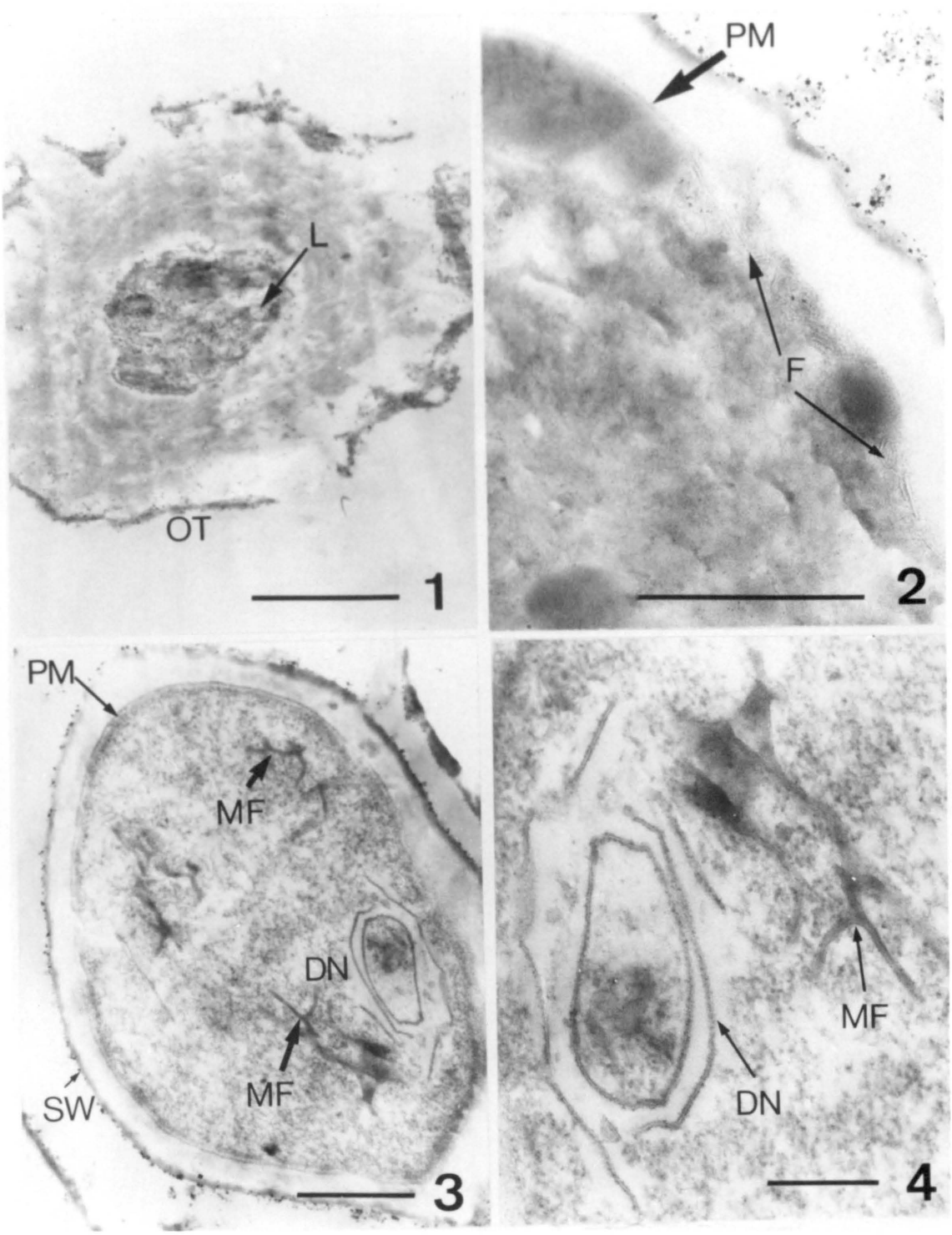
L
OT
1
PM
F
2
PM
MF
DN
MF
SW
3
MF
DN
4

CHAPTER 6

FOOD ACCEPTABILITY STUDY AND SHELF-LIFE EVALUATION OF SELECTED FOODS TREATED WITH FLASHBLAST LIGHT

6.1 INTRODUCTION

(a) Applications of ultraviolet light on foods and packaging materials

All food products are perishable under certain conditions of storage. They are subject to physiological, chemical and microbial decay depending upon their composition and storage conditions. In general, the most common form of deterioration of foodstuffs is that caused by microorganisms. Ultraviolet light has germicidal properties and it can be used for the inactivation of microorganisms on the surfaces of foods, packaging materials and equipment. Applications of UV light for the surface decontamination of many food products have been reported in the technical literature.

Harrington (1968) reported a 99% reduction in the total viable microbial count when flowing apple cider was treated in a thin film for 40 sec with UV light. The study conducted by Reagan and Smith (1973) evaluated the use of UV light for reducing microbial growth and increasing the retail caselife of beef cuts. Korhonen (1980) examined the effects of high intensity ultraviolet light on microbial

survival, growth rates and formation of oxidative rancidity in beef at the retail level. They found no significant extension in shelf life for all exposure times and intensities employed. Huang and Toledo (1982) demonstrated the effectiveness of reducing initial bacterial counts prior to packaging in prolonging the storage life of fish by UV treatments. Stermer et al., (1987) reported that a treatment dose of 150 mW s/cm^2 to 500 mW s/cm^2 reduced bacteria on smooth surface meat (beef plate) by approximately 2 to 3 log cycles. Their experimental results indicated that UV treatment of meat carcasses could effectively increase the lag phase of bacteria multiplication until adequate cooling had occurred.

Ultraviolet sterilization of containers for aseptic packaging could be used in form-fill-seal operations (Maunder, 1975). Bayliss and Waites (1979, 1982) suggested the combination of hydrogen peroxide and UV for killing bacterial spores on packaging materials used in aseptic filling. They indicated that the use of a high intensity UV lamp combined with low levels of hydrogen peroxide will allow rapid sterilization of packaging surfaces contaminated with fungal or bacterial spores.

(b) Environmental applications of ultraviolet light

UV light is widely employed in a variety of environmental applications. Galpin et al., (1985) evaluated continuous UV and chemical disinfection of a circulating

water system by studying the effectiveness of UV light versus halogenation with Legionella spp and Pseudomonas aeruginosa. They concluded that UV light disinfection may be an appropriate alternative or suppliment to chemical biocides. Disinfection of wastewater treated by UV light is gaining increasing acceptance as an alternative to the more traditional process of chlorination. There are more than 50 UV units in operation at U. S. wastewater treatment plants and more than 70 are in the design or construction phase (Kreft et al., 1986). Crandall (1986) used the combined effects of UV light and hydrogen peroxide (H_2O_2) to disinfect waters in public spas and hot tubs. He found that the UV-H_2O_2 process compared favorably with the chlorination process to control the high rate of contamination from both bacteria and non-biological organic materials commonly found in public hot-water recreational facilities.

Nagasawa et al., (1970) described the use of UV light in operating rooms and other locations, as well as in procedures such as the treatment of contaminated linen and during bed making, in hospitals in Japan. Greene (1970) pointed out in more general terms the use of UV in air and surface disinfection in American hospitals. Ultraviolet light may be used to remove ethylene from air or low oxygen atmospheres employed in the storage of fresh fruits and vegetables (Shorter and Scott, 1986).

6.2 PRELIMINARY ACCEPTABILITY STUDY OF SELECTED FOODS TREATED WITH FLASHBLAST LIGHT

MATERIALS AND METHODS

A preliminary food acceptability study was conducted with Flashblast in order to determine which combinations of energy densities and flash sequences could be applied to various food products without noticeable changes in either flavor or color characteristics. The following food products were chosen for the acceptability studies:

(1) Slices Beef Bologna (Oscar Mayer)

(2) Sliced Turkey Breast (Golden Star by Armour)

(3) American Pasteurized Process Cheese (Kroger)

(4) Natural Sliced Swiss Cheese (Kroger)

(5) Whole Almonds (Kroger)

(6) Sliced Almonds (Kroger)

(7) Snack Rye Bread (Country Oven)

(8) Almond Supreme Cookies (Pepperidge Farm)

(9) Lemon Flavored Candies (Brachs)

(10) Graham Crackers (Kroger)

(11) Dry Roasted Peanuts (Planters)

In order to observe undesirable flavor and color changes at a considerably higher Flashblast intensity, the experiment was performed with three capacitors and full (58%) voltage adjustment which corresponded to an input energy of 2053 J. The distance between the Petri plate containing a food product and the lamp head was maintained

at 10 cm. These parameters resulted in a surface energy density of 0.38 J/cm^2. The food products were spread in a monolayer within a one inch wide area at the center of the Petri plate to ensure a uniform distribution of Flashblast light. Only one flash was applied to each food product. Approximately 30 minutes after the treatment, all samples were evaluated by an experienced sensory panel for changes in odor, flavor and color using a 9-point hedonic scale. An untreated control was also presented to the panel. All the samples were blind tasted in order to determine the difference between the treated product and control.

RESULTS AND DISCUSSION

A slight change in odor was percieved when the products were evaluated immediately after treatment, however, the odor was noticeable only for a few seconds. After five minutes, it disappeared and no difference in the odor between the control and treated samples was detected. The odor of the treated samples may be due to characteristic gases, such as ozone, generated by very high intensity UV light. This odor was found to be a typical Flashblast odor which appeared similar (though with a varying degree of notes) among all food products tested.

None of the eleven products evaluated showed any significant difference in odor or flavor between the control and treated samples. The treated samples showed no visible appearance of surface burning or discoloration.

A preliminary experiment using three flash sequences on the samples of Turkey Breast and Graham Crackers was performed as previously described. A slight but insignificant Flashblast odor was observed which eventually disappeared within 10 minutes. No development of discoloration was observed by the panel. This indicated that application of multiple flashes may result in some temporary loss of a characteristic flavor without a detectable alteration of the original flavor.

It is important to note that under similar conditions, preliminary experiments with four microorganisms showed a drastic reduction in number of bacteria even when the distance between the Petri plate and the lamp head was increased to 60 cm. At a distance of 10 cm, as in case of the flavor experiments, 3 or 4 log cycle reductions in the original microorganism population was easily achieved. This clearly suggests that Flashblast treatment can inactivate or destroy food surface microorganisms, thereby extending their shelf-life without significantly altering color, flavor or odor. The potential application of Flashblast treatment for surface sterilization of foods appears promising.

The food products utilized in this experiment were identical to a previous study conducted by Julio Hidalgo. Our data are contrary to those previously reported as the highest treatment did not alter the odor, flavor or color of the food samples.

The modified Flashblast apparatus used in this experiment may be emitting a higher proportion of high intensity ultraviolet light which is responsible for microorganism destruction or inactivation rather than a larger quantity of infrared which may have caused the unacceptable odor due to burning of food components.

6.3 SENSORY EVALUATION AND SHELF-LIFE STUDY OF SELECTED FOODS TREATED WITH FLASHBLAST LIGHT

MATERIALS AND METHODS

The preliminary food acceptability study indicated that Flashblast treatment did not produce detectable changes in color, flavor or odor of the selected food products when the fluence of 0.38 Joules/cm^2 was applied on the surface. In order to compare the flavor profiles of treated samples with the control during storage, the study was modified to include a Triangle evaluation (Roessler et al., 1978) between the control and the treated samples stored at 4°C.

The following food products (Wades Supermarket Brand) were selected for this study:

(1) Home-style bread

(2) Natural sliced swiss cheese

(3) Fresh Strawberries

(4) Sliced turkey breasts

These products are very important from a shelf-life perspective because of their higher susceptibility to

microbial spoilage.

The objectives of this study were:

(1) To evaluate the effect of Flashblast light on the sensory properties of the food products over 16 days of refrigerated storage at $4^{o}C$.

(2) To determine the effectiveness of Flashblast treatment to enhance shelf-life of the food products by performing concominant microbiological and sensory analyses.

The microbiological analysis also enabled the determination as to whether the changes in flavor were due to the Flashblast treatment or a significant microbial population change during storage.

The samples of bread, cheese and turkey breast slices were cut into 3" x 1" size pieces. Each piece was placed in the center of a Petri plate along the X-axis to ensure a uniform distribution of fluence on the surface. The fresh strawberries were trimmed to remove the leaves and arranged together in a sterile Petri plate. For all the samples, a single flash of 0.38 Joules/cm^2 was applied on each side. The control and treated samples were placed inside a sterile plastic 'Whirl Bag' and stored for 16 days at $4^{o}C$.

A triangle test was conducted after 0, 4, 8, 12 and 16 days. All triangle test samples were coded and the nine panelists were served three samples at a time. They were asked to identify the sample that was different from the other two by determining a burnt or a characteristic

Flashblast odor. They were also asked to mention their preference for either the odd or even samples.

The shelf-life study was conducted by determining Total Plate Count (TPC) and Yeast Mold Count (YMC) on the control and treated samples. A portion of the samples withdrawn for sensory evaluation on each of the 16 storage days was used for the microbiological examination.

Eleven g. of each food product sample was homogenized in a stomacher bag with 99 ml of phosphate buffer (pH 7.0). Serial dilutions were then prepared for both the TPC and YMC analyses. A One ml aliquot of each dilution was used for plating. Standard Methods Agar (Difco) was used for determining the total plate count with a subsequent incubation period of 24 to 48 hours at 37^{o}C. For the yeast and mold counts, Potato Dextrose Agar (Difco) was used. The pH was adjusted to 3.5 by adding 1.6 ml of a sterile 1:10 tartaric acid dilution per 100 ml of sterile liquid medium immediately before pouring the agar.

The YMC plates were incubated in the dark at room temperature for 3 to 5 days. The plating for each dilution was performed in triplicate and the average count obtained.

RESULTS AND DISCUSSION

Triangle Test data of the sensory evaluations are contained in Table 1. It was found that there is no significant difference in sensory quality between the control and the treated samples of cheese, strawberries and

turkey breast. The treated bread samples showed a significant difference initially ($p<0.05$), but the characteristic Flashblast odor disappeared by the fourth day of storage. For the remaining food samples, the numbers of correct judgements were not significant at $p \leq 0.05$. This indicated that the panel did not have the ability to differentiate between the treated and control. The number of correct judgements for the control and treated samples varied during the storage period. The treated samples of cheese, strawberries and turkey breast were frequently preferred while the treated samples of bread were disliked by some of the panel members.

Table 2 shows the total plate counts and yeast and mold counts of the stored samples. The data indicates that the control and the treated samples of cheese and turkey breast did not show a significant difference in microbial population ($p\leq0.05$). The treated samples of bread and strawberries contained less microorganisms than the control during the entire storage period.

The room temperature storage study with strawberries and bread indicated a significant difference in texture, flavor and microbiological quality between the control and treated samples ($p\leq0.05$). The TPC and YMC data for the room temperature storage study are presented in Table 3. By the third day of room temperature storage, the control strawberries turned soft and exuded juices and were covered

with a profuse mold growth. The Flashblast treated samples of strawberries remained firm with a slight indication of mold growth on the third day of room temperature storage. However, the shelf-life extension would have been greater had refrigeration been used in the study. Similar results were obtained with the samples of bread when stored for 6 days at room temperature. The curves of the microbial counts versus storage days for all samples are contained in Appendix E.

These results indicate that Flashblast treatment is more effective for strawberries and bread than other two food products and perhaps more useful in preventing mold spoilage. The sensory data shows that bread is more susceptible to Flashblast treatment changes than any other products. This may be because of a higher absorption due to its increased surface area and porous texture. The adverse effect can be minimized to some extent by applying a lower treatment dose. This feasibility study shows promising results for the utilization of Flashblast treatment to extend the shelf-life of bread and strawberries without significantly affecting their characteristic flavor.

Table 1. Triangle test data for the four food products stored at 4°C for 16 days.

Item	Storage (Days)	Correct judgements (Number)	No. of judges liking treated samples	No. of judges disliking treated samples
BREAD	0	6/9*	2	4
	4	5/8	2	3
	8	3/9	2	1
	12	2/8	0	2
	16	3/8	1	2
CHEESE	0	3/9	1	2
	4	4/8	2	2
	8	3/9	3	0
	12	3/8	2	1
	16	2/8	1	1
STRAW-BERRIES	0	4/9	2	2
	4	5/8	3	2
	8	4/9	3	1
	12	3/8	3	0
	16	3/8	2	1
TURKEY BREASTS	0	5/9	2	3
	4	5/8	2	3
	8	4/9	3	1
	12	4/8	2	2
	16	3/8	2	1

* $p \leq 0.05$

Table 2. Shelf-life data of the control and treated food samples stored at 4°C for 16 days.

Item	Storage (Days)	TPC/g		YMC/g	
		Control	Treated	Control	Treated
BREAD	0	7.5×10^1	2.7×10^1	1.4×10^1	0
	4	8.2×10^2	4.6×10^1	9.0×10^1	0
	8	1.3×10^3	1.2×10^2	1.6×10^2	8
	12	8.6×10^3	6.1×10^2	2.5×10^3	2.1×10^1
	16	8.9×10^4	3.2×10^3	9.2×10^3	8.5×10^1
CHEESE	0	1.2×10^4	1.8×10^4	1.2×10^2	8.2×10^2
	4	7.8×10^4	2.6×10^4	4.1×10^3	1.1×10^3
	8	5.3×10^5	5.2×10^5	3.0×10^4	6.0×10^3
	12	2.1×10^6	8.0×10^5	7.2×10^5	6.1×10^4
	16	8.5×10^6	6.4×10^6	9.6×10^6	5.4×10^5
STRAW-BERRIES	0	3.1×10^1	1.8×10^1	1.9×10^1	4
	4	4.2×10^2	9.6×10^1	2.6×10^2	6
	8	8.6×10^2	1.6×10^2	6.4×10^3	8.5×10^1
	12	2.4×10^3	2.1×10^2	3.1×10^4	3.9×10^2
	16	6.0×10^4	2.8×10^2	9.2×10^4	3.2×10^3
TURKEY BREASTS	0	7.2×10^1	3.8×10^1	-	-
	4	1.8×10^3	2.5×10^3	-	-
	8	3.0×10^4	1.6×10^4	-	-
	12	2.5×10^5	4.0×10^5	-	-
	16	5.4×10^6	7.9×10^5	-	-

Table 3. Shelf-life data of the control and treated food samples stored at room temperature for 16 days.

Item	Storage (Days)	TPC/g		YMC/g	
		Control	Treated	Control	Treated
BREAD	0	7.5×10^1	2.7×10^1	1.4×10^1	0
	2	1.8×10^5	2.4×10^3	2.3×10^2	1.2×10^1
	4	2.4×10^7	4.1×10^5	6.0×10^3	1.1×10^2
	6	7.6×10^9	4.2×10^6	4.2×10^5	8.6×10^3
STRAW-BERRIES	0	3.1×10^1	1.8×10^1	1.9×10^1	4.0
	2	7.8×10^4	2.9×10^3	8.6×10^1	1.2×10^1
	4	4.1×10^7	2.8×10^5	4.2×10^4	1.3×10^2
	6	8.6×10^{10}	2.5×10^7	6.7×10^7	3.8×10^5

CHAPTER 7

EFFECT OF FLASHBLAST LIGHT ON EIGHT TYPES OF AFLATOXINS

7.1 INTRODUCTION

Aflatoxins are secondary metabolites of Aspergillus flavus and Aspergillus parasiticus and are the most carcinogenic of the known mycotoxins which are potent liver toxins in all the animals in which they have been tested. Aflatoxins have been found in a wide variety of foods including milk, beer, cocoa, raisins, soybean meal and peanut meal (Jay, 1986). The eight most common types of aflatoxins are B_1, B_2, G_1, G_2, B_{2a}, G_{2a}, M_1 and M_2. The primary products contaminated with B_1, B_2, G_1 and G_2 include peanuts, corn, wheat, rice, cottonseed, copra and nuts. The M toxins are found in milk, eggs and cheese products. Aflatoxins have been produced in whole-rye and whole-wheat breads, tilsit cheese, and apple juice stored at 22°C (Frank, 1968). Higher temperature and moisture environments favor the growth of molds and hence the production of aflatoxins. The toxicity of the six most potent aflatoxins is listed in decreasing order: $B_1 > M_1 > G_1 > B_2 > M_2$ (Ayres et al., 1980). The U. S. Food and Drug Administration has established allowable levels of 20 ppb for food, feeds, and nuts, and 0.5 ppb for milk.

Aflatoxins are intensely fluorescent under long wave UV

light and hence are most readily detected by thin layer chromatography. The aflatoxins are resolved in the increasing order of polarity: B_1, B_2, G_1, G_2 and M_1 (Touchstone, 1982). Miyaki et al., (1967) demonstrated, chemically and biologically, the resistance of aflatoxins to gamma irradiation. Andrellos et al., (1967) studied photochemical changes of aflatoxin B_1 and reported as under:

> "Irradiation of aflatoxins B1 and G1 with UV light (principal wavelength ~365 m) converts both compounds to new fluorescent photoproducts which have much lower R_f values than aflatoxins B1 and G1 when chromatographed on silica gel thin layer plates. Photoproducts of aflatoxin B1 form much faster on a silica gel surface than in methanol solution. Photoconversion of aflatoxin B1 is shown to alter fluorescence comparision assays and identification tests. Studies show that the principal photoproduct developed from aflatoxin B1 is significantly less toxic than the parent aflatoxin."

Waiss and Wiley (1969) reported that ultraviolet irradiation of aflatoxin B_1 in methanol results in addition of methanol across the double bond in the furan ring, giving two isomers, 2-hydro-1-methyl aflatoxin and 1-hydro-2-methoxy aflatoxin. The study conducted by Lillard and Lantin (1970) showed that the exposure of solutions of aflatoxins B_1 and G_1 to UV irradiation for two hours or more resulted in decreased toxicity to chick embryo, altered UV and IR absorption spectra, and the development on TLC plates of compounds with R_f values lower than those of the parent compounds. Wei and Chu (1973) investigated the effect of UV light on the fluorescence intensity of aflatoxins in various solvents and on the photocatalized addition of alchohols and

water to the vinyl ether double bond of aflatoxins B_1 and G_1. The photoproducts resulting from the UV catalized aflatoxin-solvent interaction were found to be less toxic to chicken embryo than the parent toxin.

MATERIALS AND METHODS

Aflatoxin standards of types B_1, B_2, G_1, G_2, B_{2a}, G_{2a}, M_1 and M_2 were obtained from SIGMA Chemical Company (Cat. No. AF-1 and AF-2). All aflatoxins except AF-M_2 were dissolved in chloroform and the concentration of each type of aflatoxin was adjusted to 100 ppm. AF-M_2 was dissolved in acetonitrile to obtain a concentration 100 ppm. The aflatoxin solutions were vigorously agitated for one minute on a Vortex shaker. Pre-coated silica gel TLC plates (EM Science, West Germany) were used for spotting one micro-liter of each aflatoxin solution. The dried spots were treated with Flashblast at an input energy of 2053 Joules. The distance of the spots on TLC plates from the flashlamp remained constant at 5 cm. These parameters corresponded to an incident fluence of 0.76 Joules/cm^2.

Our preliminary single flash experiments indicated no observable effect of Flashblast treatment on B_1 and B_2 aflatoxins. Consequently, the treatment was increased to three consecutive flashes. In order to determine whether the rate of photochemical degradation is dose responsive, AF-B_1 and AF-B_2 were further treated with 15 flashes at the same fluence. All the control and treated TLC plates were

simultaneously placed in the solvent chambers.

The developing solvents used were: (AOAC, 1980)

(1) Chloroform-Acetone-Water (88:12:1.5) for AF-B_1, AF-B_2, AF-G_1 and G_2.

(2) Chloroform-Acetone-Isopropanol-Water (87:10:3:1.5) for AF-B_{2a}, AF-G_{2a}, and AF-M_2.

(3) Ether-Methanol-Water (95:4:1) for AF-M_1.

All the TLC plates with the control and treated aflatoxin spots were developed using the appropriate solvents for 1.5 hr with the solvent front travelling 15 cm. The plates were air dried at room temperature and the spots were visible under long-wave ultraviolet light (366 nm) in a UV detector (Model UVSL-58, Ultra-Violet Products, Inc.). The positions of all fluorescent spots were noted and the R_f values calculated. The TLC plates were photographed in long-wave UV light with a Polaroid camera without using spray reagent.

The spots on all the aflatoxin plates, except the AF-M_2, were scanned with a CAMAG TLC Scanner II using a mercury lamp at 365 nm. AF-M_2 spots were scanned under visible light with the scanner wave length adjusted to zero. The scanning speed was adjusted to 1.0 mm/sec for AF-B_1 and AF-B_2 while for all other aflatoxins, the scanning was performed at 0.5 mm/sec. The sensitivity was set on automatic and spans were varied to obtain an appropriate chromatogram size.

The chromatograms were printed and quantified as area percentages on a CAMAG SP4270 TLC integrator (CS=4, AT=128, PW=6 and PT=12). The positions of all fluorescent spots in the control and the treated plates were determined with respect to their retention times (the time or distance elapsed between the point of injection and the maximum of peak) and each peak area was calculated after normalization.

RESULTS AND DISCUSSION

The Polaroid photographs of all the control and treated TLC plates are shown in Plates 1 and 2. AF-B_1 was found to be the most susceptible aflatoxin to Flashblast treatment as observed in Figure 1 of Plate 1. The control AF-B_1 migrated on a silica gel TLC plate as a single spot with an R_f of approximately 0.58 (Figure 1.a). A treatment with three flashes produced several breakdown products in the vicinity of the starting position as seen in figure 1.b of Plate 1. The molecules of the treated AF-B_1 presumed to be unaffected, travelled the same distance as the control aflatoxin. The decrease in the intensity of this spot suggests a probable decrease in its concentration after photodegradation. This component disappeared completely when 15 flashes were applied (Figure 1.c of Plate 1). Only two fluorescent spots were visible under long-wave UV light; one at the point of injection and the other, a prominent blue-fluorescent spot, with an R_f of 0.07. The intense fluorescent spot at the point of injection indicates that

all the AF-B_1 molecules are not converted into a principal photoproduct with an R_f value of 0.07. The Flashblast treatment may have either substantially altered their polarity, induced polymerization or produced chemical fragmentation, making them unable to migrate with the developing solvent.

Similar treatments on AF-B_2 did not produce breakdown products as seen in Figure 2.b of Plate 1. A treatment with 15 flashes is capable of altering the polarity of some of the molecules that remained as a fluorescent spot at the injection point. There was no visible breakdown product with a different R_f value. AF-G_1 showed additional fluorescent spots near the point of injection when treated with three flashes while AF-G_2 was not affected as seen in Figures 3 and 4 of Plate 1. With AF-B_{2a}, some of the breakdown products possessed higher R_f values than the control aflatoxin. One of the predominant photoproducts was found at an R_f value of 0.64 as seen in Figure 5 of Plate 2.

AF-G_{2a} was found to be less susceptible to Flashblast treatment as compared to AF-B_{2a} (Figure 6 of Plate 2). There were no breakdown photoproducts with different R_f values for treated aflatoxins AF-M_1 and AF-M_2 (Figures 7 and 8 of Plate 2). AF-M_2 had a very poor fluorescence at 365 nm under UV light which is evidenced by the dull gray spots observed in Figure 8 of Plate 2. The chromatograms of the control and treated aflatoxins are presented in Figures 1-4

which indicate similar positions of breakdown products as observed in a UV detector. The peak position, area, retention time, and R_f value of each aflatoxin component is presented in Tables 1 and 2. Based on these data and observations, it may be inferred that aflatoxin B_1 is the most susceptible to Flashblast treatment among all types of aflatoxins. These results are in accordance with the report published by Andrellos et al., (1967). The treated AF-B_{2a} produced several breakdown products with higher R_f values than the control aflatoxin. Aflatoxins B_2, G_1, G_{2a} and M_1 were slightly affected while aflatoxins G_2 and M_2 were not.

This experiment provides preliminary information concerning the effect of Flashblast treatment on eight types of aflatoxins. The results are sufficiantly promising to suggest that Flashblast treatment can induce photodegradation of aflatoxins B_1, G_1 and B_{2a}. Most of the photoproducts were found to be fluorescent at variable intensities under a long-wave UV light. The Xenon lamp used as a source of ultraviolet light in the Flashblast apparatus also emits a significant proportion of visible light.

Hence, there may be some contribution of thermal effects as well as the photochemical breakdown of the aflatoxins. The toxicity of these photoproducts were not evaluated and should be studied in order to establish the potential use of Flashblast treatment to destroy or detoxify aflatoxins from the surfaces of foods, feeds or equipment.

Table 1. Effect of Flashblast treatment on aflatoxins B_1, B_2, G_1 and G_2.

AF-Types and Treatment	Position of the Peak	Retention Time (min)	Area (%)	R_f
(1) Control AF-B_1	1	1.67	100	0.58
Treated (3 Flashes)	1	0.07	2.1	0
	2	0.17	9.7	0.03
	3	0.34	25.5	0.07
	4	0.46	9.6	0.12
	5	1.24	7.0	0.42
	6	1.58	46.1	0.58
Treated (15 Flashes)	1	0.18	34.7	0
	2	0.33	59.5	0.07
	3	0.45	5.8	0.12
(2) Control AF-B_2	1	1.55	100	0.54
Treated (3 Flashes)	1	1.56	100	0.54
Treated (15 Flashes)	1	0.21	2.5	0
	2	1.56	97.5	0.54
(3) Control AF-G_1	1	0.49	14.5	0
	2	0.80	7.2	0.07
	3	1.60	8.4	0.24
	4	2.78	69.9	0.47
Treated (3 Flashes)	1	0.55	14.9	0
	2	0.71	41.2	0.03
	3	1.56	2.8	0.21
	4	2.00	3.0	0.29
	5	2.68	38.0	0.43
(4) Control AF-G_2	1	2.47	100	0.40
Treated (3 Flashes)	1	0.52	1.0	0
	2	0.73	1.5	0.05
	3	2.34	97.5	0.38

Table 2. Effect of Flashblast treatment on aflatoxins B_{2a}, G_{2a}, M_1 and M_2.

AF-Types and Treatment	Position of the Peak	Retention Time (min)	Area (%)	R_f
(1) Control AF-B_{2a}	1	0.34	2.0	0
	2	0.42	2.7	0.03
	3	0.98	2.2	0.13
	4	1.67	53.4	0.29
	5	1.71	39.7	0.29
Treated (3 Flashes)	1	0.35	9.0	0
	2	0.59	2.8	0.03
	3	0.94	4.2	0.13
	4	1.57	65.3	0.25
	5	1.97	5.6	0.32
	6	2.39	3.4	0.41
	7	3.53	9.7	0.64
(2) Control AF-G_{2a}	1	0.35	7.5	0
	2	0.49	11.0	0.03
	3	1.25	76.6	0.19
	4	2.13	1.7	0.37
	5	2.98	3.2	0.52
Treated (3 Flashes)	1	0.34	42.8	0
	2	1.21	17.3	0.18
	3	1.24	18.7	0.18
	4	1.56	3.4	0.25
	5	1.87	2.8	0.31
	6	2.81	3.4	0.50
	7	3.08	11.6	0.55
(3) Control AF-M_1	1	2.39	100	0.42
Treated (3 Flashes)	1	0.39	6.7	0
	2	0.78	2.3	0.07
	3	2.38	38.7	0.42
	4	2.43	52.3	0.42
(4) Control AF-M_2	1	0.38	13.8	0
	2	4.29	7.1	0.83
	3	4.91	79.1	0.92
Treated (3 Flashes)	1	0.35	17.2	0
	2	4.39	10.8	0.82
	3	5.00	72.0	0.94

PLATE 1. Photographs of TLC plates with the control and Flashblast treated aflatoxins B_1, B_2, G_1 and G_2.

1. **AFLATOXIN B_1**
   (a) Control
   (b) Treated with three flashes
   (c) Treated with fifteen flashes

2. **AFLATOXIN B_2**
   (a) Control
   (b) Treated with three flashes
   (c) Treated with fifteen flashes

3. **AFLATOXIN G_1**
   (a) Control
   (b) Treated with three flashes

4. **AFLATOXIN G_2**
   (a) Control
   (b) Treated with three flashes

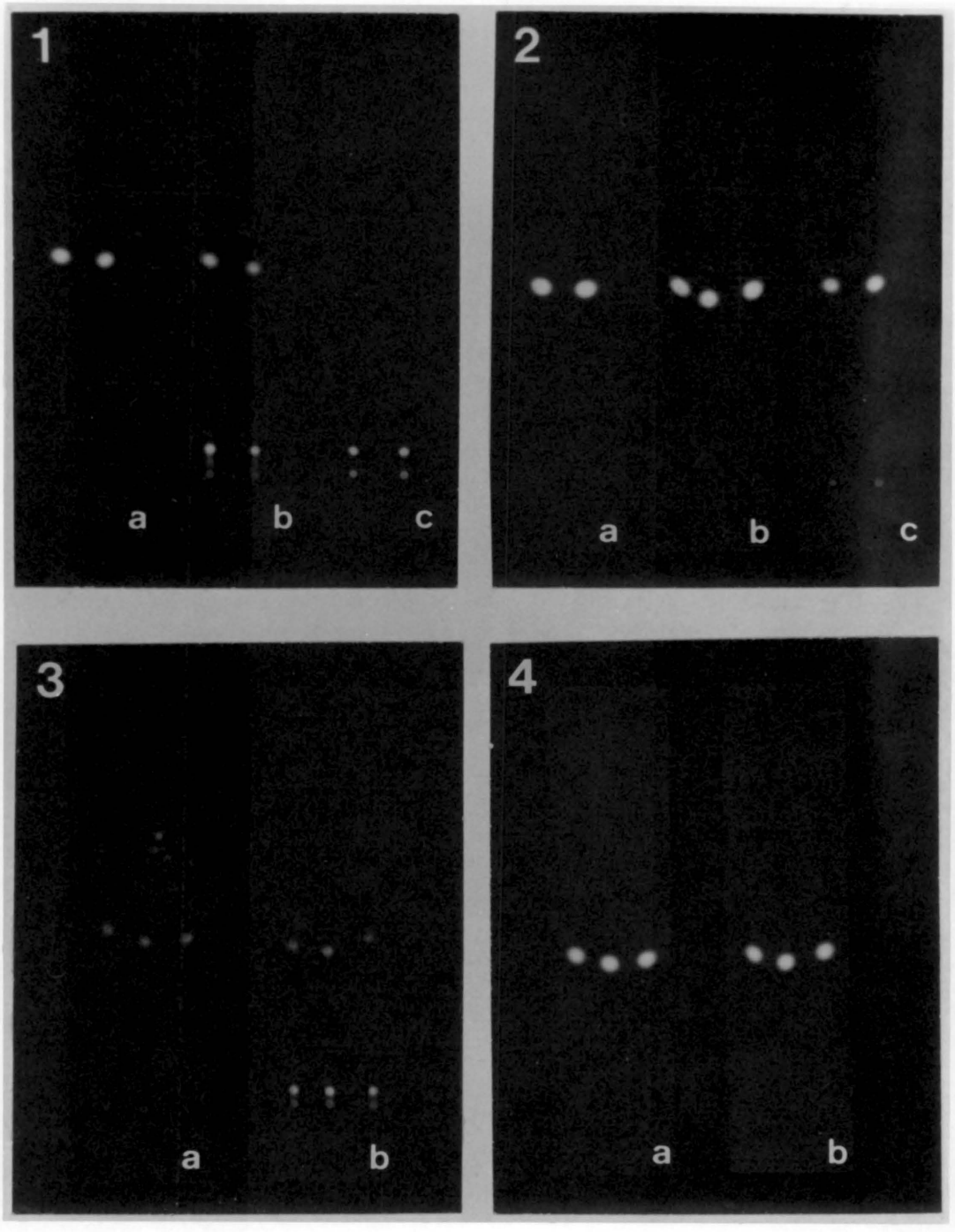
1
a
b
c
2
a
b
c
3
a
b
4
a
b

PLATE 2. Photographs of TLC plates with the control and Flashblast treated aflatoxins B_{2a}, G_{2a}, M_1 and M_2.

5. **AFLATOXIN B_{2a}**
   (a) Control
   (b) Treated with three flashes

6. **AFLATOXIN G_{2a}**
   (a) Control
   (b) Treated with three flashes

7. **AFLATOXIN M_1**
   (a) Control
   (b) Treated with three flashes

8. **AFLATOXIN M_2**
   (a) Control
   (b) Treated with three flashes

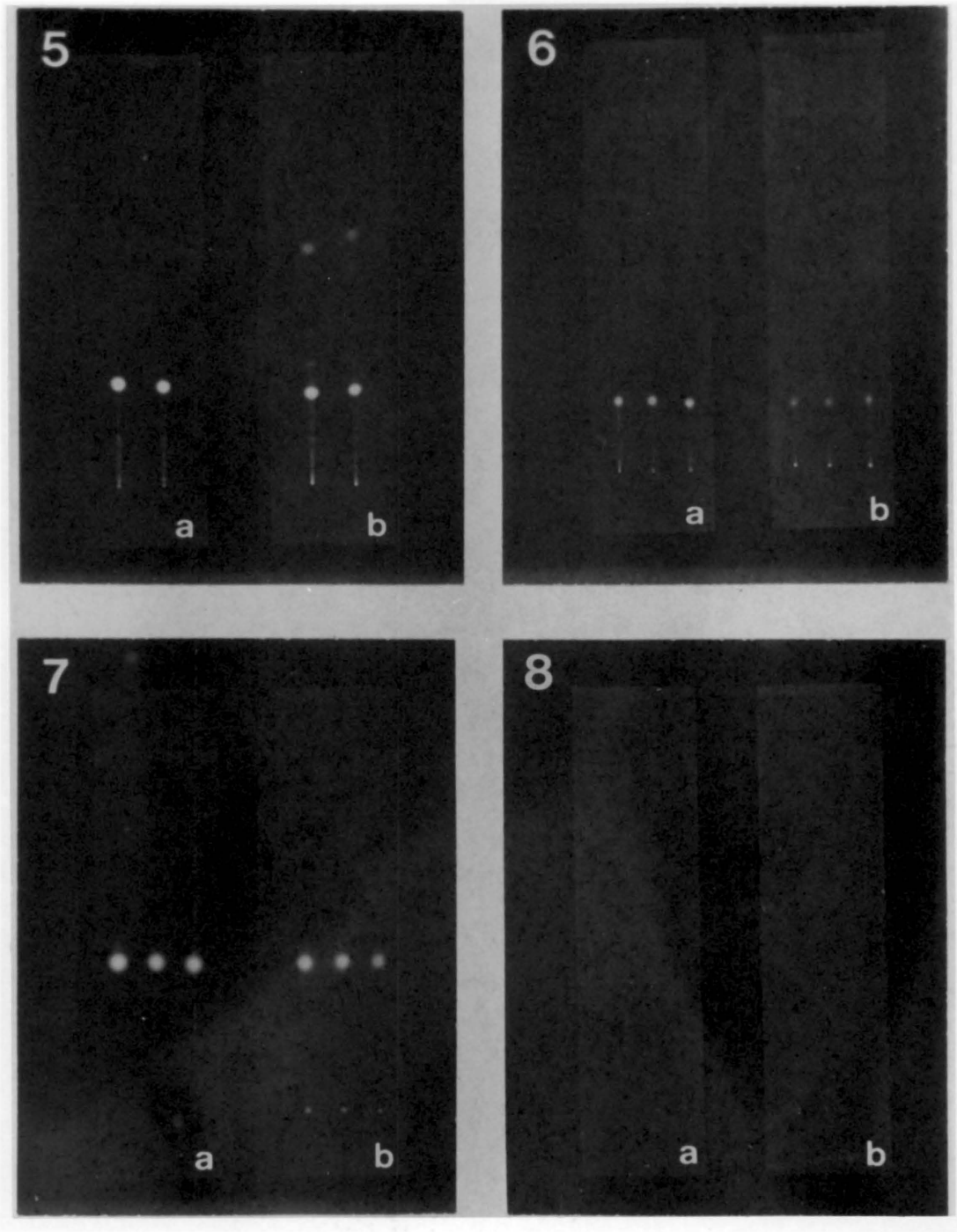
5
a
b
6
a
b
7
a
b
8
a
b

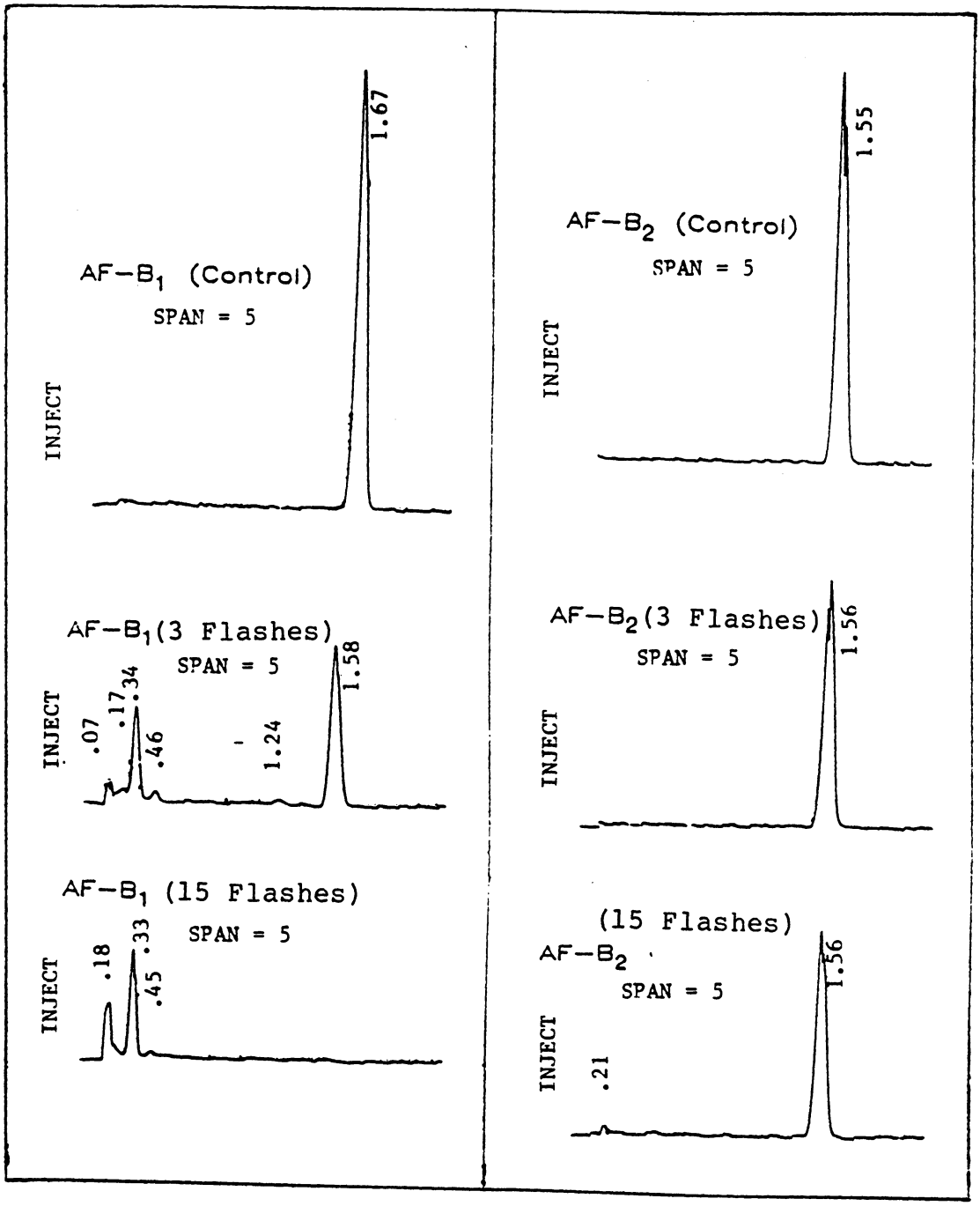

Figure 1. Chromatograms of the control and Flashblast treated B_1 and B_2 aflatoxins.

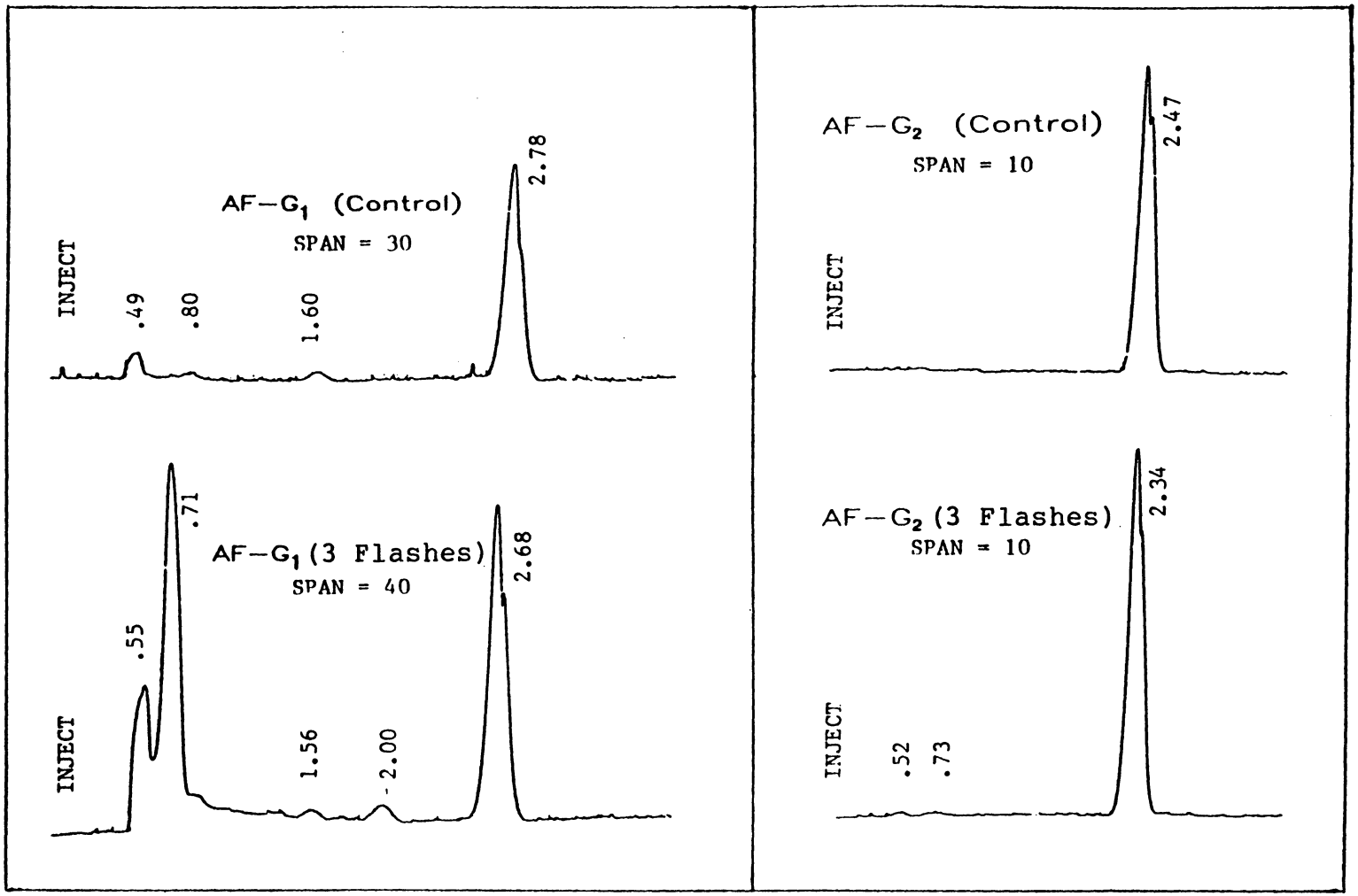

Figure 2. Chromatograms of the control and Flashblast treated G_1 and G_2 aflatoxins.

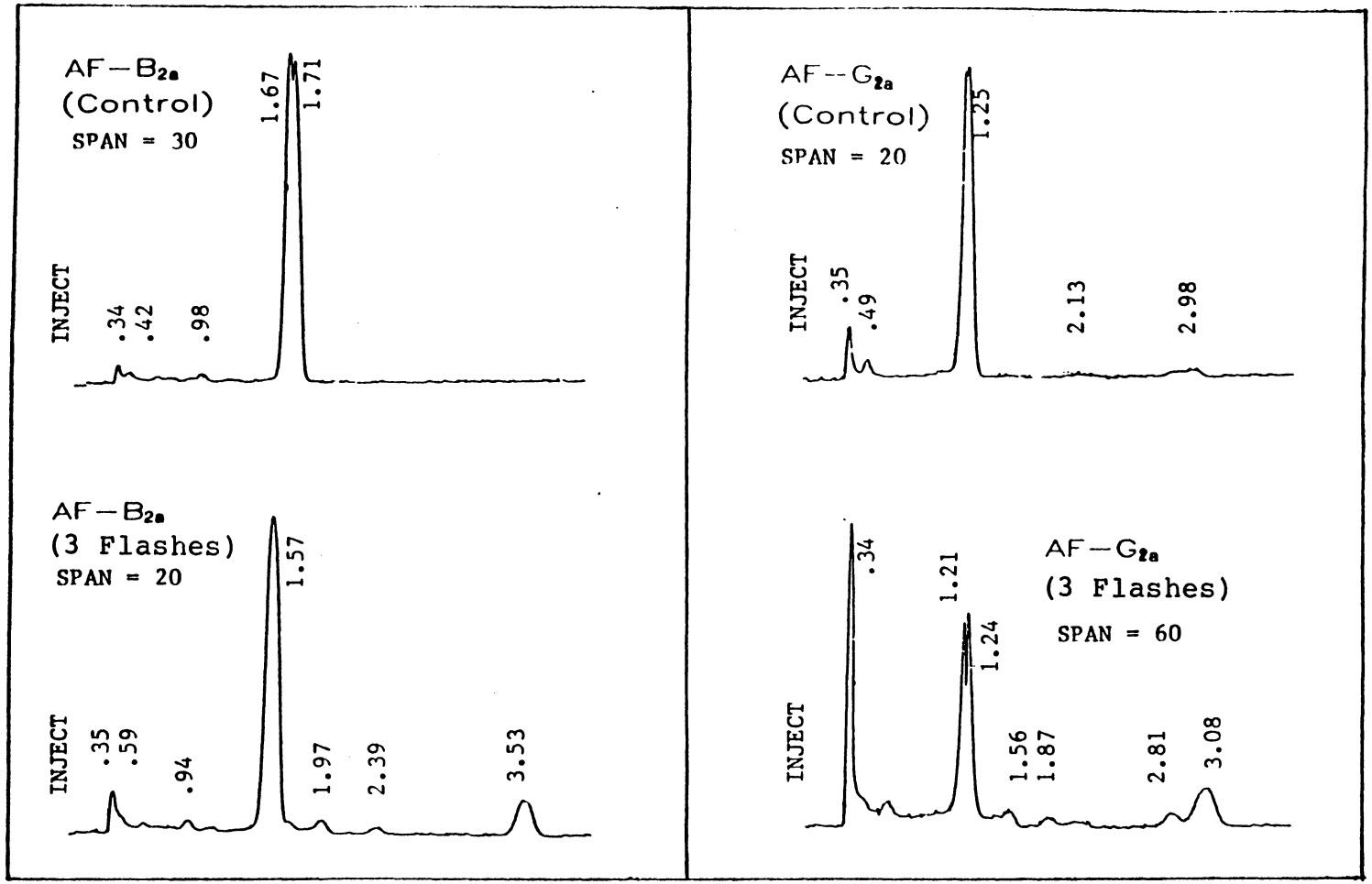

Figure 3. Chromatograms of the control and Flashblast treated B_{2a} and G_{2a} aflatoxins.

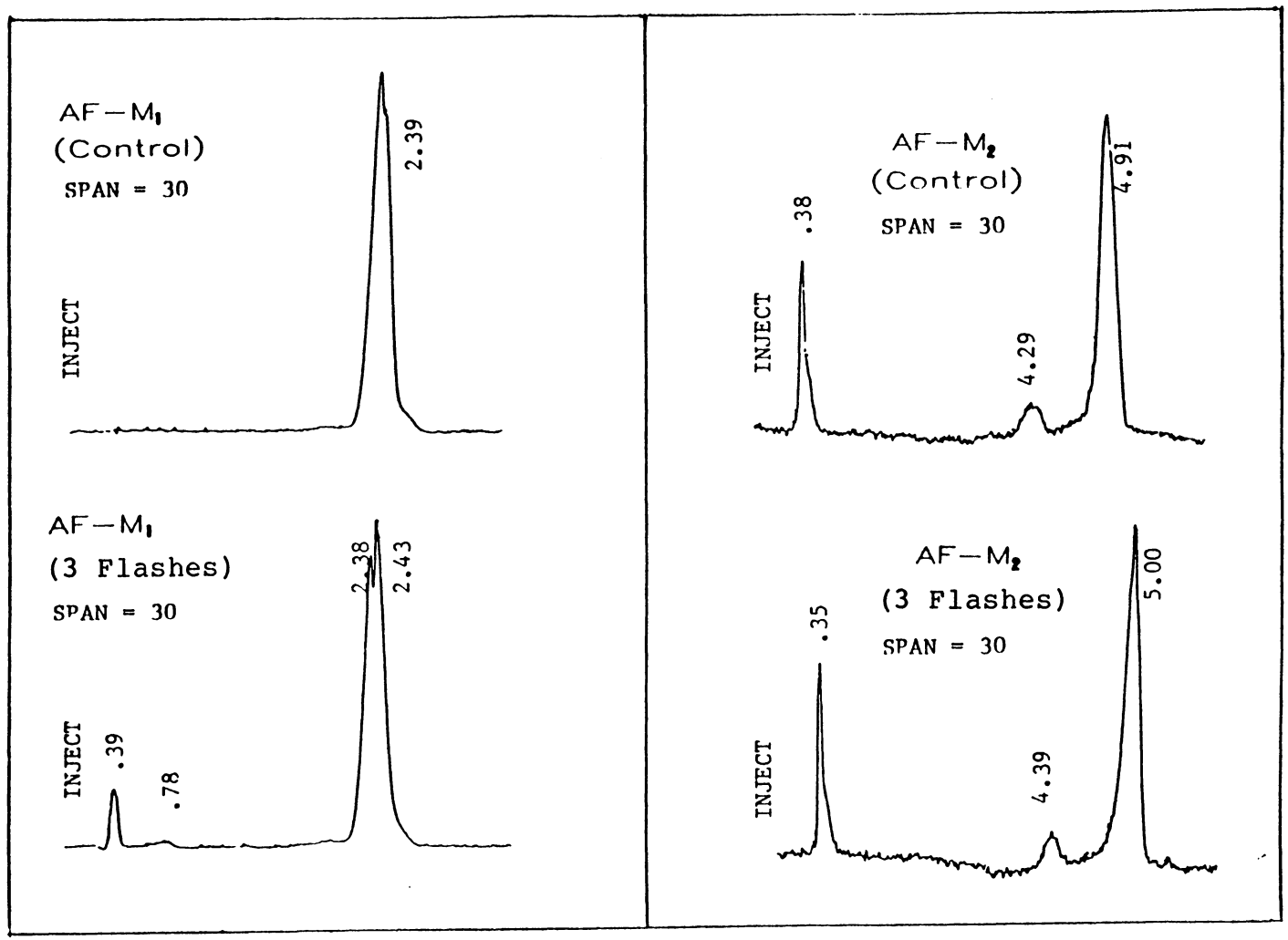

Figure 4. Chromatograms of the control and Flashblast treated M_1 and M_2 aflatoxins.

APPENDIX

A

Surviving Fractions of Microorganisms and LD_{90} Values at Different Input Energies

TABLE 1. Surviving fractions (N/No) of four microorganisms at different input energies after Flashblast treatment.

Input Energy (J)	Dist. (cm)	Fluence (J/cm^2)	Vegetative Cells			
			E. coli	*S. aureus*	*B. cereus*	*B. subtilis*
171	50	0.0043	0.9768	-	-	-
171	40	0.0061	0.9075	0.9433	0.8943	0.9619
171	30	0.0081	0.8250	0.8981	0.7317	0.6571
171	20	0.0173	0.5412	0.5660	0.3740	0.3809
171	10	0.0472	0.1518	0.2113	0.0650	0.1143
406	60	0.0043	0.8316	0.8415	0.7723	0.7714
406	50	0.0087	0.7425	0.6528	0.6666	0.6952
406	40	0.0133	0.5280	0.4830	0.3902	0.4476
406	30	0.0184	0.2570	0.2188	0.1626	0.2666
406	20	0.0357	0.0298	0.0226	0.0000	0.0571
513	50	0.0143	0.9326	0.9615	0.6938	0.7215
513	40	0.0194	0.6205	0.8384	0.5646	0.3411
513	30	0.0296	0.3617	0.5384	0.2789	0.1941
513	20	0.0485	0.0213	0.1615	0.0476	0.0490
1218	60	0.0173	0.1489	0.4769	0.2789	0.2352
1218	50	0.0280	0.0993	0.3538	0.2040	0.1294
1218	40	0.0383	0.0283	0.0692	0.0544	0.0705
1218	30	0.0000	0.0000	0.0000	0.0000	0.0000

TABLE 2. Surviving fractions (N/No) of three microorganisms after Flashblast treatment at different input energies using three capacitors.

Input Energy (J)	Dist. (cm)	Fluence (J/cm^2)	Spores		
			B. cereus	*B. subtilis*	*A. niger*
513	40	0.0194	0.7863	0.8962	1.0000
513	30	0.0296	0.6837	0.7924	1.0000
513	20	0.0485	0.5812	0.7169	1.0000
513	10	0.1225	0.3675	0.1698	0.9821
1218	50	0.0280	0.9230	0.8679	-
1218	40	0.0383	0.6410	0.4905	1.0000
1218	30	0.0510	0.5641	0.4528	1.0000
1218	20	0.0919	0.1795	0.2452	0.8392
1218	10	0.2169	0.0171	0.0377	0.3928
2053	50	0.0485	0.6666	0.5666	-
2053	40	0.0664	0.4188	0.4528	0.9285
2053	30	0.0919	0.1538	0.3396	0.8750
2053	20	0.1735	0.0940	0.0471	0.6428
2053	10	0.3828	0.0000	0.0000	0.1250

TABLE 3a. Fluences (Joules/cm^2) required for a one log cycle reduction (LD_{90}) in the initial population of bacteria vegetative cells at different input energies.

Input Energy	Vegetative Cells			
(J)	*E. coli*	*S. aureus*	*B. cereus*	*B. subtilis*
171	0.052	0.064	0.036	0.050
406	0.021	0.018	0.020	0.027
513	0.023	0.052	0.033	0.035
1218	0.029	0.025	0.030	0.042

TABLE 3b. Fluences (Joules/cm^2) required for a one log cycle reduction (LD_{90}) in the initial population of microbial spores at different input energies.

Input Energy	Spores		
(J)	*B. cereus*	*B. subtilis*	*A. niger*
513	0.360	0.140	*
1218	0.115	0.135	0.420
2053	0.150	0.110	0.360

* Too high to measure

APPENDIX

B

Survival Curves (Surviving Fraction versus Fluence) of Microorganisms at Different Input Energies

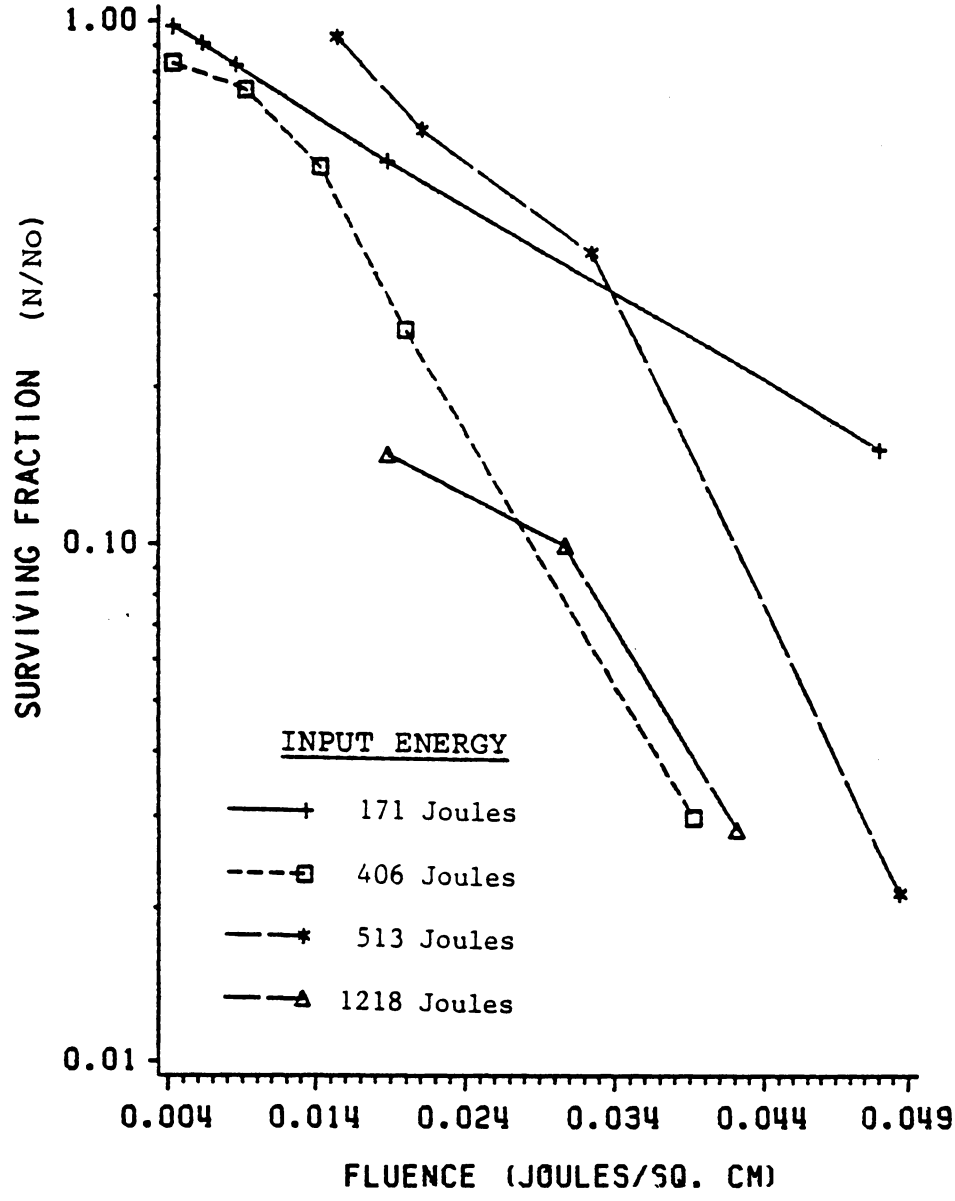

FIG. 1

Survival of E. coli at different Flashblast input energies.

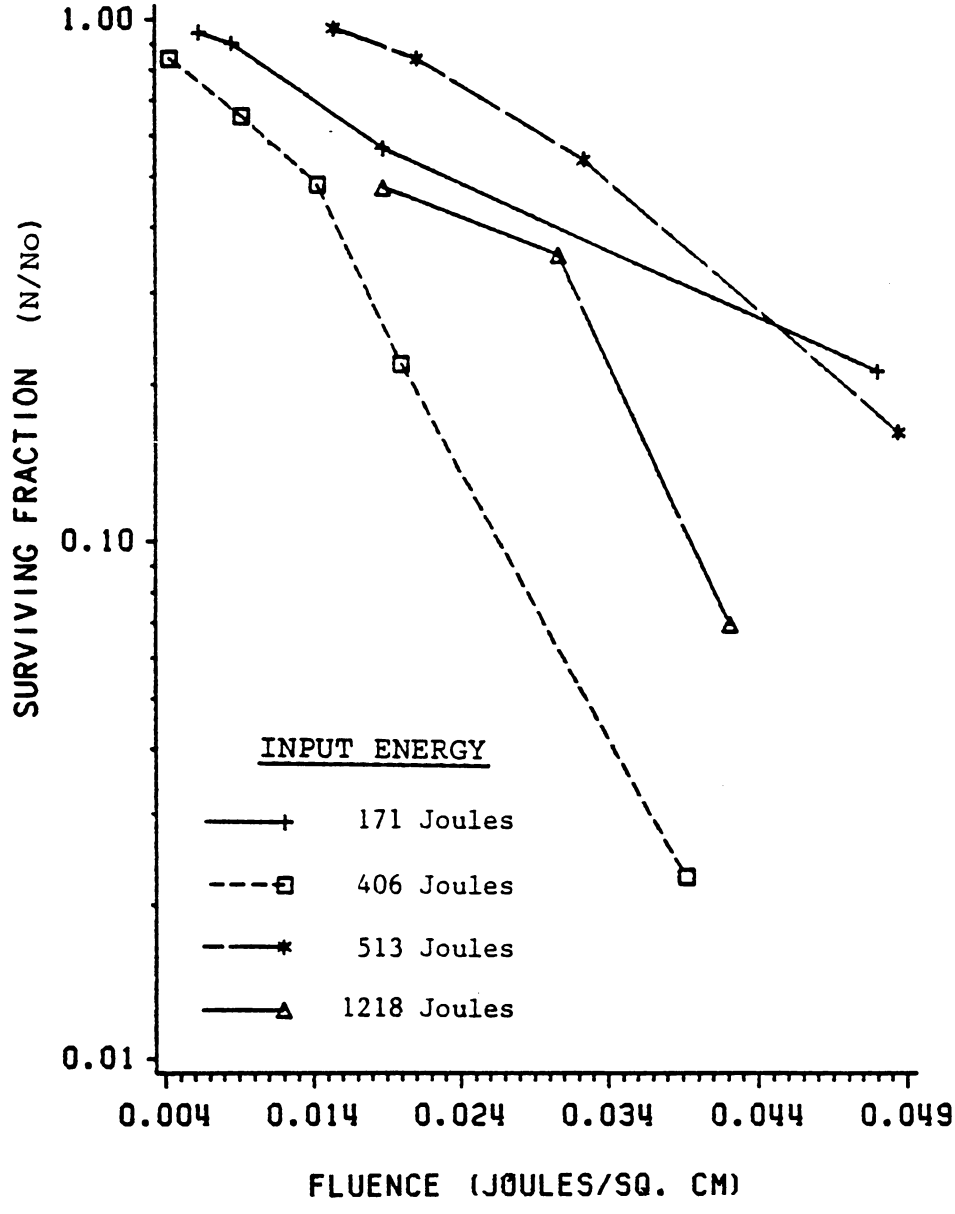

FIG. 2

Survival of S. aureus at different Flashblast input energies.

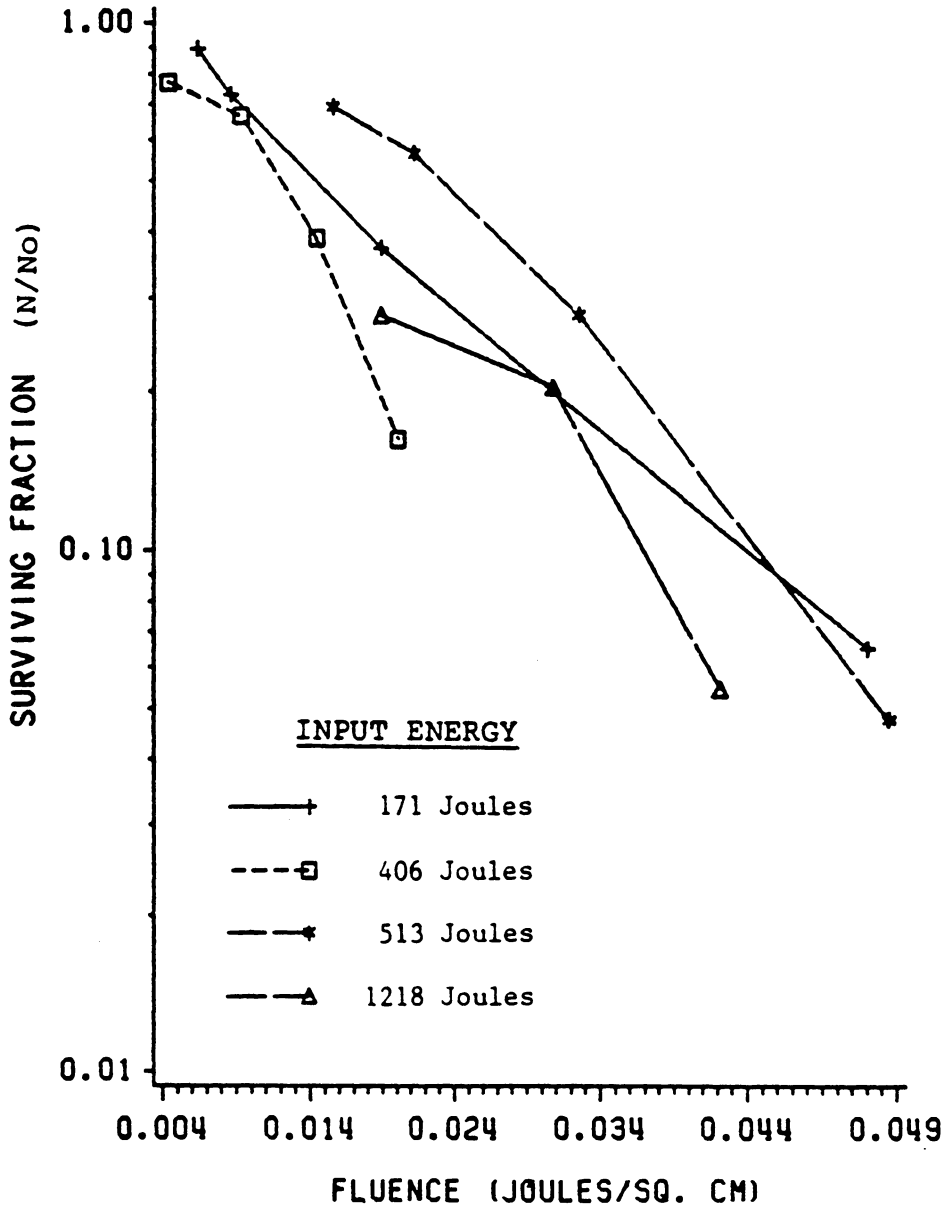

FIG. 3

Survival of B. cereus (veg. cells) at different Flashblast input energies.

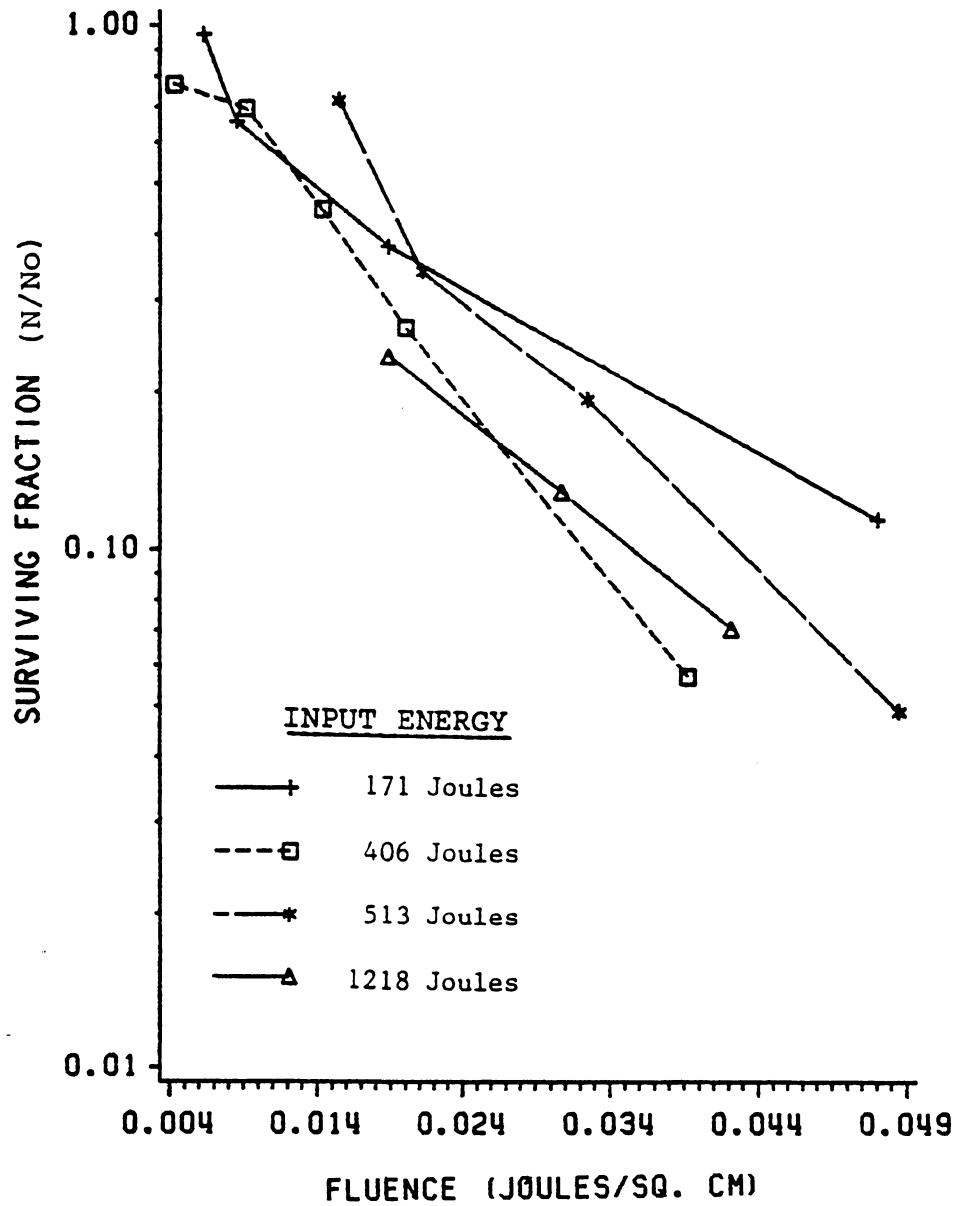

FIG. 4

Survival of B. subtilis (veg. cells) at different Flashblast input energies.

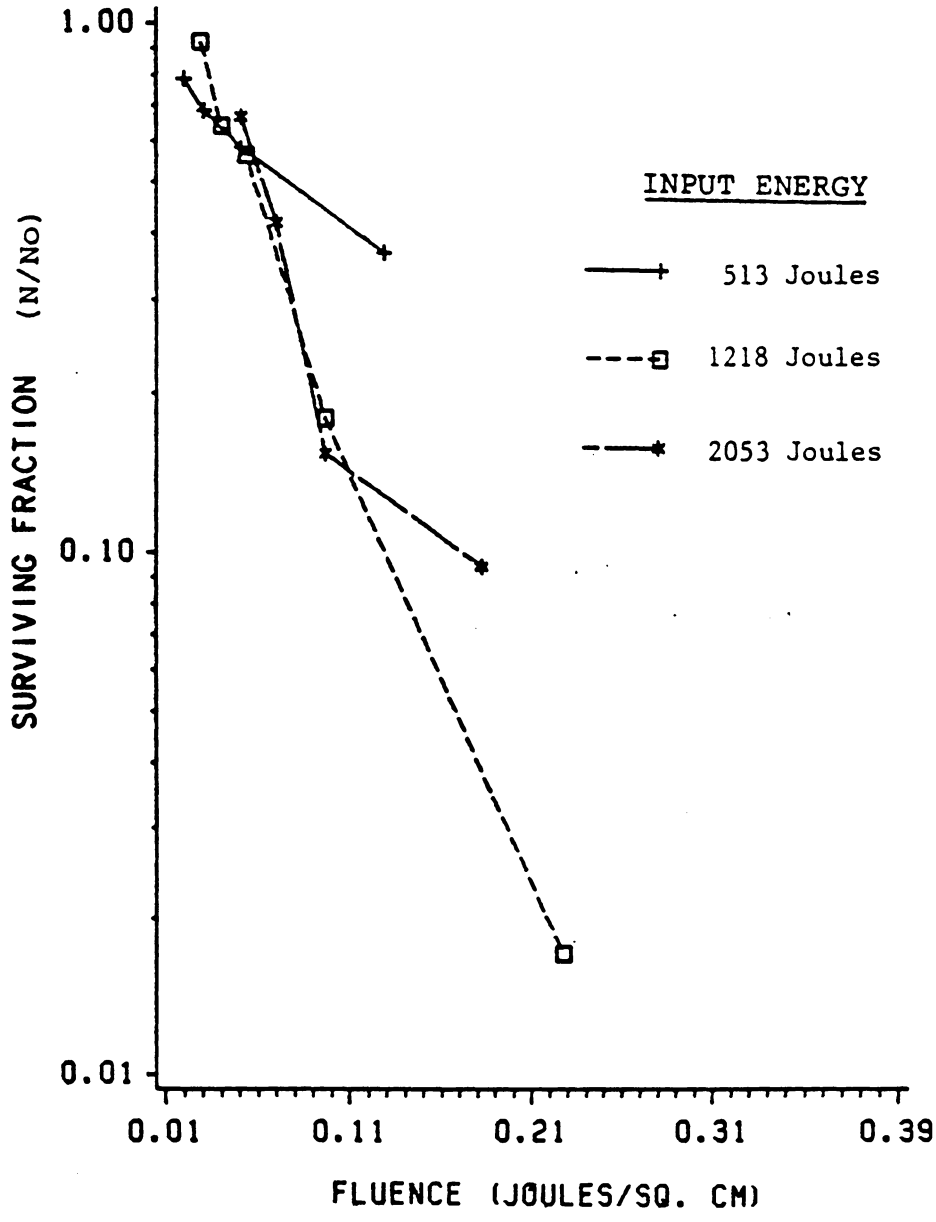

FIG. 5

Survival of B. cereus (spores) at different Flashblast input energies.

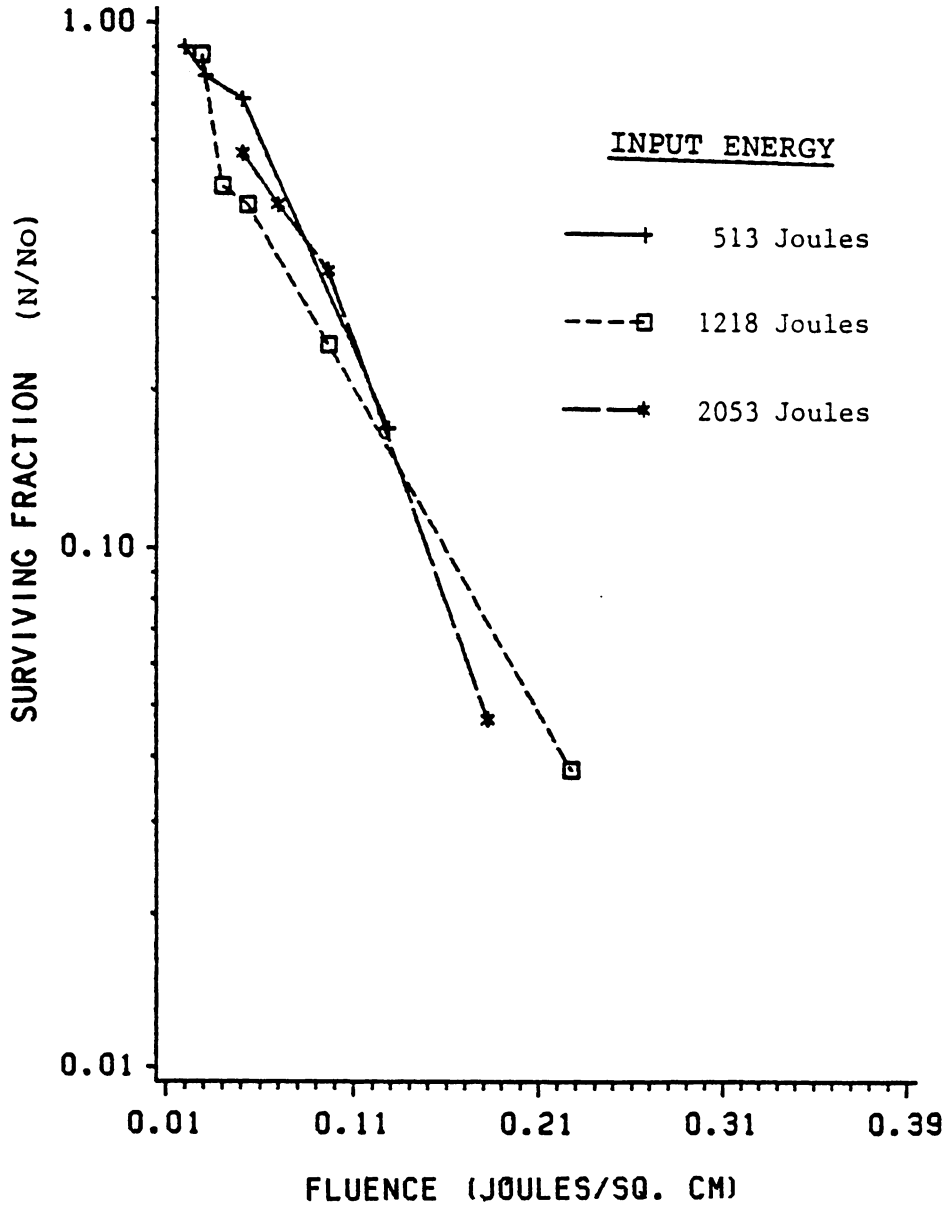

FIG. 6

Survival of B. subtilis (spores) at different Flashblast input energies.

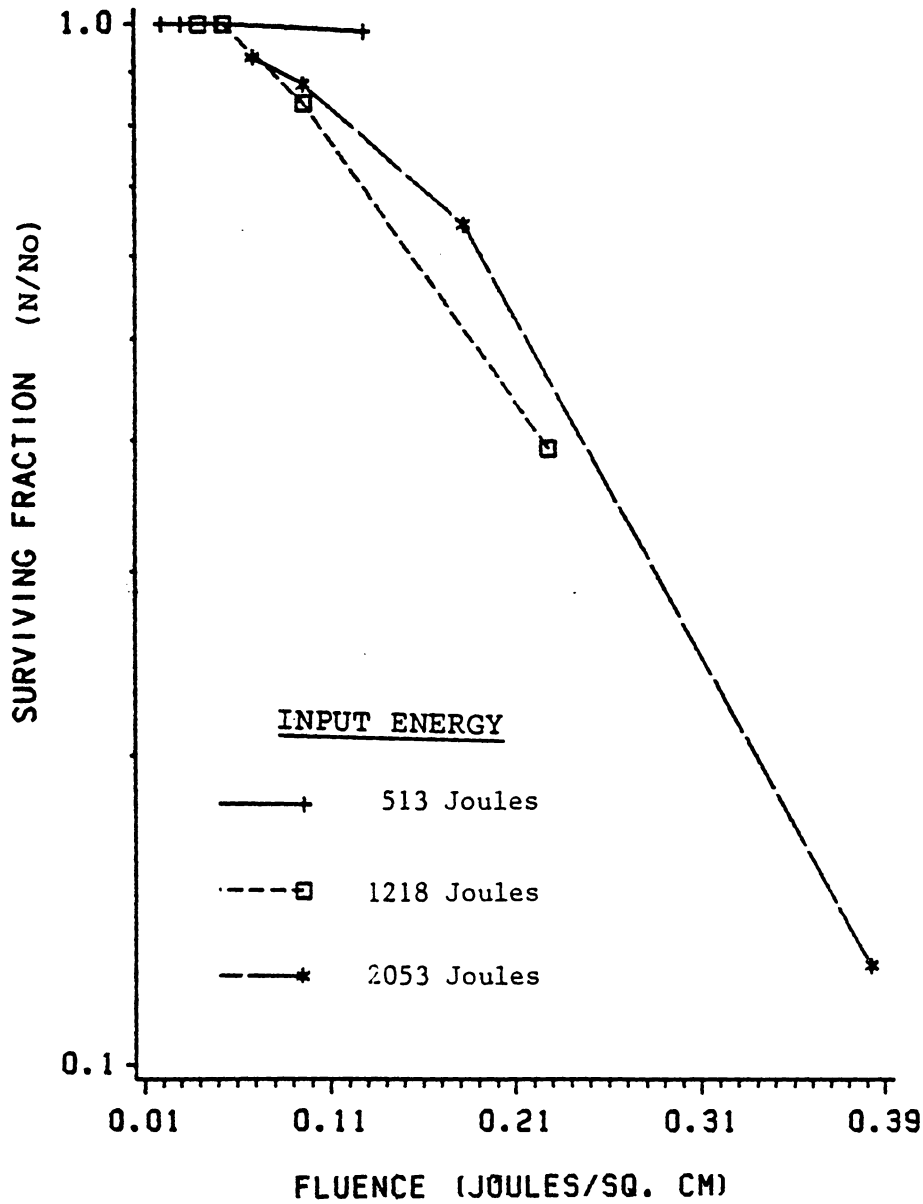

FIG. 7

Survival of A. niger (spores) at different Flashblast input energies.

APPENDIX

C

Survival Curves (Log Survivor Number versus Fluence) of Microorganisms at Different Input Energies

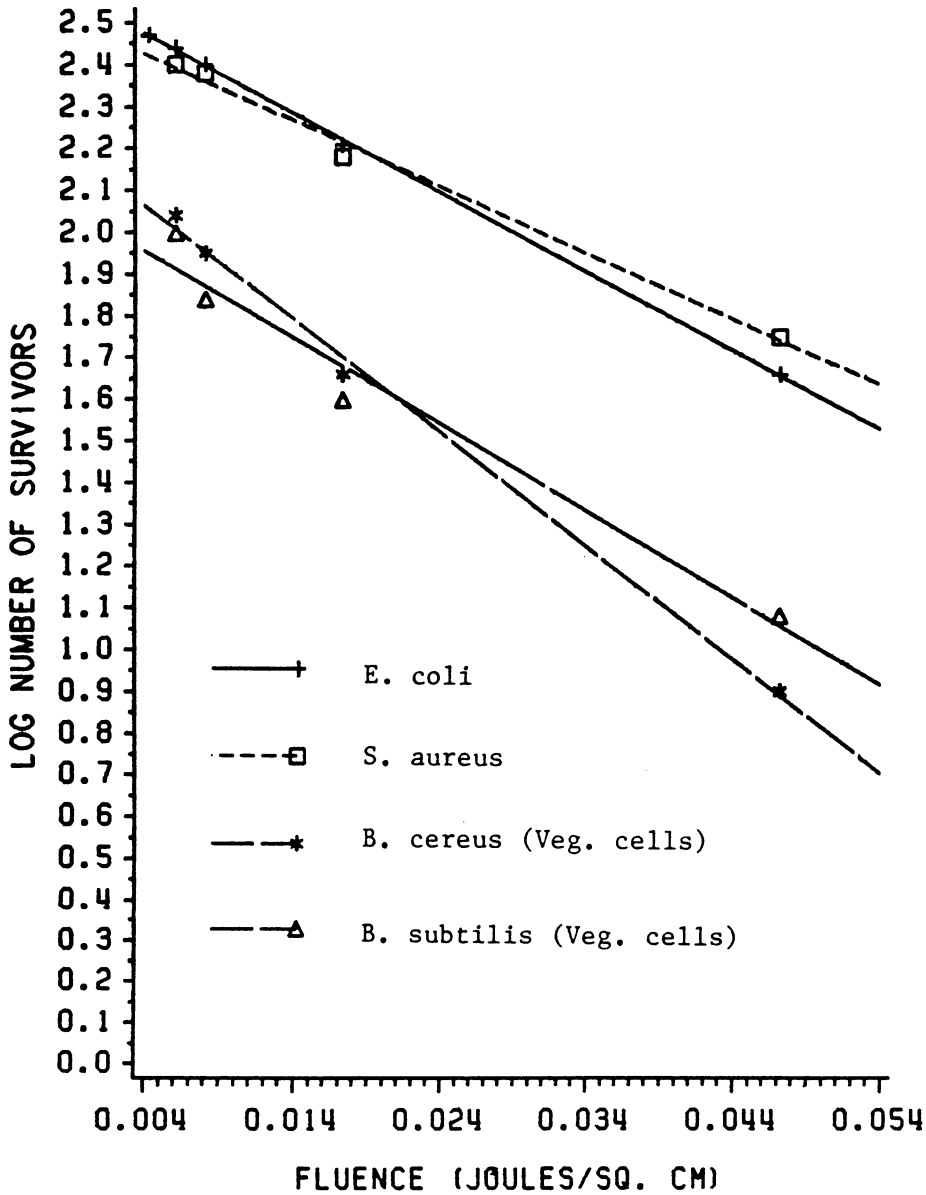

Figure 1. Survival of four microorganisms at a Flashblast input energy of 171 Joules.

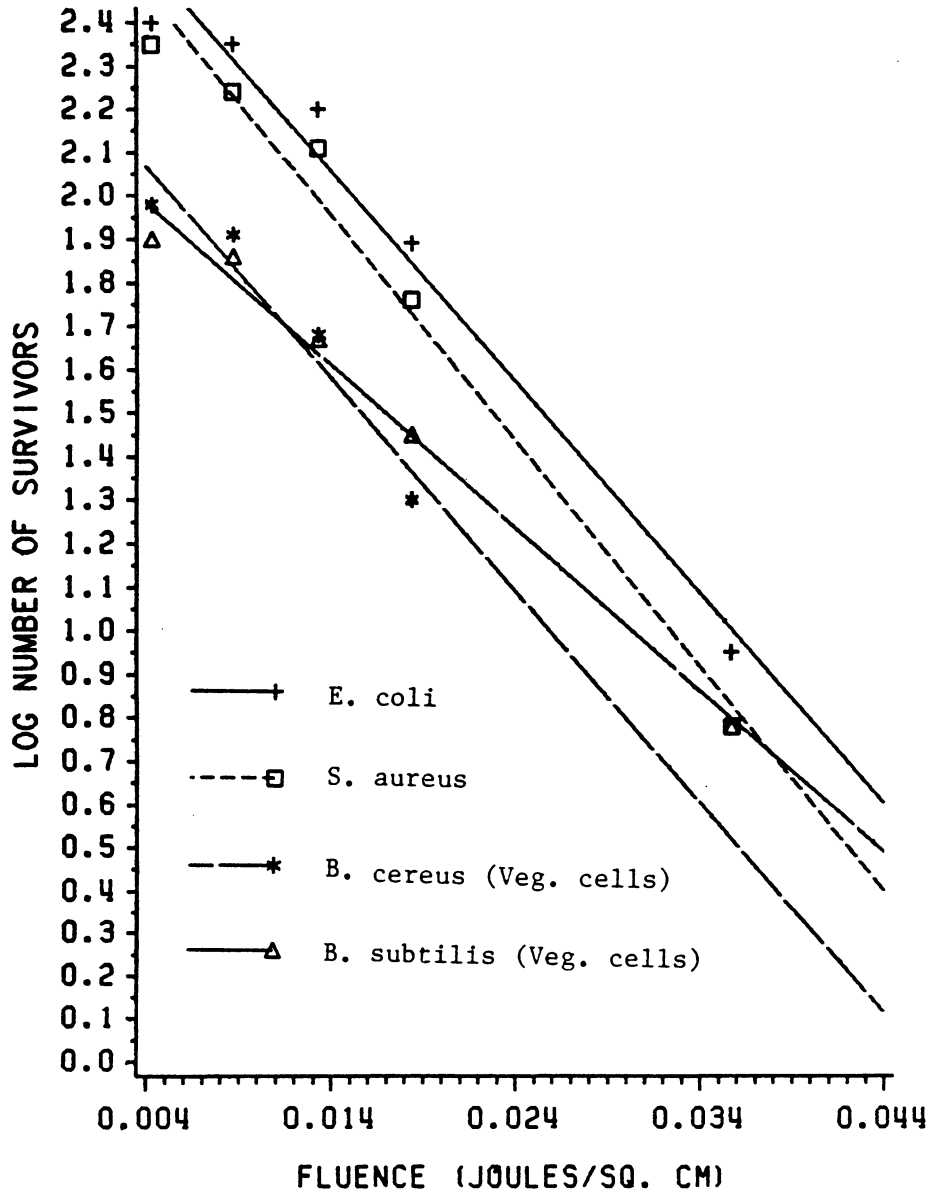

Figure 2. Survival of four microorganisms at a Flashblast input energy of 406 Joules.

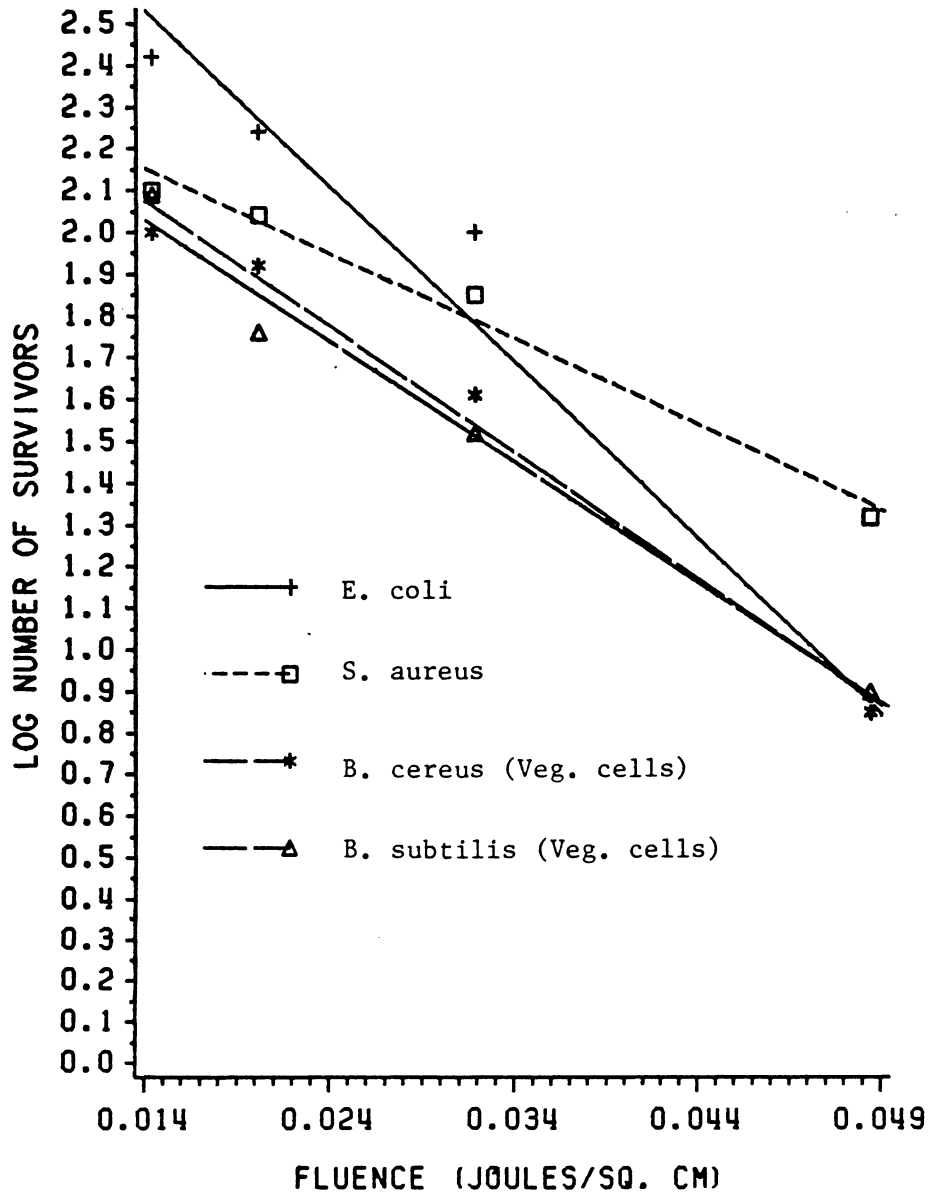

Figure 3. Survival of four microorganisms at a Flashblast input energy of 513 Joules.

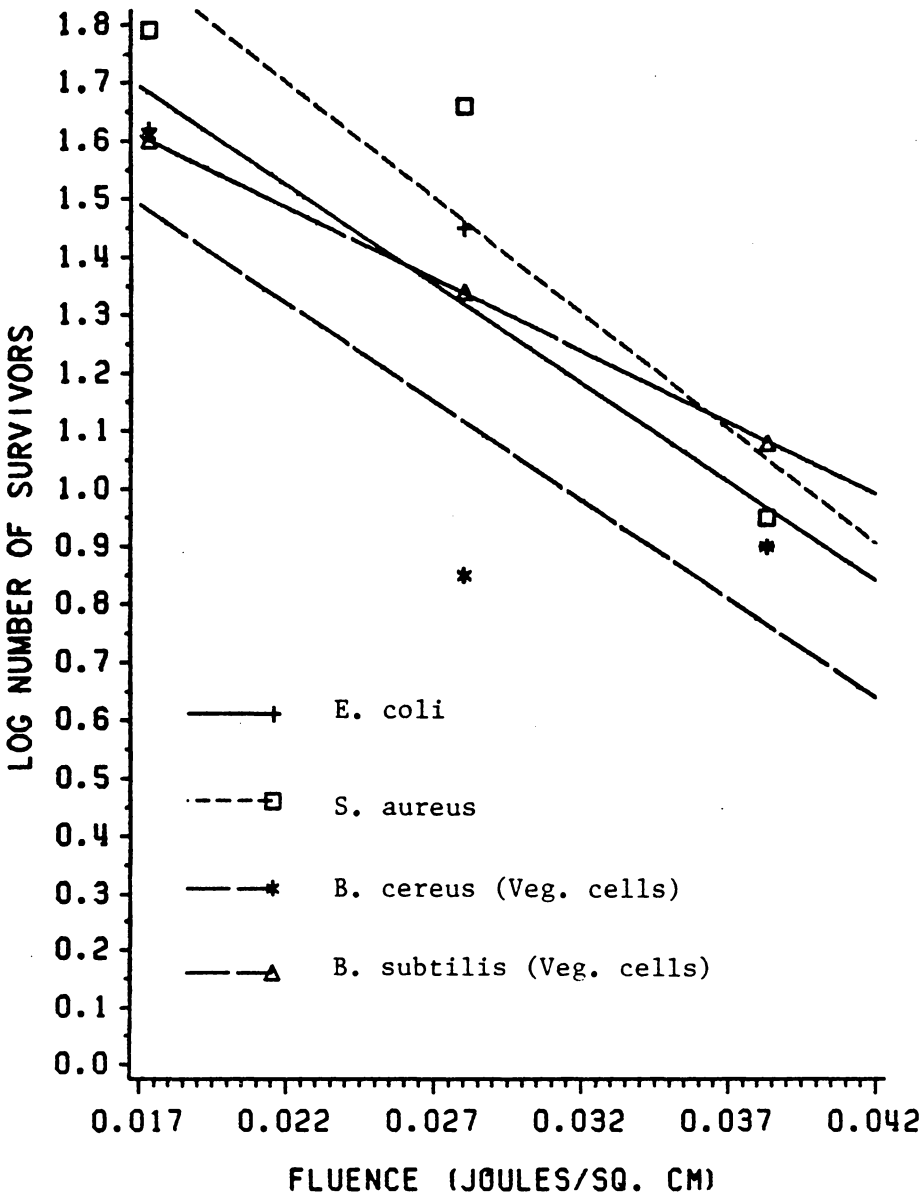

Figure 4. Survival of four microorganisms at a Flashblast input energy of 1218 Joules.

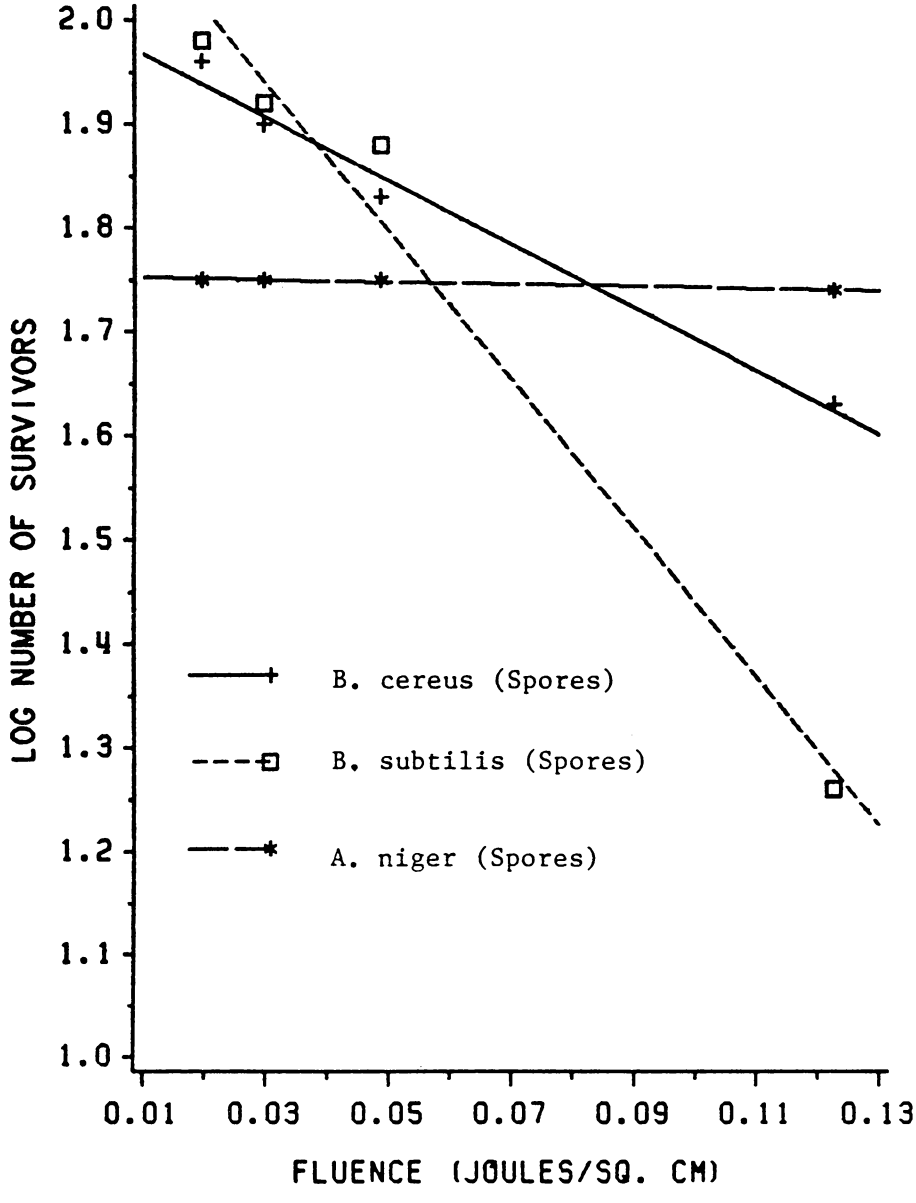

Figure 5. Survival of three spore species at a Flashblast input energy of 513 Joules.

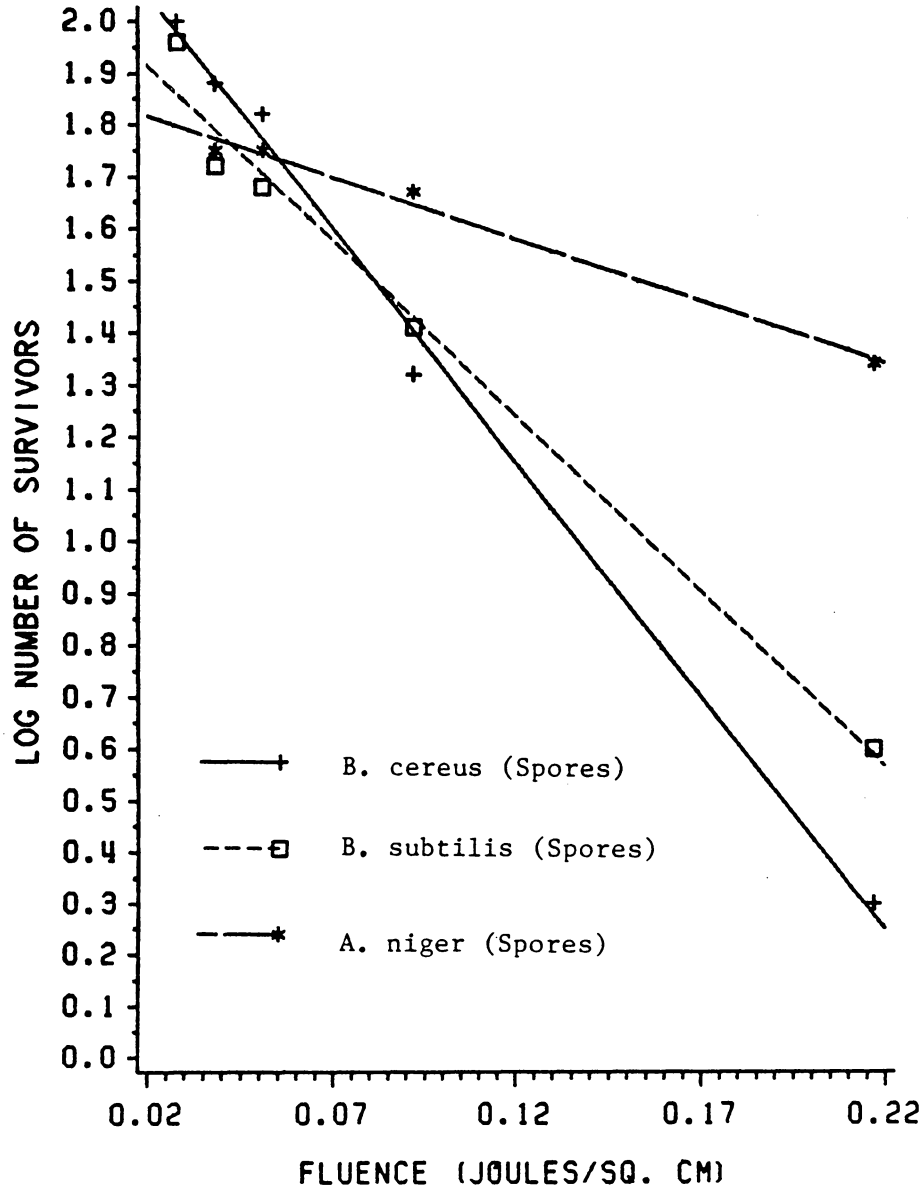

Figure 6. Survival of three spore species at a Flashblast input energy of 1218 Joules.

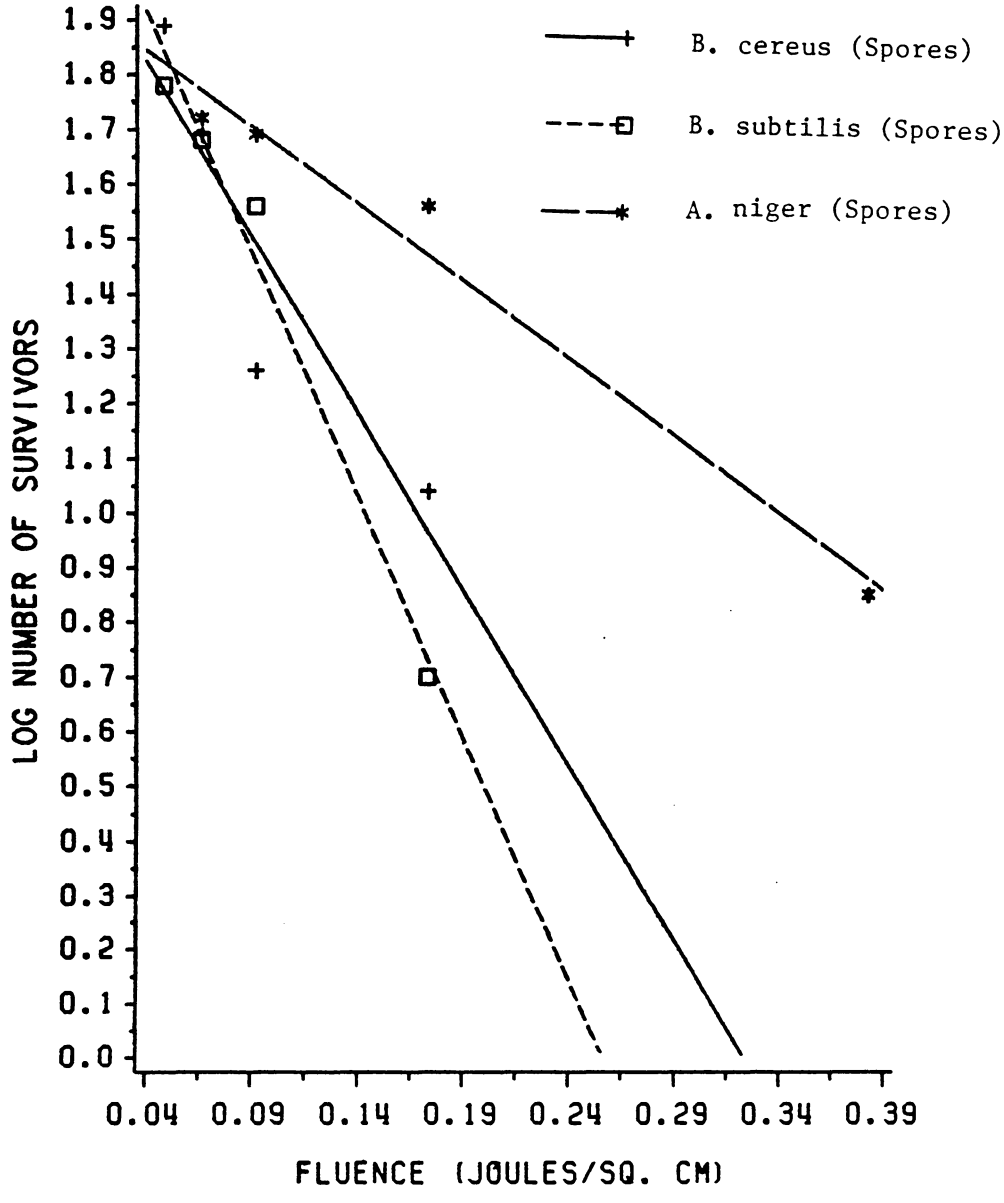

Figure 7. Survival of three spore species at a Flashblast input energy of 2053 Joules.

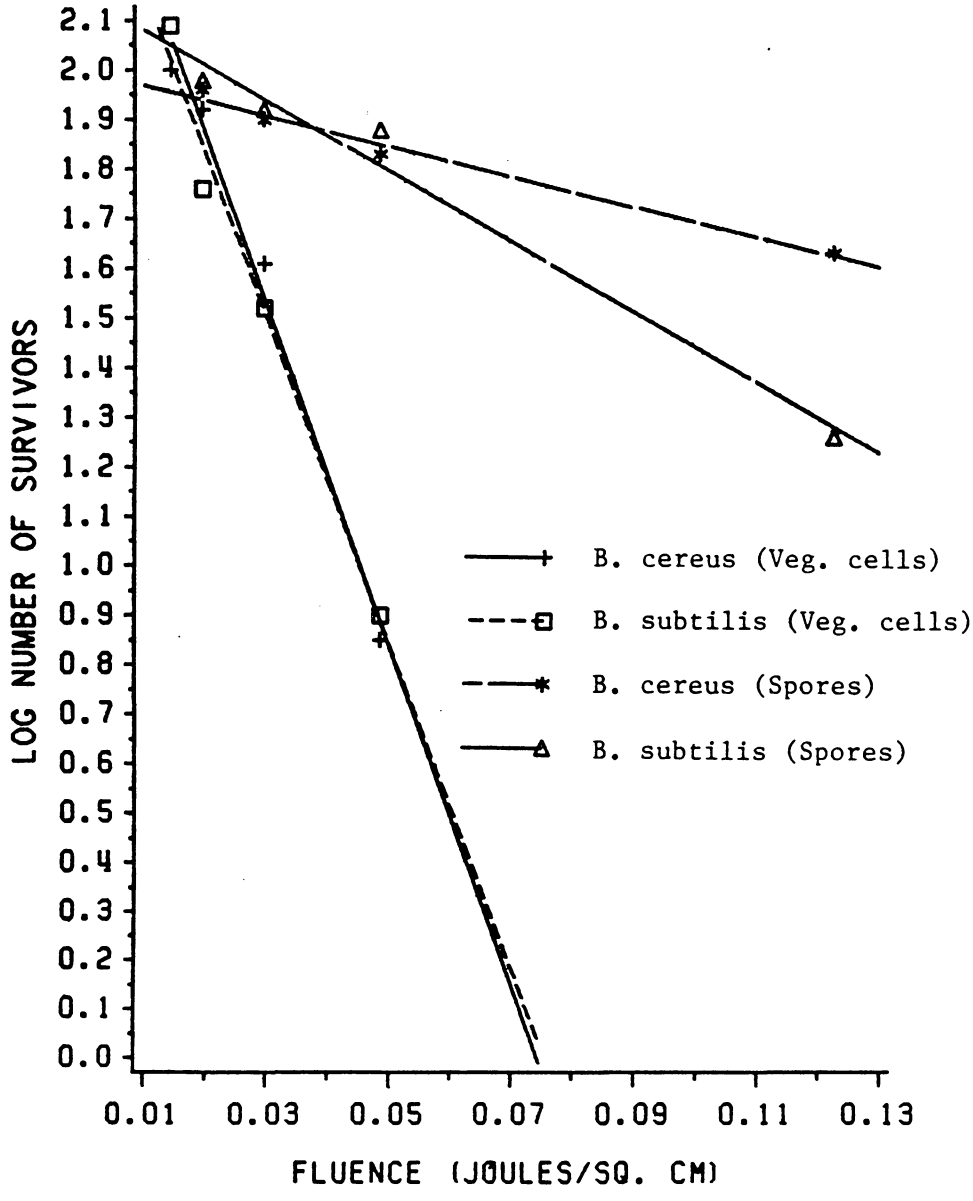

Figure 8. Survival of Bacilli vegetative cells and spores at a Flashblast input energy of 513 Joules.

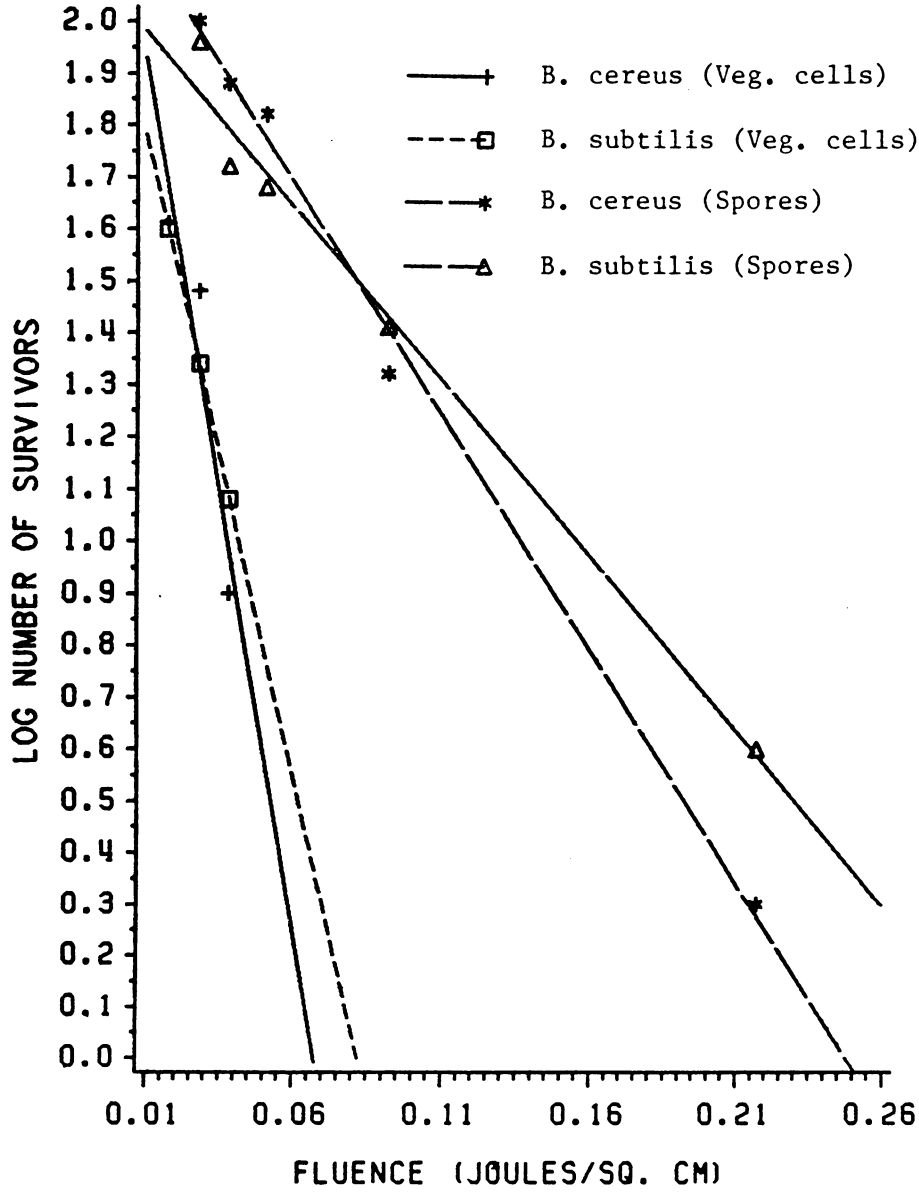

Figure 9. Survival of Bacilli vegetative cells and spores at a Flashblast input energy of 1218 Joules.

APPENDIX

D

Bar Charts of Microorganism Survival at Different Input Energies

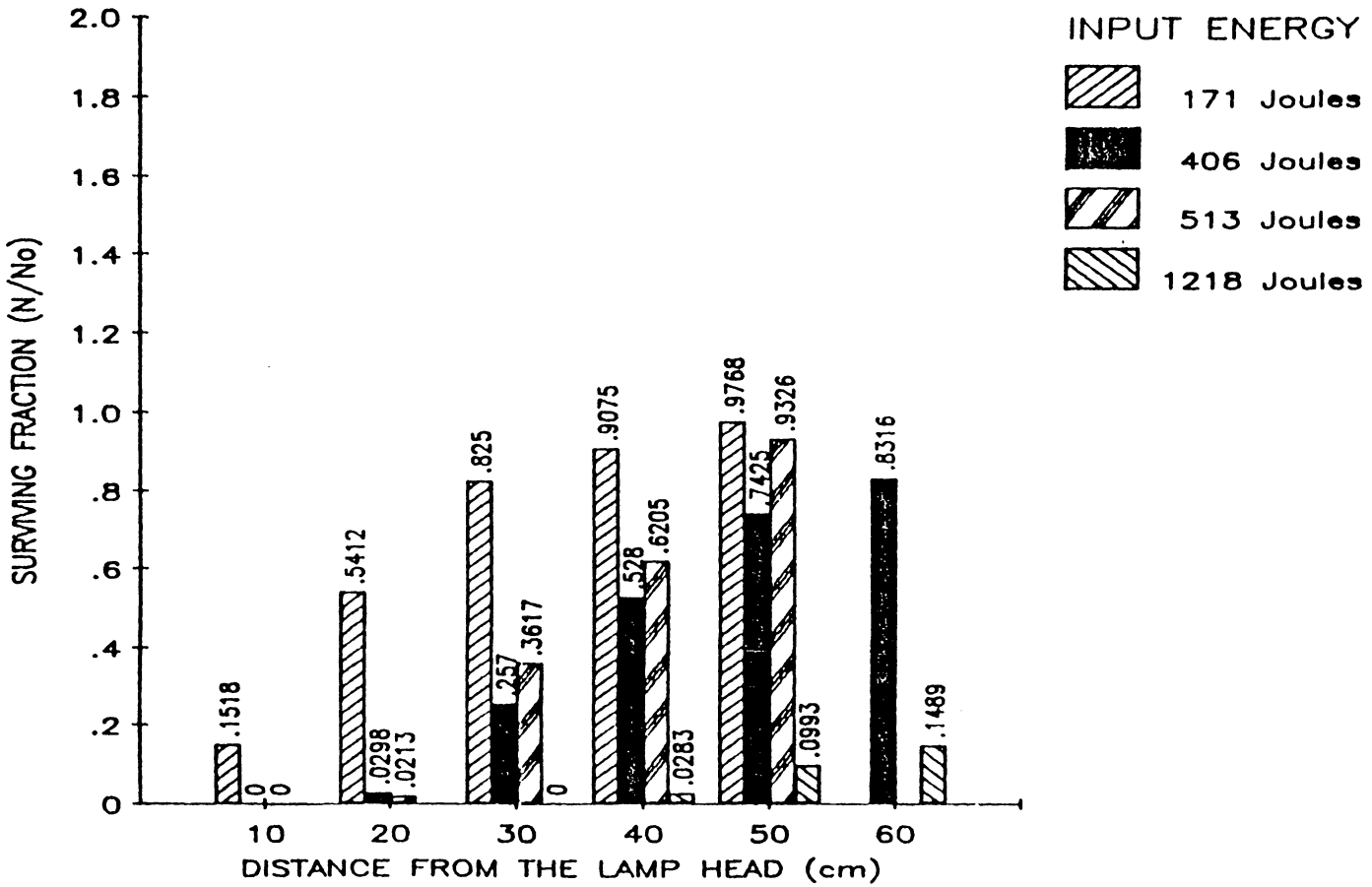

Figure 1. Survival of Flashblast treated E. coli at different input energies. Distance between the Petri plate and the flashlamp varied from 60 cm to 10 cm.

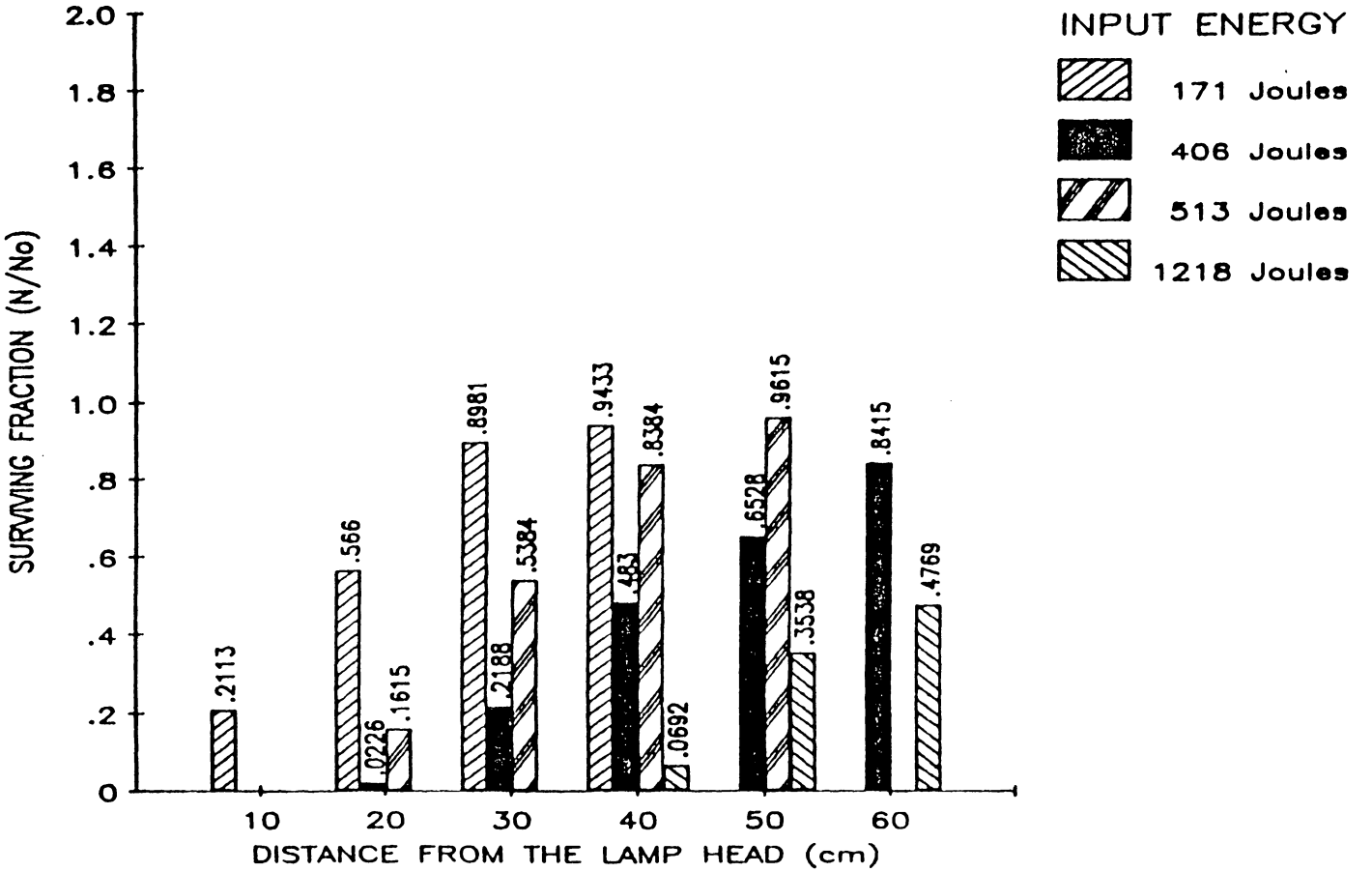

Figure 2. Survival of Flashblast treated S. aureus at different input energies. Distance between the Petri plate and the flashlamp varied from 60 cm to 10 cm.

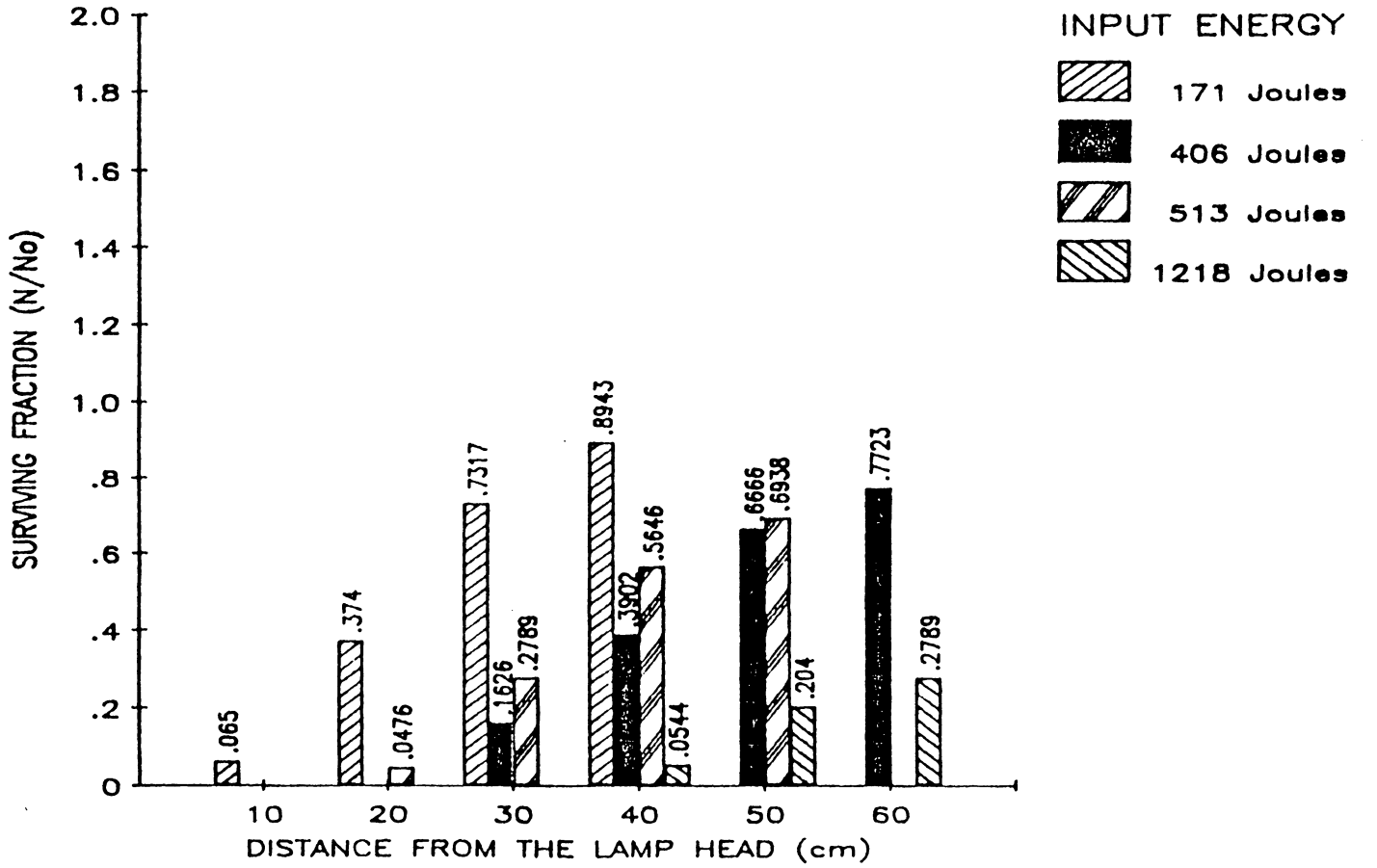

Figure 3. Survival of Flashblast treated B. cereus (vegetative cells) at different input energies. Distance between the Petri plate and the flashlamp varied from 60 cm to 10 cm.

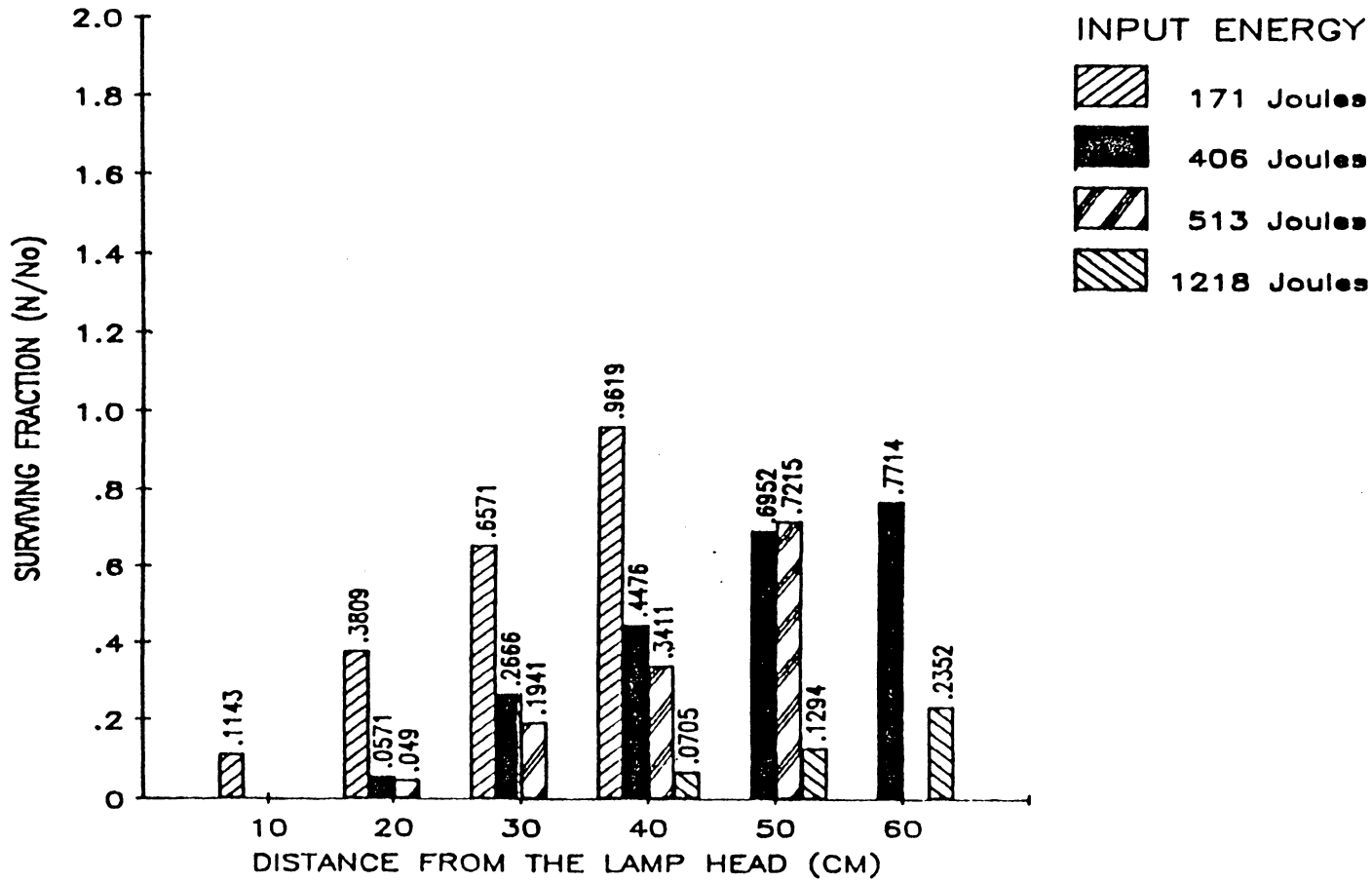

Figure 4. Survival of Flashblast treated B. subtilis (vegetative cells) at different input energies. Distance between the Petri plate and the flashlamp varied from 60 cm to 10 cm.

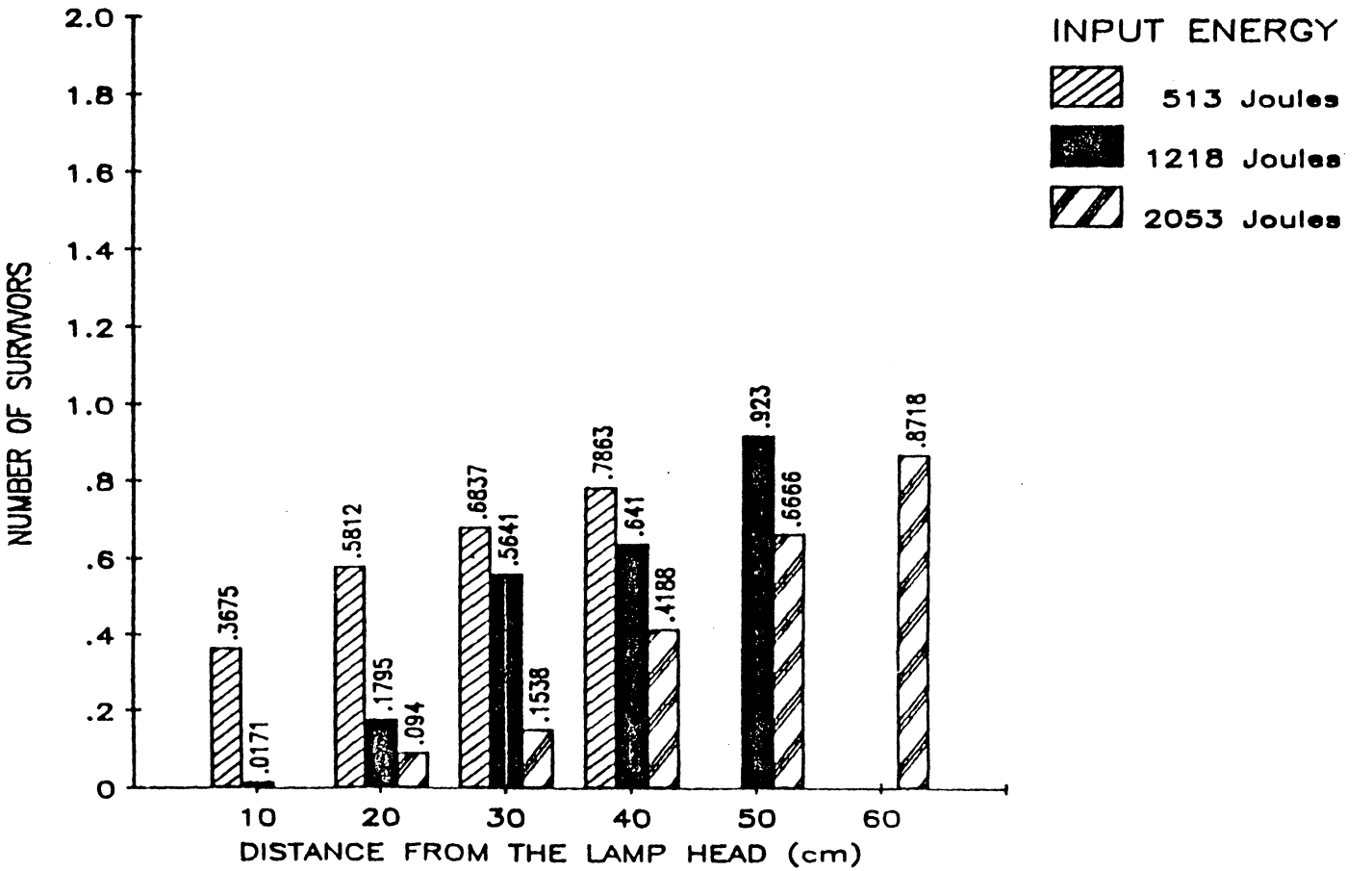

Figure 5. Survival of Flashblast treated B. cereus (spores) at different input energies. Distance between the Petri plate and the flashlamp varied from 60 cm to 10 cm.

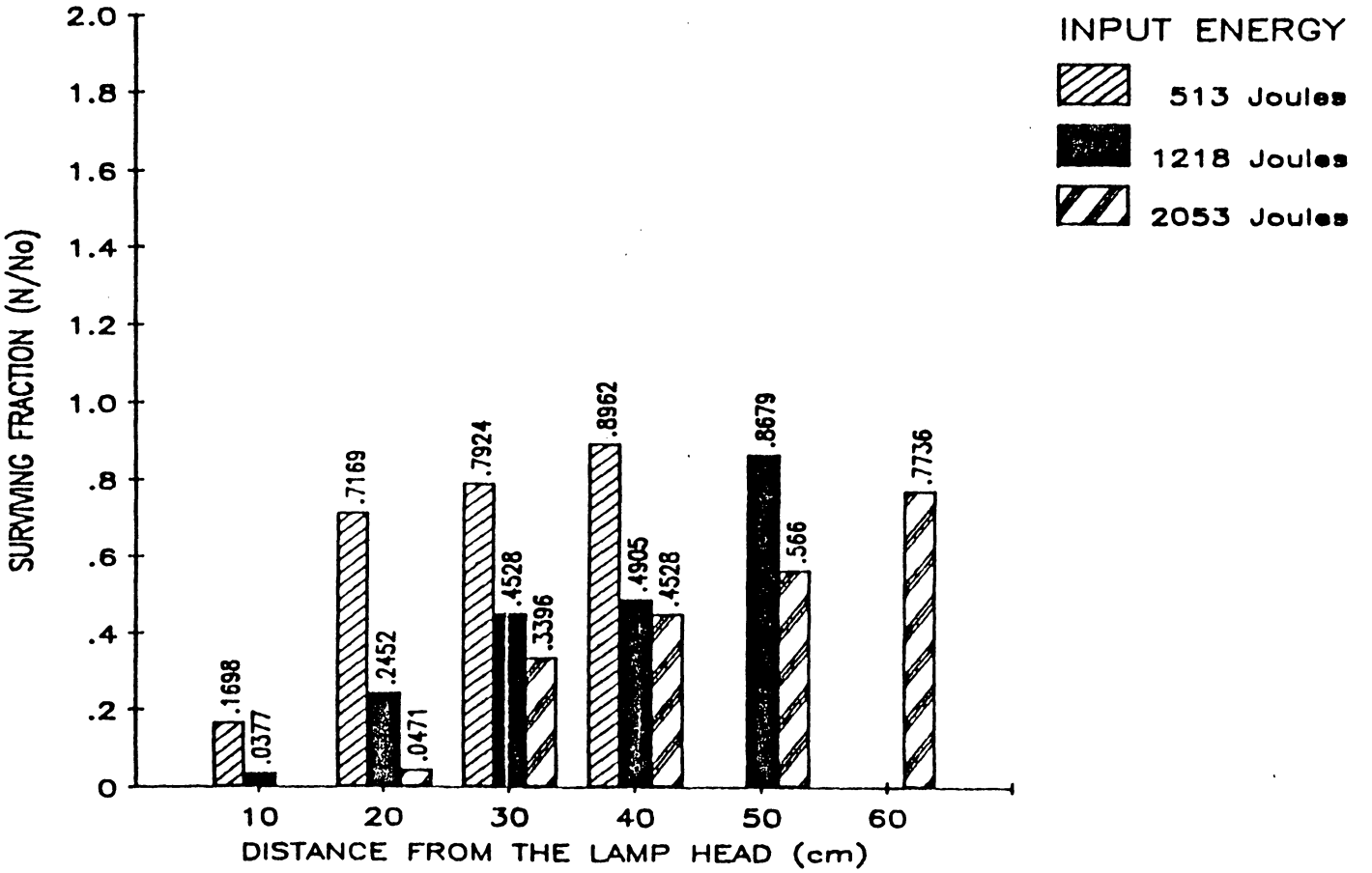

Figure 6. Survival of Flashblast treated B. subtilis (spores) at different input energies. Distance between the Petri plate and the flashlamp varied from 60 cm to 10 cm.

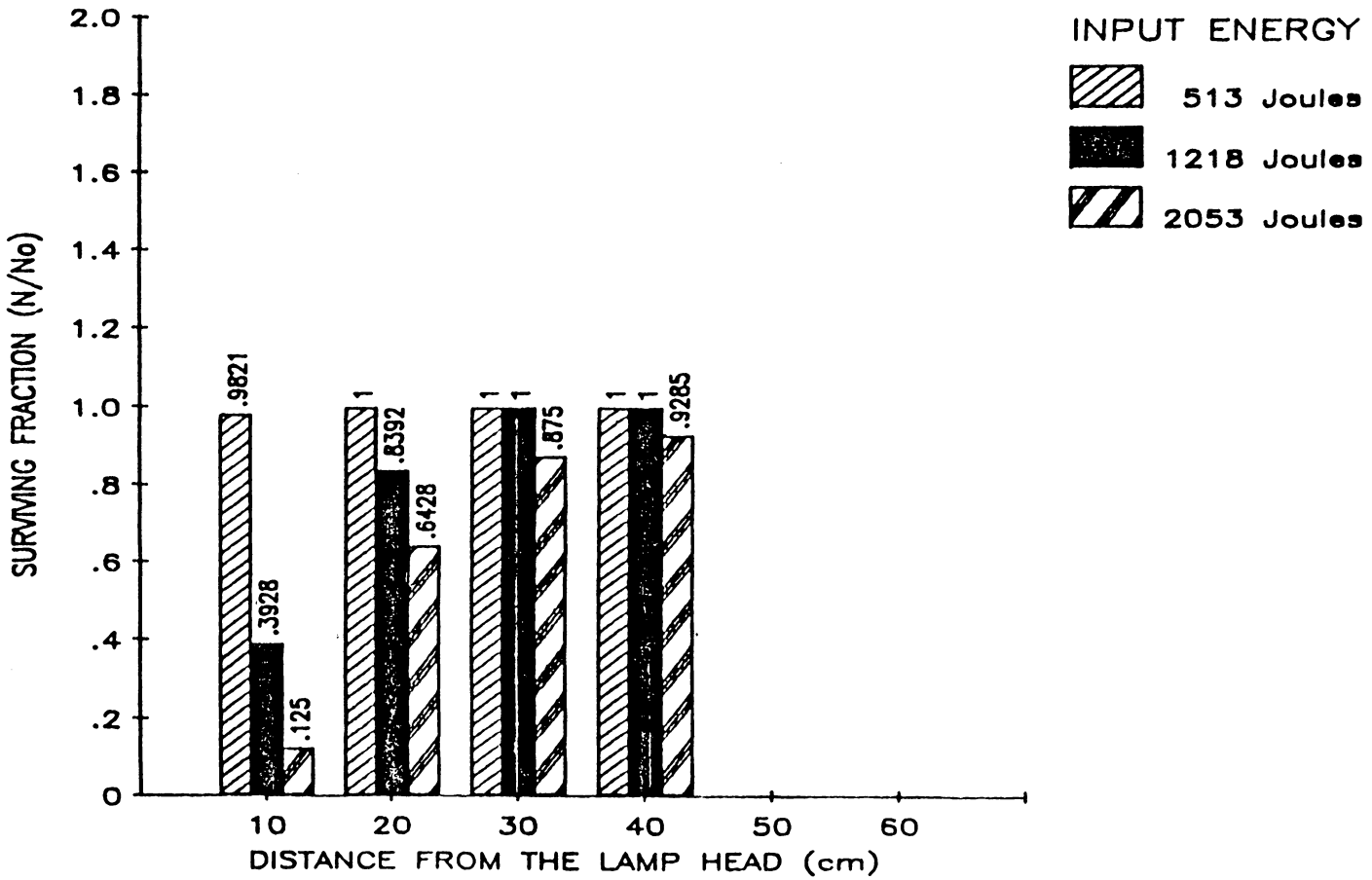

Figure 7. Survival of Flashblast treated A. niger (spores) at different input energies. Distance between the Petri plate and the flashlamp varied from 40 cm to 10 cm.

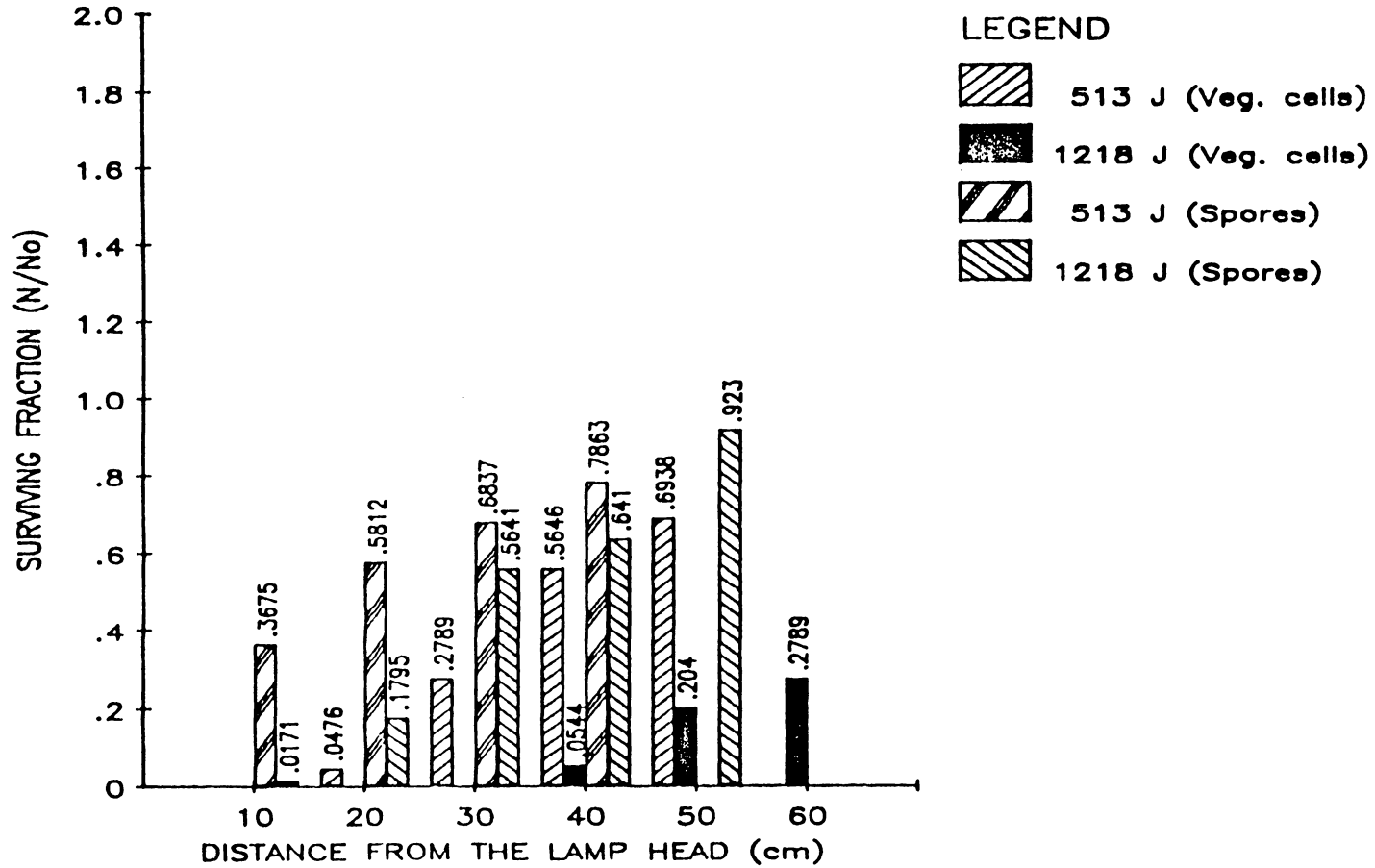

Figure 8. Survival of B. cereus vegetative cells and spores at different Flashblast input energies. Distance between the Petri plate and the flashlamp varied from 60 cm to 10 cm.

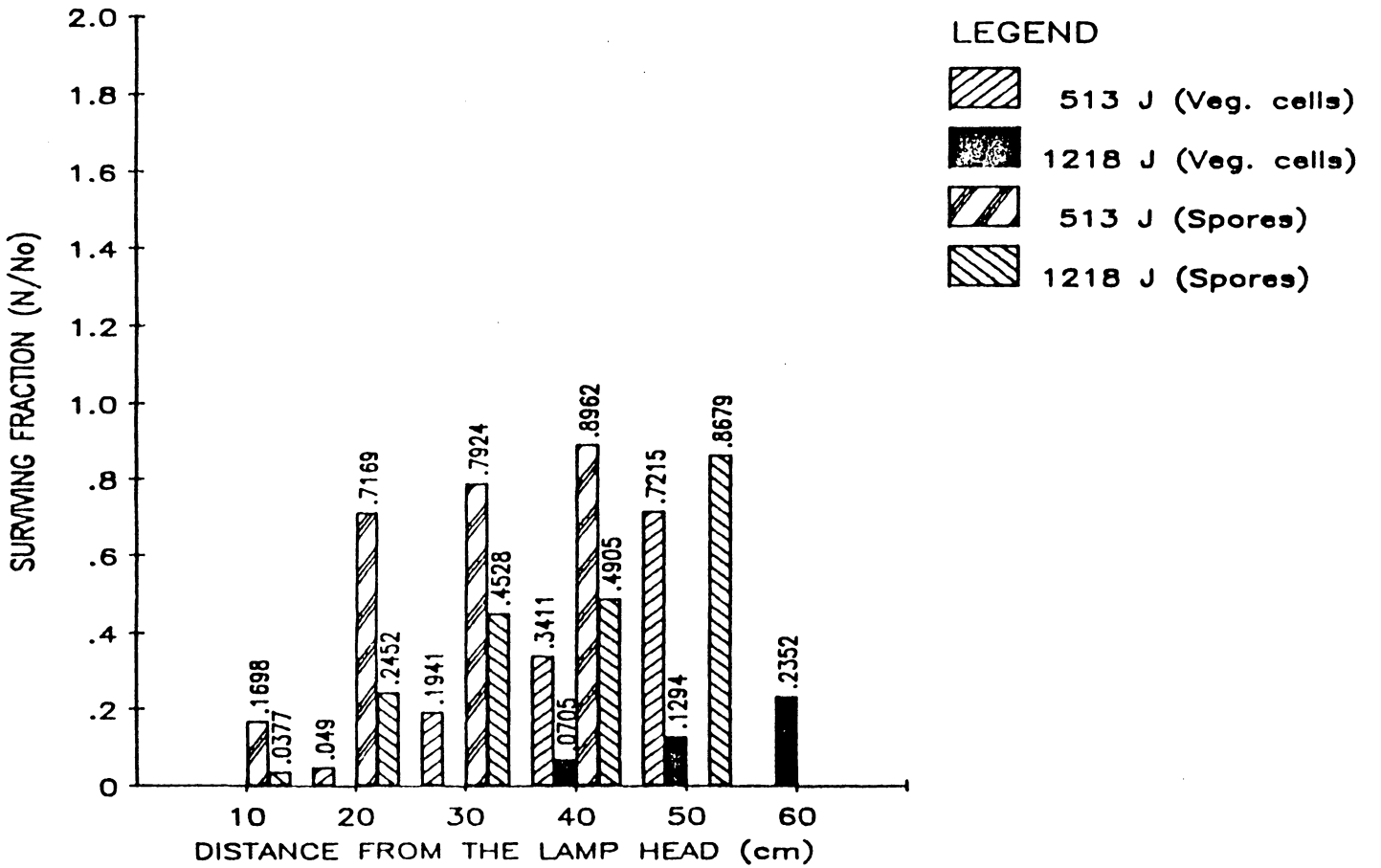

Figure 9. Survival of B. subtilis vegetative cells and the spores at different Flashblast input energies. Distance between the Petri plate and the flashlamp varied from 60 cm to 10 cm.

APPENDIX

E

Effect of Flashblast^{TM} Treatment On the Microbial Counts of Selected Food Products Stored at 4°C and Room Temperature

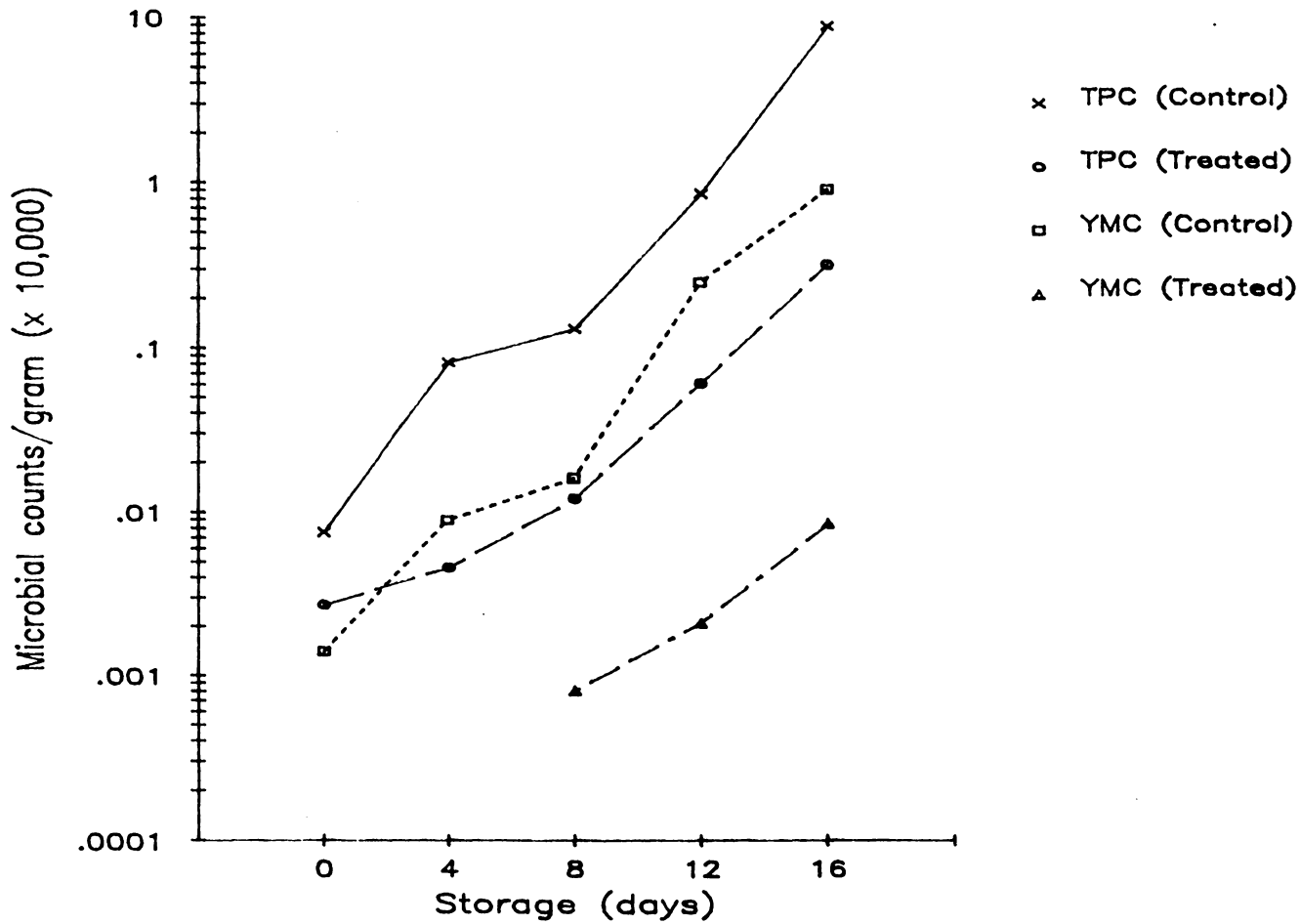

Figure 1. The effect of Flashblast treatment on Total Plate Count (TPC) and Yeast & Mold Count (YMC) of bread during storage at $4^{o}C$.

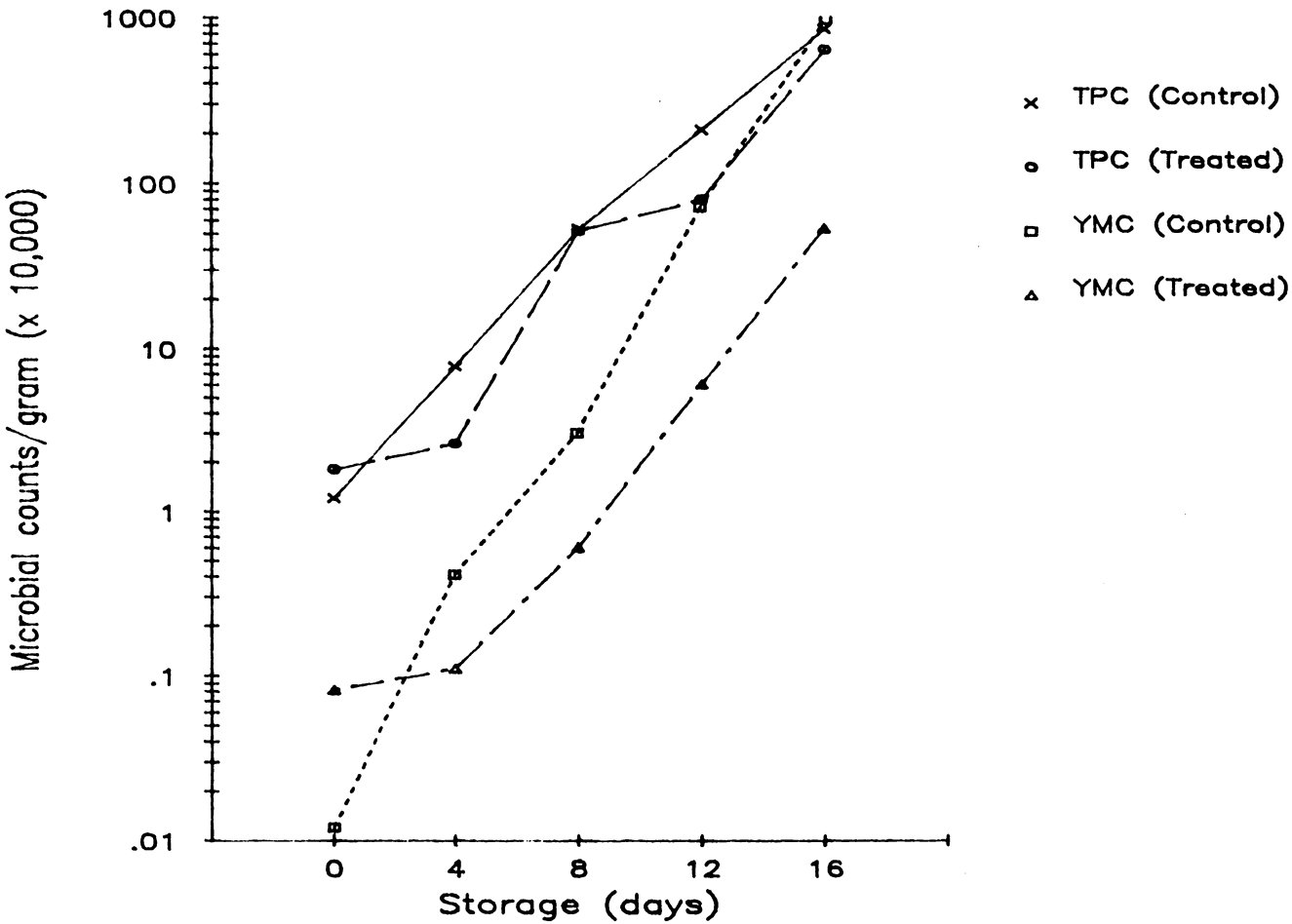

Figure 2. The effect of Flashblast treatment on Total Plate Count (TPC) and Yeast & Mold Count (YMC) of cheese during storage at 4°C.

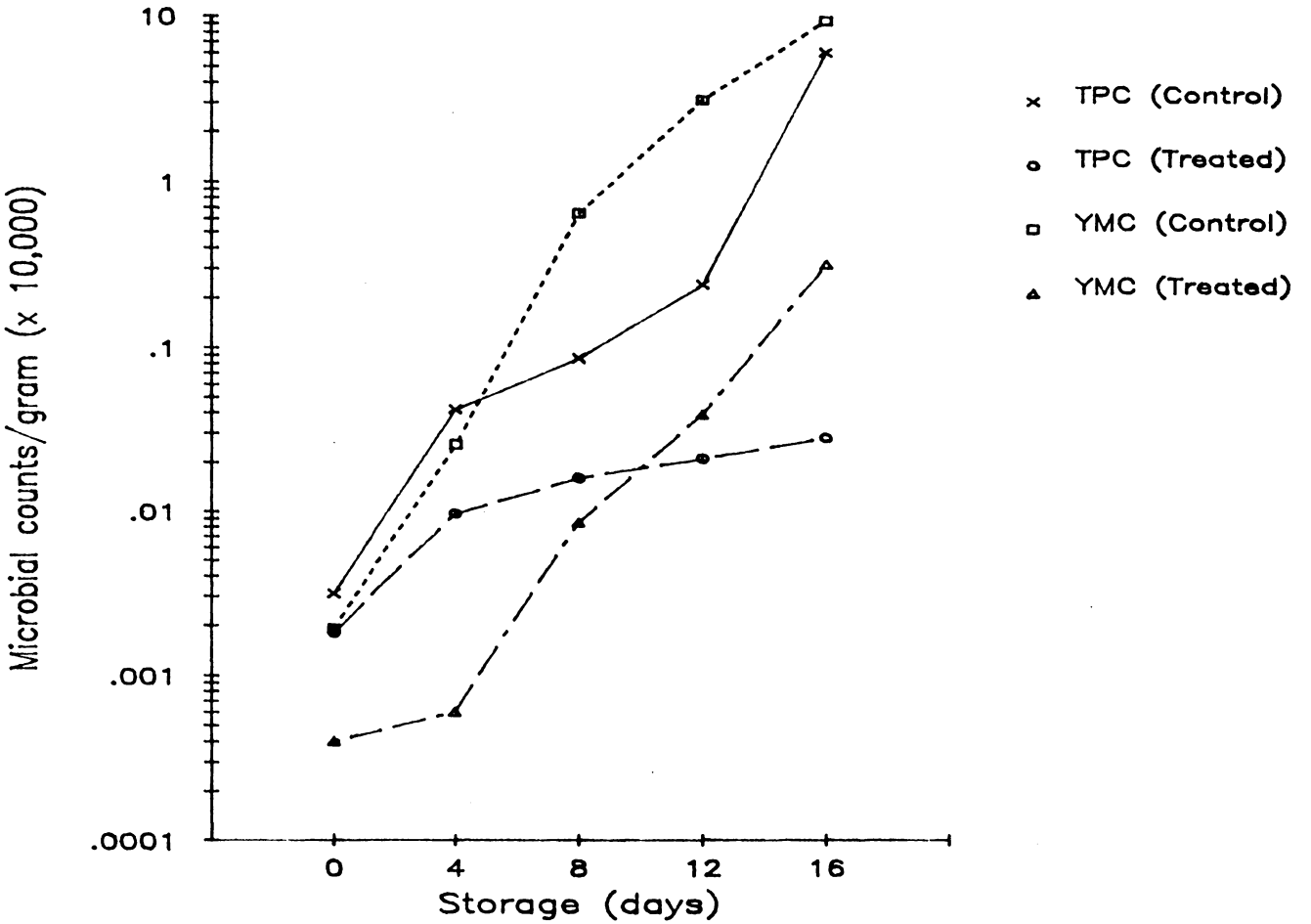

Figure 3. The effect of Flashblast treatment on Total Plate Count (TPC) and Yeast & Mold Count (YMC) of strawberries during storage at 4°C.

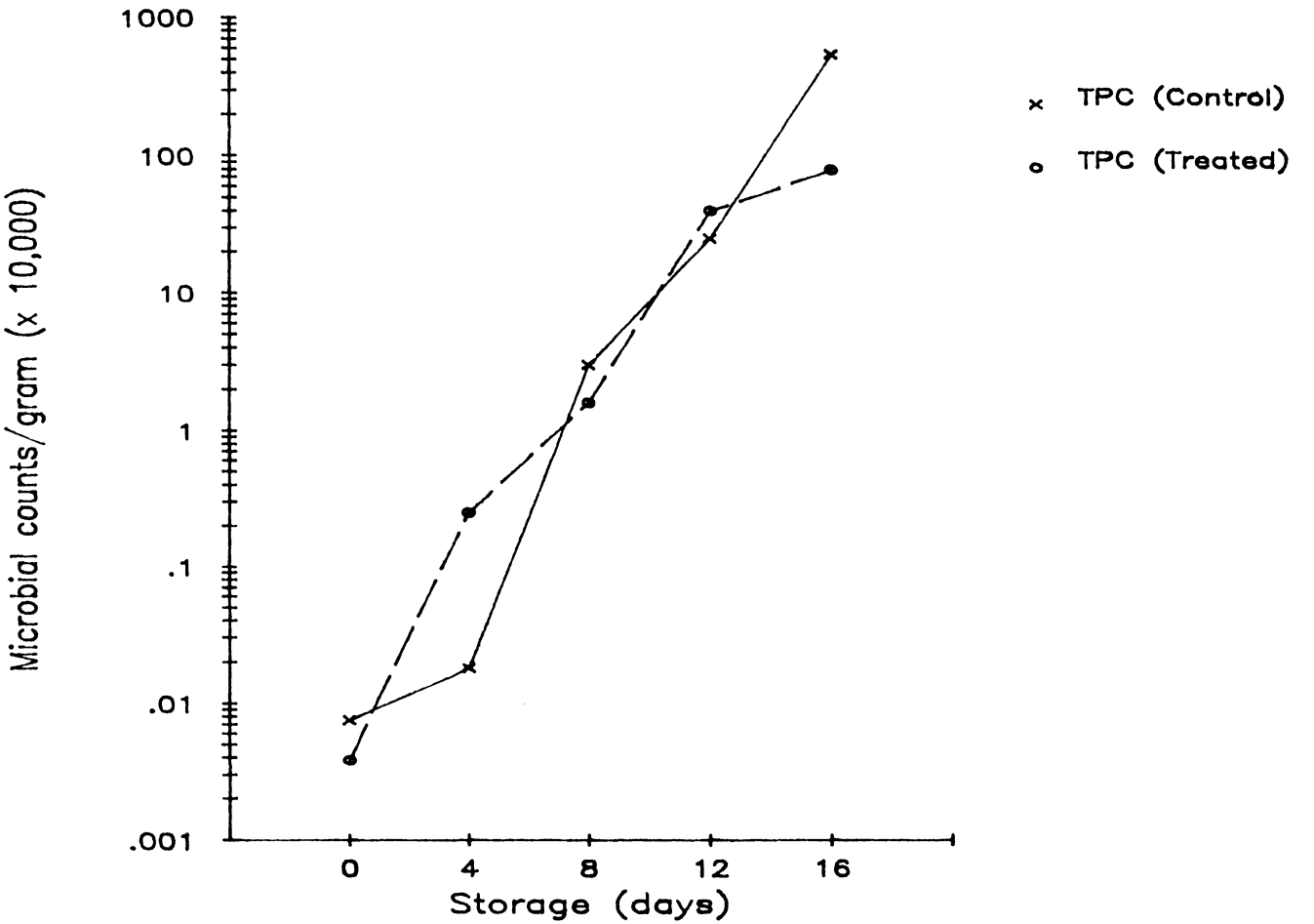

Figure 4. The effect of Flashblast treatment on Total Plate Count (TPC) of turkey breasts during storage at 4°C.

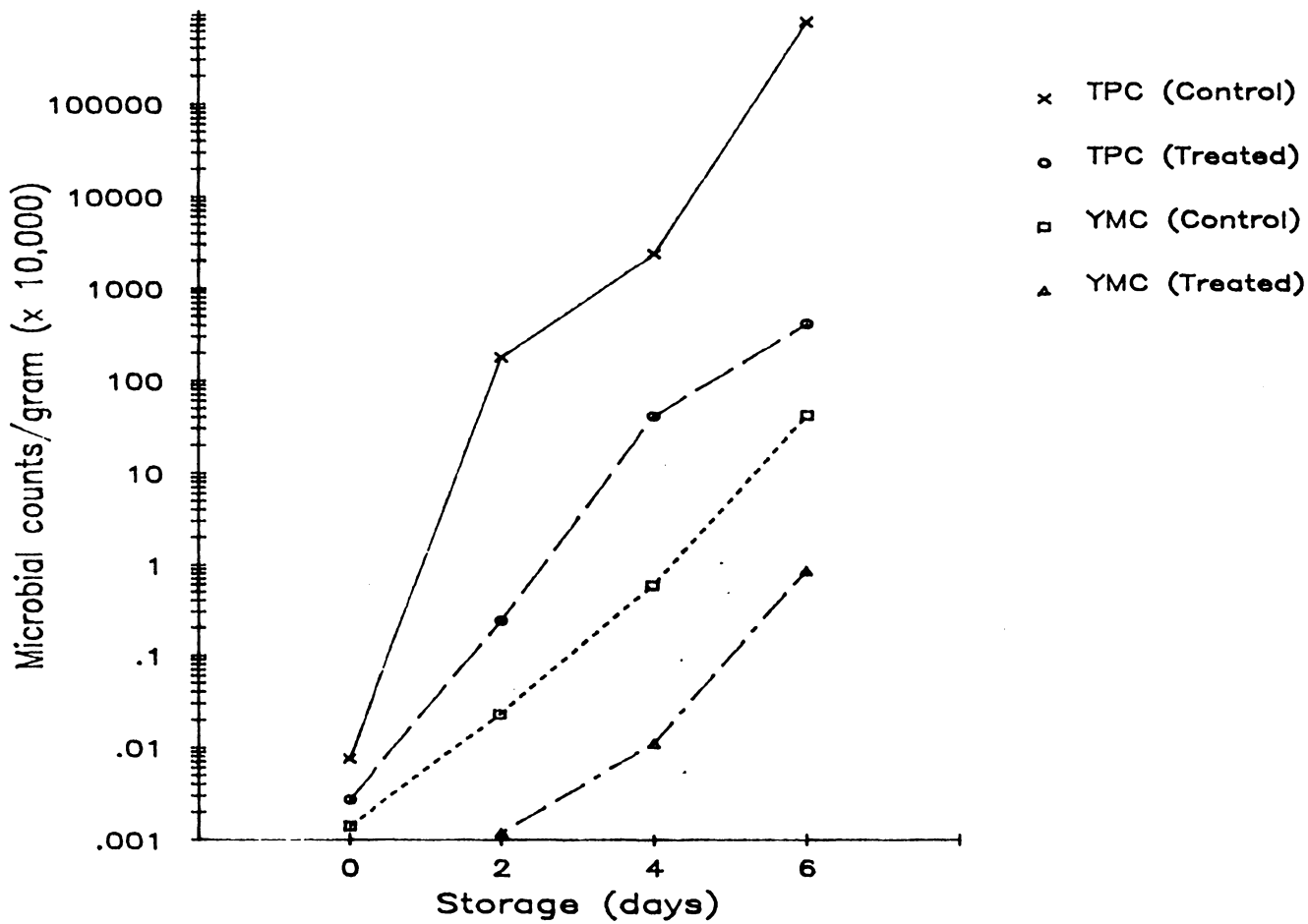

Figure 5. The effect of Flashblast treatment on Total Plate Count (TPC) and Yeast & Mold Count (YMC) of bread during storage at room temperature (25°C).

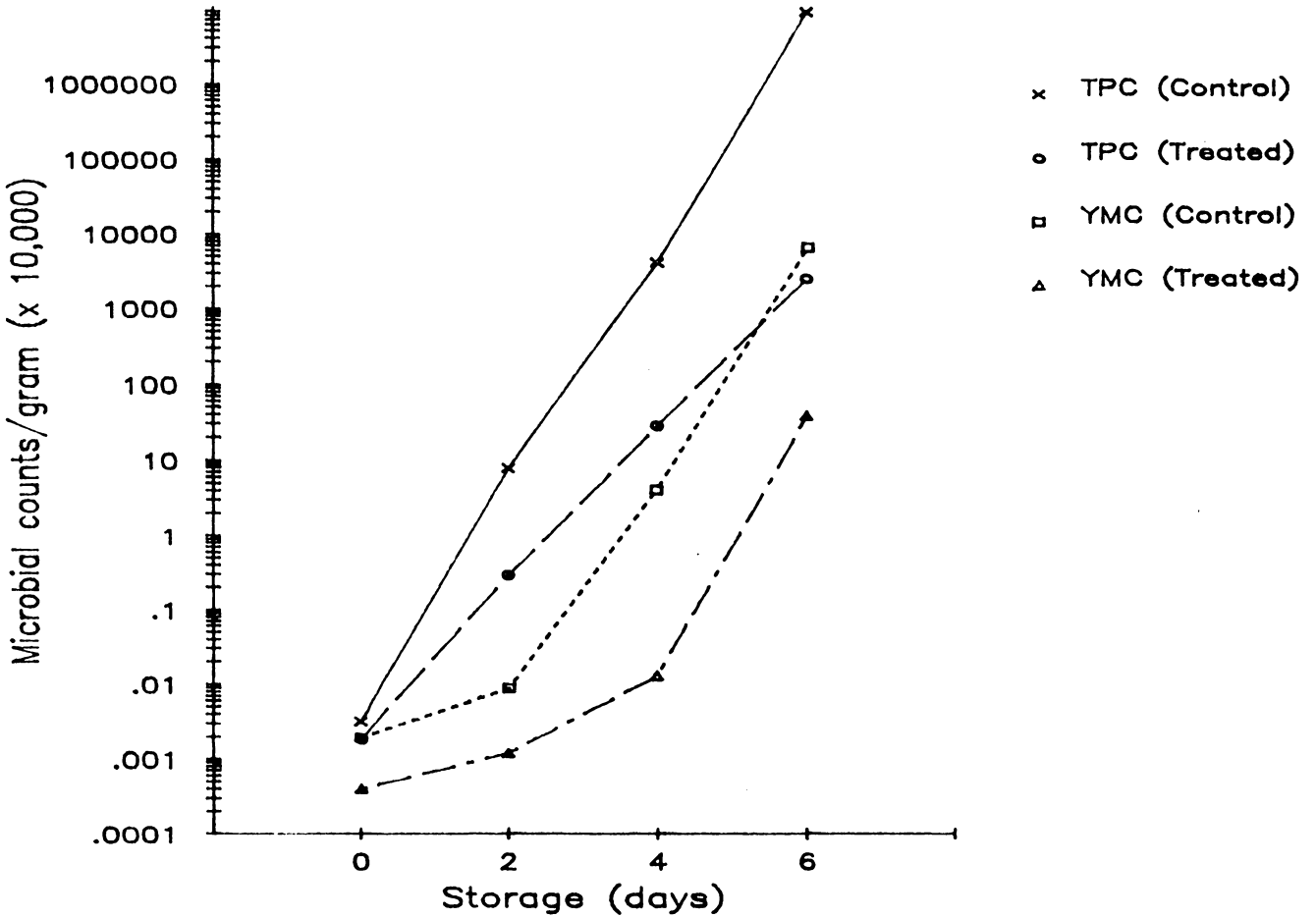

Figure 6. The effect of Flashblast treatment on Total Plate Count (TPC) and Yeast & Mold Count (YMC) of strawberries during storage at room temperature (25°C).

APPENDIX (F)

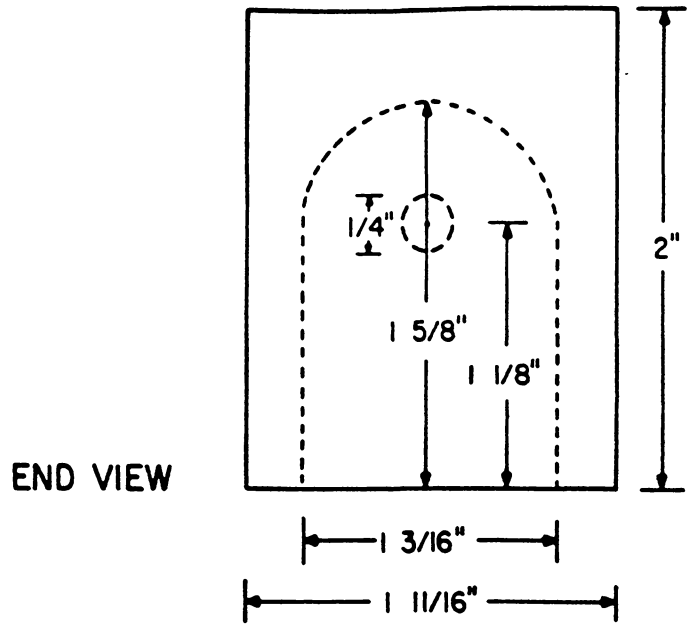

END VIEW

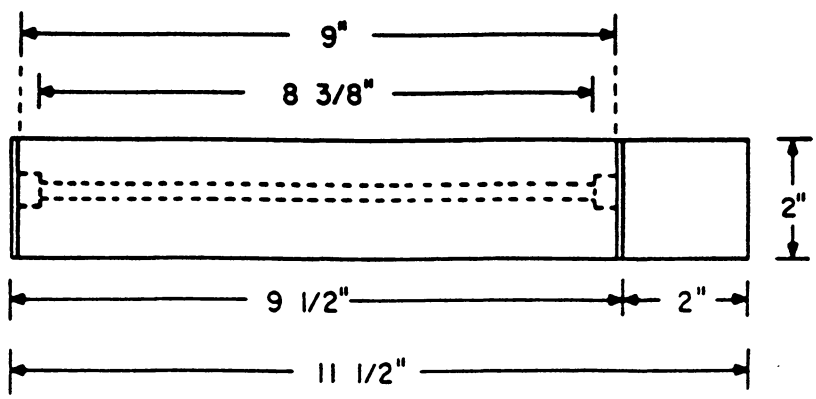

SIDE VIEW

Diagram of the Maxwell Laboratories, Inc., Flashblast Lamphead.

APPENDIX (G)

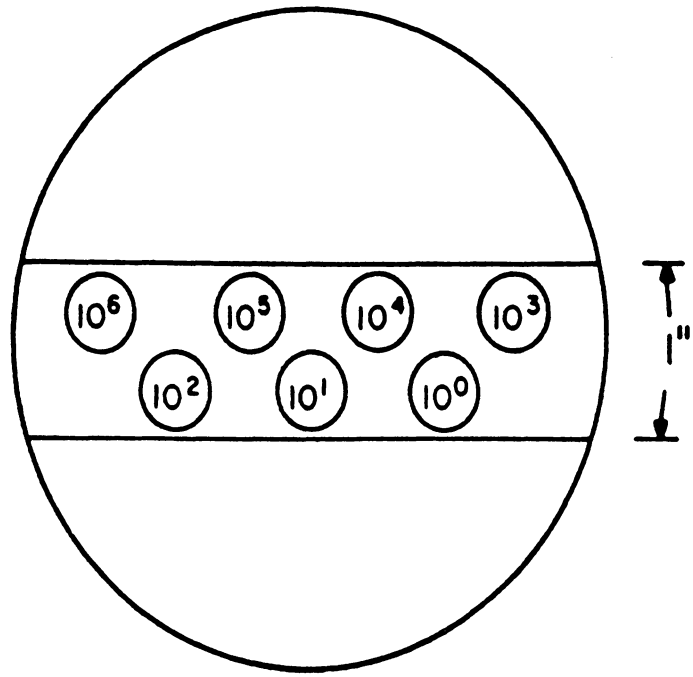

Figure 1. Microdrop positions containing different microorganism concentrations within a one cm^2 area on a Petri plate.

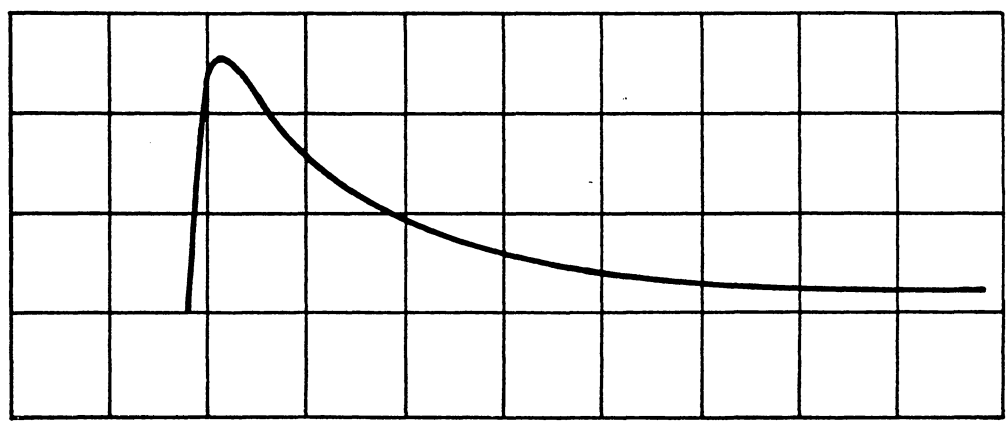

Figure 2. Calorimeter trace indicating a peak amplitude of 2.5 cm on an oscilloscope screen.

APPENDIX (H)

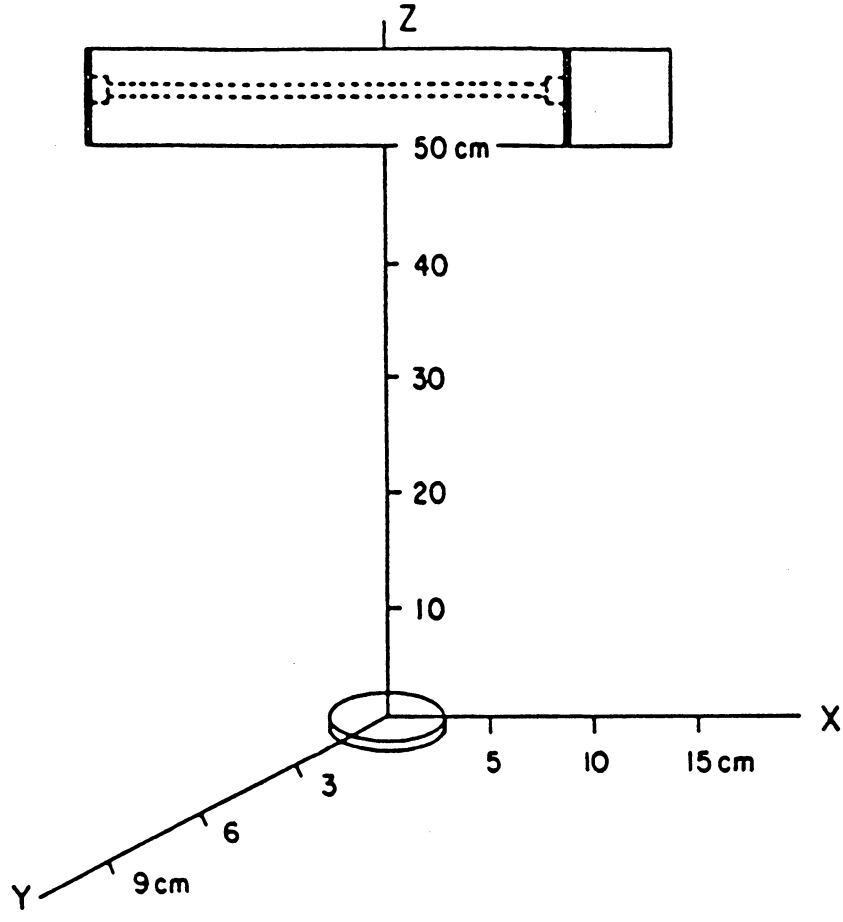

Flashblast Lamphead Cartesian Coordinates for Energy Density Calibration.

REFERENCES

Andrellos, P. J., Beckwith, A. C. and Eppley, R. M. 1967. Photochemical changes of Aflatoxin B_1. J. Assoc. Off. Anal. Chem. 50:346-350.

AOAC. 1980. Aflatoxins. In: Official Methods of Analysis. Washington, D.C. : Association of Official Analytical Chemists. pp. 415-427.

Ayres, J. C., Mundt, J. O. and Sandine, W. E. 1980. "Microbiolology of foods". Freeman, San Francisco. pp. 658-683.

Bayliss, C. E. and Waites, W. M. 1979. The combined effect of hydrogen peroxide and UV irradiation on bacterial spores. J. Appl. Bacteriol. 47:263-269.

Bayliss, C. E. and Waites, W. M. 1982. Effect of simultanious high intensity UV irradiation and hydrogen peroxide on bacterial spores. J. Food. Technol. 17:467-470.

Beukers, R. and Berends, W. 1960. Isolation and identification of the irradiation product of thymine. Biochem. Biophys. Acta. 41:550-551.

Butler, R. C.,Lund, Vidal and Carlson, D. A. 1987. Susceptibility of Campylobacter jejuni and Yersinia enterocolitica to UV radiation. Appl. Environ. Microbiol. 53:375-378.

Chang, J. C., Ossott, S. F., Lobe, D. C., Dorfman, M. H., Dumais, C. M., Qualls, R. G. and Johnson, J. D. 1985. UV inactivation of pathogenic and indicator microorganisms. Appl. Environ. Microbiol. 6:1361-65.

Crandall, R. A. 1986. The use of ultraviolet light in the treatment of water in public spas and hot tubs. J. Environ. Health. 49:16-23.

Davis, B. D., Dulbecco, R., Eisen, H. N., Ginsberg, J. S. and Wood, W. B. 1970. "Microbiology". 6th Edition. Harper and Row Publishers, New York. pp. 340-341.

Elenbaas, W. 1972. "Light Sources", Phillips Technical Library. Macmillan, London.

Frank, H. K. 1968. Diffusion of aflatoxins in food stuffs. J. Food Sci. 33:98-100.

Gates, F. L. 1928. On nuclear derivatives and the lethal action of ultraviolet light. Science. 68:479-480.

Gates, F. L. 1929. A study of bactericidal action of ultraviolet light. Part II. The effects of various environmental factors and conditions. J. Gen. Physiol. 13:249-260.

Gilpin, R. W., Dillon, S. B., Keyser, P., Androkites, A., Berube, M., Carpendale, N., Skorina, J., Hurley, J. and Kaplan, A. M. 1985. Disinfection of circulating water systems by ultraviolet light and helogenation. Water Res. 19:839-848.

Grecz, N., Tang, T. and Frank, H. A. 1973. Photoprotection by dipicolinate against inactivation of bacterial spores with ultraviolet light. J. Bacteriol. 113:1058-1060.

Greene, V. W. 1970. Disinfection and sterilization practices in American hospitals. In: Disifection (M. A. Benarde, Ed.). Marcel Dekker, New York. pp. 702-756.

Harm, W. 1980. "Biological Effects of Ultraviolet Radiation". Cambridge University press, Cambridge. pp. 31-39.

Harrington, W. O. and Hills, H. H. 1968. Reduction of the microbial population of Apple Cider by ultraviolet irradiation. Food Technol. 22:117-120.

Haynes, R. H. 1964. Role of DNA repair mechanisms in microbial inactivation and recovery phenomena. Photochem. Photobiol. 3:429-450.

Hidalgo, J. G. 1985. Feasibility study of surface applications for Flashblast radiation in the food industry. Virginia, V. P. I. & S. U., Thesis.

Hoyt, G. D. and McCormick, W. W. 1950. A study of the short duration, high intensity, electric arc as asource of visible light. J. Opt. Soc. Amer. 40:658-663.

Huang, Y. W. and Toledo, R. 1982. Effect of high doses of high and low intensity UV irradiation on surface microbiological counts and storage-life of fish. J. Food Sci. 47:1667-1669, 1731.

Jagger, J. 1985. "Solar-UV actions on living cells". Praeger Publishers, New York.

Jay, J. M. 1986. "Modern Food Microbiology". 3rd Edition. Van Nostrand Reinhold, New York. pp. 542-543.

Jones, S. B., Palumbo, S. A. and Smith, J. L. 1986. Improved fixation of Staphylococcus aureus for electron microscopy. J. Electron Microsc. Tech. 3:455-456.

Korhonen, R. W., Reagan, J. O., Carpenter, J. A. and Campion, D. R. 1981. Effects of brief exposure of high intensity ultraviolet light on microbial survival and growth rates and formation of oxidative rancidity in beef at the retail level. J. Food Quality. 4:217-229.

Kreft, P., Karl Scheible, O. and Venosa, A. 1986. Hydraulic studies and cleaning evaluations of ultraviolet disinfection units. J. Water Pollut. Control Fed. 58:1129-1137.

Leif, W. R. and Herbert, J. E. 1960. Effect of uronic acid and dipicolinic acid on bacteria exposed to ultraviolet radiation. Amer. J. Hygiene. 71:285-291.

Lillard, D. A. and Lantin, R. S. 1970. Some chemical characteristics and biological effects of photomodified aflatoxins. J. Assoc. Off. Anal. Chem. 53:1060-1063.

Maruyama, Y. and Hayaski, K. 1963. Effect of UV irradiation on nucleic acid synthesis in germinating Aspergillus niger conidia. J. Gen. Appl. Microbiol. (Tokyo). 9:425-431.

Maunder, D. T. 1977. Possible use of UV sterilization of containers for aseptic packaging. Food Technol. 4:36-37.

McCulloch, E. C. 1945. "Disinfection and Sterilization". Kimpton, London.

McNair Scott, D. B. and Lesher, E. C. 1963. Effect of ozone on survival and permeability of Escherichia coli. J. Bacteriol. 85:567-576.

Meissel, M. N. 1955. The biological effect of ionizing radiations on microorganisms. Proc. Intern. Conf. Peaceful Uses of Atomic Energy. 11:227-230.

Miyaki, K., Aibara, K. and Miura, T. 1967. In: Microbiological Problems in Food Preservation by Irradiation (Proc. panel, Vienna, IEAE 1966). Vol 57.

Morita, R. Y. and Burton, S. D. 1963. Influence of moderate temperature of growth and malic dehydrogenase activity of a marine psychrophile. J. Bacteriol. 86:1025-1029.

Munakata, N. and Rupert, C. S. 1972. Genetically controlled removal of "Spore Photoproduct" from deoxyribonucleic acid of ultraviolet-irradiated Bacillus subtilis spores. J. Bacteriol. 11:192-198.

Nagasawa, S., Tsuchiya, T. and Nishimura, H. 1970. Hospital Infection. In: Disinfection (M. A. Benarde, Ed.). Marcel Dekker, New York, pp. 257-290.

Phillips, R. 1983. "Sources and Application of Ultraviolet radiation". Academic Press, New York.

Raynolds, E. S. 1963. The use of lead citrate at high pH as an electron-opeque stain in electron microscopy. J. Cell Biol. 17:208-210.

Reagan, J. O., Smith, G. C. and Carpenter, Z. C. 1973. Use of ultraviolet light for extending the case life beef. J. Food Sci. 38:929-931.

Roessler, E. B., Pangborn, R. M., Sidel, J. L. and Stone, H. 1978. Expanded statistical tables for estimating significance in paired- preference, paired-difference, duo-trio and triangle tests. J. Food Sci. 43:940-943.

Russell, A. D. and Harries, D. 1968. Damage to Escherichia coli on exposure to moist heat. Appl. Microbiol. 16:1394-1399.

Schechmeister, I. L. 1977. Sterilization by ultraviolet radiations. In: Disinfection, Sterilization and Preservation, (Seymour S. Block, Ed.). 2nd Edition. Lea & Febiger, Philadelphia. pp. 522-541.

Sharp, D. G. 1939. The lethal action of short ultraviolet rays on several common pathogenic bacteria. J. Bacteriol. 37:447-460.

Shepherd, C. J. 1962. Germination of conidia of Peronospora tabacina Adam. Austral. J. Biol. Sci. 15:483-508.

Shorter, A. J. and Scott, K. J. 1986. Removal of ethylene from air and low oxygen atmospheres with ultraviolet radiation. 19:176-179.

Stermer, R. A., Lasater-Smith, M. and Brasington, C. F. 1987. Ultraviolet Radiation- An effective bactericide for fresh meat. J. Food Prot. 50:108-111.

Smith, K. C. and Hanawalt, P. C. 1969. "Molecular Photobiology, Inactivation and Recovery". Academic Press, London and New York.

Sussman, A. S. and Halvorson, H. O. 1966. Spores, their dormancy and germination. Harper and Row, New York and London.

Touchstone, J. C. 1982. "Advances in Thin Layer Chromatography, Chemical and environmental applications". Wiley, New York.

Waiss, A. J. and Wiley, M. 1969. Anomalous photochemical addition of methanol to 6-methoxydifurocoumarone. Chem. Comm. 18:512-513.

Wei, Ru-dong and Chu Fun Sun. 1973. Aflatoxin-Solvent interaction induced by ultraviolet light. J. Assoc. Off. Anal. Chem. 56:1425-1430.

Zarmenhof, S. and Reddy, T. K. R. 1967. Induction of mutations by ultraviolet irradiation of spores of Bacillus subtilis. Radiation Research. 31:112-120.

The vita has been removed from the scanned document